Universidade do Minho
Escola de Engenharia

Rita Alexandra Carpinteiro Domingues

Characterization of novel *Acinetobacter baumannii* phage-derived depolymerases with anti-virulence properties

November 2021

Characterization of novel *Acinetobacter baumannii* phage-derived depolymerases with anti-virulence properties

Rita Alexandra Carpinteiro Domingues

UMinho | 2021

Universidade do Minho
Escola de Engenharia

Rita Alexandra Carpinteiro Domingues

Characterization of novel *Acinetobacter baumannii* phage-derived depolymerases with anti-virulence properties

Master's Thesis
Master's degree in Biothecnology

Work supervised by
Doctor Hugo Oliveira

November 2021

DIREITOS DE AUTOR E CONDIÇÕES DE UTILIZAÇÃO DO TRABALHO POR TERCEIROS

Este é um trabalho académico que pode ser utilizado por terceiros desde que respeitadas as regras e boas práticas internacionalmente aceites, no que concerne aos direitos de autor e direitos conexos.

Assim, o presente trabalho pode ser utilizado nos termos previstos na licença abaixo indicada.

Caso o utilizador necessite de permissão para poder fazer um uso do trabalho em condições não previstas no licenciamento indicado, deverá contactar o autor, através do RepositóriUM da Universidade do Minho.

Atribuição-NãoComercial-SemDerivações
CC BY-NC-ND

https://creativecommons.org/licenses/by-nc-nd/4.0/

Acknowledgements

Este trabalho traduz o fim de um capítulo na minha vida profissional e pessoal. Um capítulo que me permitiu evoluir e aprender bastante. Desta forma, gostaria de expressar o meu agradecimento a todos os que me acompanharam e permitiram que este trabalho fosse possível.

Em primeiro lugar, ao meu orientador, Dr. Hugo Oliveira, por toda a disponibilidade, paciência, motivação e conhecimento. Não tenho forma de agradecer pela preocupação constante, bem como a excelente orientação e a confiança que depositaste em mim. Mereces todo o reconhecimento por este trabalho e agradeço-te imenso por toda a ajuda e apoio.

Ao grupo do LPhage, agradeço por me terem proporcionado um ambiente incrível para desenvolver a minha tese. Agradeço todos os conselhos que me foram dados, as conversas, a simpatia e as gargalhadas. Em especial, agradeço ao Dr. Sílvio Santos e à Dra. Priscila Pires pela ajuda e orientação em partes deste trabalho. Agradeço ainda toda a disponibilidade e sugestões que permitiram a conclusão desta tese. À Ana Barbosa, agradeço pela ajuda constante e por ter sido a minha parceira de laboratório durante este trabalho.

À minha família, agradeço pelo apoio incondicional e pelo carinho. À minha mãe, agradeço a paciência e por acreditar sempre em mim. Às minhas avós, agradeço por serem um exemplo de força e perseverança para mim. Ao meu pai, dedico esta tese. Espero que estejas orgulhoso e que consigas ver mais um objetivo alcançado. És e serás sempre a minha estrelinha.

Ao Miguel, agradeço por todo o amor e apoio constante. És a minha âncora e fazes-me sempre acreditar que consigo fazer tudo. Agradeço por acreditares sempre em mim e por estares sempre presente. A minha vida sem ti não seria a mesma coisa. Agradeço-te do fundo do coração.

Aos meus amigos, a família que escolhi, agradeço a paciência, o apoio e o carinho. Em especial, à Beatriz, Inês, Mariana e Marta, agradeço por tolerarem todas as inseguranças e receios. Tenho muita sorte por vos ter na minha vida.

STATEMENT OF INTEGRITY

I hereby declare having conducted this academic work with integrity. I confirm that I have not used plagiarism or any form of undue use of information or falsification of results along the process leading to its elaboration.

I further declare that I have fully acknowledged the Code of Ethical Conduct of the University of Minho.

Resumo

Acinetobacter baumannii é uma bactéria patogénica e a maior causa de infeções nosocomiais em ambiente hospitalar. O tratamento de infeções causadas por *A. baumannii* com antibióticos é extremamente difícil devido a multi-resistências. Adicionalmente, a maioria das estirpes de *A. baumannii* possui um polissacarídeo capsular, considerado o maior fator de virulência desta espécie, e uma grande variedade de tipos capsulares são produzidos por esta bactéria. Os fagos são vírus que apenas infetam bactérias, usando a sua maquinaria celular para propagar. Alguns fagos evoluíram para codificar depolimerases capsulares, que se ligam especificamente a certos tipos capsulares e degradam os polissacarídeos presentes nas cápsulas bacterianas, permitindo que o fago infete as bactérias. Desta forma, as depolimerases capsulares têm demonstrado ser uma poderosa arma antivirulenta, com a capacidade de degradar e remover as cápsulas das bactérias. Previamente a este trabalho, 17 diferentes depolimerases capsulares-específicas foram identificadas e caracterizadas (K1-2, K9, K19, K27, K30, K32, K37, K44-45, K47-48, K87, K89, K91, K93 e K116).

Neste trabalho, os genes codificantes para as β-lactamases *oxa-51* e *oxa-23* foram os mais predominantes encontrados em isolados clínicos de *A. baumannii* resistentes a carbapenemos, seguidos pelos genes correspondentes às β-lactamases *Imp-like* e *oxa-24*. Adicionalmente, 6 novas depolimerases capsulares derivadas de novos fagos isolados foram identificadas (F70, 3042, 3043, 3060, 3073 e 3082). Estas foram clonadas e expressas recombinantemente em *E. coli,* juntamente com depolimerases capsulares previamente identificadas (B1, B3, B9, P1 e P2). Os espetros de atividade das depolimerases capsulares B1, B3, B9, P1, P2, F70, 3042, 3043 e 3073 corresponderam aos espetros líticos dos seus fagos parentais (K9, K2/K19, K30/K45, K1, K67, K44, K38 e K32 respetivamente). Desta forma, a coleção destas enzimas expandiu para 19 diferentes depolimerases capsulares-específicas. Posteriormente, estas enzimas foram caracterizadas, demonstrando possuir uma elevada estabilidade estrutural e capacidade de degradação dos polissacarídeos capsulares, deixando as bactérias mais suscetíveis a serem eliminadas pelo sistema complemento do soro. Porém, um efeito sinergético entre as enzimas e diferentes antibióticos na disrupção de biofilmes e em células planctónicas não foi observado.

Palavras-chave: *Acinetobacter*, bacteriófagos, depolimerases, tipos capsulares, atividade antimicrobiana

Abstract

Acinetobacter baumannii is a pathogenic bacterium and is the major cause of nosocomial infections in hospital environment. Treatment of *A. baumannii* infections with antibiotics is extremely difficult due to their multi-resistance antibiotics. Moreover, most *A. baumannii* strains carry a capsular polysaccharide that is considered its main virulence factor, and a high variety of capsular types are produced by this bacterium. Phages are viruses that only infect bacteria, using their cellular machinery to propagate. Some phages produce polysaccharide depolymerases, that bind specifically to certain capsular types and degrade the polysaccharides present in the bacterial capsules, allowing phages to infect. Therefore, capsular polysaccharide depolymerases have demonstrated to be a very powerful anti-virulence weapon with the capability to degrade and strip bacterial cells from their capsule. Prior to this work, 17 distinct *A. baumannii* capsular-specific depolymerases were identified and characterized (K1-2, K9, K19, K27, K30, K32, K37, K44-45, K47-48, K87, K89, K91, K93 and K116).

In this study, *oxa-51* and *oxa-23* β-lactamases-encoding genes were the most predominant found within carbapenem-resistant *A. baumannii* clinical isolates, followed by *Imp-like* and *oxa-24* β-lactamases-encoding genes. Furthermore, 6 novel phage derived-CPS depolymerases were identified (F70, 3042, 3043, 3060, 3073 and 3082). They were cloned and expressed in *E. coli* alongside with previously identified CPS depolymerases (B1, B9, P1 and P2). The activity spectra of the capsular depolymerases B1, B3, B9, P1, P2, F70, 3042, 3043 and 3073 matched the lytic spectra of their parental phages (K9, K2/K19, K30/K45, K1, K67, K44, K38 and K32 respectively), expanding the collection of enzymes to infect 19 different K types. However, the capsular depolymerases belonging to phages 3060 and 3082 did not demonstrate any activity against any strain. Furthermore, these enzymes were characterized, demonstrating a high structural stability and degrading activity against the capsular polysaccharides, leaving bacteria more susceptible to be eliminated by the serum's complement system. However, no synergy was found between the combination of these enzymes and different antibiotics in the disruption of biofilms and in planktonic cells.

Keywords: *Acinetobacter*, bacteriophages, CPS depolymerases, capsular types, antimicrobial activity

Table of contents

List of publications

Domingues R, Barbosa A, Santos SB, Pires DP, Save J, Resch G, Azeredo J, Oliveira H. Unpuzzling Friunavirus-Host Interactions One Piece at a Time: Phage Recognizes *Acinetobacter pittii* via a New K38 Capsule Depolymerase. *Antibiotics*. 2021;10(11):1304. doi:10.3390/antibiotics10111304

List of abbreviations and symbols

Abs	Absorbance
ANOVA	Analysis of variance
BLAST	Basic Local Alignment Search Tool
BLASTN	Nucleotide Blast
BLATP	Protein Blast
bp	Base pair
C-terminal	Carboxyl-terminal
CD	Circular Dichroism
CDS	Coding region
CFUs	Colony forming units
CPS	Capsular polysaccharides
DNA	Deoxyribonucleic acid
DNase I	Deoxyribonuclease I
DNS	3,5-Dinitrosalicylic acid
dNTP	Deoxynucleotide triphosphate
E-value	Expected value
EDTA	Ethylenediamine tetraacetic acid
EPS	Extracellular polysaccharides
gp	Gene product
HF	High-fidelity
ICUs	Intensive care units
Imp	Imipenemase metallo-β-lactamase
IPTG	Isopropyl-B-D-thiogalactopyranoside
KAN	Kanamycin
kDa	Kilodalton
KL	Chromosomal K locus
KPC	*Klebsiella pneumoniae* carbapenemases
K type	Capsular polysaccharide-based structure
K units	Oligosaccharide units
LB	Lysogeny broth

LPS	Lipopolysaccharides
MBLs	Metallo-β-lactamases
$MgCl_2$	Magnesium chloride
MHB	Mueller-Hinton broth
MIC	Minimum inhibitory concentration
MW	Molecular Weight
N-terminal	Amino-terminal
NaCl	Sodium chloride
NCBI	National Center for Biotechnology Information
NCBI SRA	NCBI Sequence Read Archive
Ndm	New Delhi metallo-β-lactamases
Ni^{2+}-NTA	Nickel-charged affinity resin
OD	Optical Density
ORF	Open Reading Frame
Oxa-enzymes	Oxacillin-hydrolysing carbapenemases
PBS	Phosphate buffered saline
PCR	Polymerase chain reaction
PFUs	Plaque forming units
RNase A	Ribonuclease A
rpm	Rotations per minute
RT	Room temperature
SDS	Sodium dodecyl sulphate
SDS-PAGE	Sodium dodecyl sulfate polyacrylamide gel electrophoresis
SOC	Super Optimal Broth with Catabolite repression
STR	Streptomycin
TAE buffer	Tris-Acetate-EDTA Buffer
TET	Tetracycline
Tm	Melting temperature
Tris-HCl	Tris-Hydrochloride
tRNA	Transfer Ribonucleic acid
TSA	Tryptic soy agar
TSB	Tryptic soy broth

UV	Ultraviolet
V	Volts
Vim	Verona integron-borne metallo-β-lactamase
WHO	World Health Organization
w/v	Weight/volume

List of figures

List of tables

CHAPTER I

General Introduction

1.1. Antibiotic problematic

We have been living in the "antibiotic era" for the past decades, where antibacterial drugs have been used to cure threatening bacterial infections. However, that era may be coming to an end since development of resistance to antibiotics has been increasing.[1] Due to this, antibiotics are demonstrating decreased efficacy and, aside from three new antibiotic classes discovered between 2005 and 2018, there has not been significant development in this area since the 1980's.[2]

Indeed, these antibacterial drugs have been largely used in medicine due to their effectiveness against a wide range of bacterial infections. Still, the appearance of resistance mechanisms to antibiotics has been predicted since their discovery, as bacteria are able to adjust to the environment surrounding them, demonstrating a great ability to endure stress conditions, including developing mechanisms to resist antimicrobial agents.[3,4] Unfortunately, mechanisms to resist every class of antibiotics produced until this date have been established over time.[4]

The major cause of resistance is the misuse of these drugs, as they were being administrated for all types of infections, resulting in a selective pressure which determined that strains able to resist antibiotics' action, due to mutations, were able to survive, grow and transmit those resistance mechanisms to the descendent bacterial community.[4–6] As a result, many bacteria, previously susceptible to antibiotics, obtained resistance.

Bacteria can prevent the entrance of antibiotics by modifying their cell envelope, expel them through efflux pumps and modify or destroy these drugs by producing enzymes.[4,7,8] Furthermore, microbial cells can also achieve resistance through metabolic dormancy, persistence and growth in biofilms, which are communities enclosed in an extracellular matrix.[7,9] Ultimately, multidrug-resistant strains have emerged throughout the years, especially in hospital environment. These bacteria can cause significant nosocomial infections and are the major cause of mortality in hospitalized patients. However, lately, they have spread to the community, causing severe illness in non-vulnerable patients.[4]

1.2. *Acinetobacter baumannii*

Recently, some species have become a focus of scientific attention as they can cause nosocomial infections that seem to be difficult to overcome. The most clinically relevant strains within the *Acinetobacter* genus belong to the *Acinetobacter calcoaceticus-baumannii* (ACB)

complex. This complex consists of five pathogenic species: *Acinetobacter baumannii*, *Acinetobacter nosocomialis*, *Acinetobacter pittii*, *Acinetobacter seifertii* and *Acinetobacter dijkshoorniae*, and also one non-pathogenic species: *Acinetobacter calcoaceticus.*[9] Due to the high phenotype similarities between the species belonging to the ACB complex, it is difficult to distinguish *A. baumannii* from the others. So, all members of the complex are usually identified as *A. baumannii*, hence the high characterization of this species.[9]

A. baumannii is a non-fermentative, strictly aerobic, gram-negative, motile, catalase positive and oxidase-negative coccobacillus bacterium.[10,11] Generally, *A. baumannii* can be found in wet environments as mud, wastewater and ponds.[12] Once thought to be harmless, *A. baumannii* first received attention when it was uncovered in wounds of veterans and soldiers coming back from wars in Iraq and Afghanistan.[13,14] Ultimately, *A. baumannii* multidrug-resistant strains have emerged throughout the years, especially in hospital environment (e.g. assisted ventilation and hospital sink traps and floors).[11,12,14,15] This is on account of the high selective pressure exerted by the inappropriate or excessive usage of antibiotics and due to the spread to civilian hospitals by injured military patients repatriated from the war zones.[11,12,14,15]

This pathogen is the major cause of nosocomial infections in hospital environment, including complications as bacteremia, urinary tract infections, bloodstream infections, meningitis, septicemia, endocarditis and, particularly, pneumonia in patients confined to hospital intensive care units (ICUs). Thus, this is an opportunist human pathogen, that generally infects critically vulnerable and immuno-compromised patients.[9,11,15,16] Less frequently, *A. baumannii* has also been linked to complicated skin and soft tissue and central nervous system infections. It is commonly transmitted to patients through surfaces and colonization on the hands of health care workers. Moreover, spread of this bacterium by colonized patients has been documented.[12]

Infections caused by *Acinetobacter* spp. account for 1.8% of all health care-associated infections in the United States.[9,12] Also, these infections account for up to 20% of ICUs' infections worldwide and there are an estimated 1 million cases of *Acinetobacter* spp. infections per year around the globe.[9,12] This occurrence seems to be similar in ICUs across Europe and Latin America.[9,12] However, these rates are twice as high in Asia and the Middle East.[9,12] *A. baumannii* is the most prevalent, responsible for 95% of infections, followed by *A. nosocomialis* and *A. pitti*.[15] The lethality of *Acinetobacter* spp. infections is very high, with mortality rates averaging 45-60%, even reaching 80% when patients are infected with multidrug-resistant strains, and they are estimated

to directly and indirectly cause 100,000 deaths yearly, which comes with a huge expense, resulting in an addition $34 billion in health care costs per year in the United States only.[12,15,17–19]

Treatment of *A. baumannii* infections is extremely challenging due to 1) its intrinsic resistance to sometimes all classes of antibiotics (including carbapenems and β-lactams, aminoglycosides, quinolones, tetracyclines, fluoroquinolones and polymyxins), 2) its remarkable capacity to acquire new resistance mechanisms at never foreseen rates and 3) its ability to survive long periods in hospital environment and unfavored conditions, such as surfaces, spreading between patients (biotic) or via inanimate objects (abiotic) by colonizing and forming biofilms.[9–11,15,16,20–22]

Antibiotic resistance is not considered a traditional virulence factor. Nonetheless, currently is the biggest mishap in the efficient treatment of *A. baumannii* infections.[12] Unfortunately, recent statistics demonstrate a high prevalence (45%) of *A. baumannii* multidrug-resistant isolates found in ICUs' patients across the United States and Europe, and in Latin America and in the Middle East the rates are higher (around 70%).[9] It is one of the species that consistently demonstrates an extensive drug-resistant (XDR) phenotype, defined as resistant to all available antibiotics, except for those that are less effective or more toxic compared to first-line agents used in the treatment of these infections.[12] It is of great concern that a high number of *A. baumannii* strains display multidrug-resistance mechanisms to even "last line of defense" antibiotics.[15] In those cases, there are limited or even non-existent treatment options, which is a major health burden and a problem of global concern.[23] So, as previously exposed, the threat of a "post-antibiotic era" is increasingly becoming a reality.[15]

In light of all these data, the World Health Organization (WHO) has included carbapenem-resistant *A. baumannii* in the list of the critical bacteria that carry the greatest danger to human health, prioritizing research efforts for new antimicrobial treatments.[9] Also, *A. baumannii* is one of the most serious ESKAPE organisms (*Enterococcus faecium*, *Staphylococcus aureus*, *Klebsiella pneumoniae*, *A. baumannii*, *Pseudomonas aeruginosa* and *Enterobacter* spp).[14,21] The ESKAPE bacteria were classified due to their ability to escape antibiotic treatments, resulting in high mortality rates.[21]

Alongside with the intrinsic resistance to antibiotics, *A. baumannii* also possesses a massive resistance library within its genome, comprised of 45 resistance genes.[12] Correspondingly, *A. baumannii* can acquire antibiotic-resistant genes from other bacteria that colonize the same environment, such as *Escherichia coli*.[10,11,16] Moreover, this pathogen is able to develop resistance

mechanisms to antibiotics in the middle of a course of treatment, hampering the attempts to eliminate infections.[12]

Some of the resistance mechanisms harbored by this pathogen are the reduced number and size of porins, which are channels that allow the transport of molecules across the outer membrane, that confer a low permeability to antibiotics, and the overexpression of chromosomal efflux systems.[12,14] However, the major form of resistance to antibiotics is the synthesis of enzymes that can degrade antibiotics, such as β-lactamases and aminoglycoside-modifying enzymes. In *A. baumannii*, carbapenem resistance is mainly mediated by class B (Metallo-β-lactamases; MBLs) and class D (oxacillin-hydrolysing carbapenemases; Oxa-enzymes) β-lactamases.[14,23] Regarding the oxa-enzymes, four sub-groups are most relevant in *A. baumannii*, of which oxa-23-like, oxa-24-like, oxa-51-like and oxa-58-like carbapenemases.[23] In addition, the MBL family includes Verona integron-borne (VIM), Imipenemase (IMP) and New Delhi (NDM) metallo-β-lactamases.[23] Also, *Klebsiella pneumoniae* carbapenemase (KPC) was found in a high percentage of multidrug-resistant *A. baumannii* isolates, disseminated from *K. pneumoniae*.[24]

Furthermore, Farrow et al. (2018) and Bravo et al. (2019) found some strains that exhibited a profound resistance to desiccation and uncovered that the majority of their cells could survive without loss of viability and cultivability on a dry solid surface for a long time, enhancing the knowledge that this bacterium can colonize and persist in medical equipment and hospital environment for a long period of time.[25,26] Moreover, *A. baumannii* was able to adapt to disinfection regimes that integrate health-care procedures.[9] All these factors may explain its propensity for causing extended outbreaks.[11]

Adding to the factors mentioned previously that cause this bacterium to be clinically dangerous, *A. baumannii* is also able to sense and respond to signals that allow it to adapt to its surrounding environment. Light is one of the environmental signals that it can respond through a photoreceptor, allowing it to recognize its surroundings. On that note, the pathogen is able to control biofilm formation, adjusting its lifestyle to persist, colonize and inflict contamination. It can also adapt to changes in the abundance of iron and zinc, which are critical metals for most living cells, allowing it to maintain its virulence.[12,27]

1.2.1. *A. baumannii* capsular polysaccharide

Most *A. baumannii* strains carry a thick capsular polysaccharide (CPS) and an O-linked protein glycosylation system. This glycosylation system favors short-chain, branched, negatively charged amino-containing surface sugars that protect against host immunity and serve as a target to help clear the pathogen.[12] Moreover, cells that lack this glycosylation system are usually deficient in biofilm formation, indicating that this system is required for a successful adaption to the environment.[9]

Considered to be the main virulence factor of *A. baumannii*, the capsule helps cells to 1) evade immunity by shielding them from the host's complement effect, antibodies and engulfment by macrophages, 2) avoid predators (such as bacteriophages) by hiding their receptors and 3) allow interactions with prokaryotic and eukaryotic cells and with abiotic surfaces (e.g. biofilms).[9,18,28] Furthermore, the capsule is also responsible to retain water, protecting the bacteria from desiccation, which enables *A. baumannii* to maintain its viability under water limitation conditions.[9] Also, besides being a critical protection requirement for *A. baumannii*, it also grants intrinsic resistance to antibacterial agents.[29,30] Interestingly, the presence of antibiotics induces the hyperproduction of the capsule, since it increases the bacterium's resistance to be killed by the host's complement system and it also increases its virulence.[14]

The capsule is the outer layer surrounding bacteria and it consists of long-chain capsular polysaccharides, also labeled as K-antigens in *A. baumannii,* that are connected to the outer membrane of gram-negative bacteria via a lipid anchor.[31] As a result of the different abovementioned selective pressure, *A. baumannii* produces a highly variable capsule structure. The capsule is produced by the polymerization of an oligosaccharide by a Wzy polymerase. Usually, the different sets of genes that encode those enzymes are located within the CPS biosynthesis gene cluster, that is positioned at the chromosomal K locus (KL) and are responsible for the synthesis, assembly and exportation of the capsule (**Figure 1**).[31,32] The KL determines the capsular polysaccharide-based structures (K types) by defining the oligosaccharide units (K units) formed.[33]

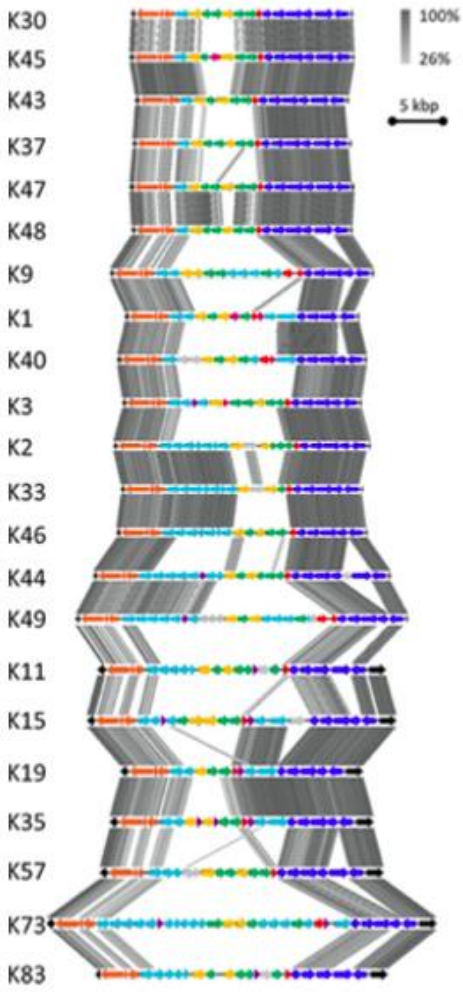

Figure 1. Chromosomal K locus (KL) of different *A. baumannii* K types. Capsular polysaccharide synthesis clusters (n=22) represented with EasyFig drawn at scale. The K locus genes are colored according to function. Adapted from Oliveira et al. (2019).[34]

In **Figure 1**, it is possible to observe a typical arrangement for *A. baumannii* KL gene clusters. There is a variable gene region in the center, responsible for nucleotide sugar and glycosyltransferase biosynthesis, flanked by several conserved genes, involved in the extraction of the capsule (on the left) and synthesis of simple sugars (on the right).[34–36] At this moment, 125 different K types have been described in *A. baumannii*. This variety might be related to different degrees of clinical manifestation of infections and antibiotic resistance.[31] However, due to the lack of serotyping or genotyping systems, the availability of the prevalence of *A. baumannii* K types in nosocomial infections is sparce.[30]

Recently, the *Kaptive* software was developed to screen new genomes for their K types.[37] Through this software, the authors validated *in silico* typing of K locus through the genomes of *A. baumannii* assembled in different databases. According to the 642 genomes assembled from

reads available in National Center for Biotechnology Information (NCBI) Sequence Read Archive (SRA) and the 3415 genomes assembled from NCBI GenBank, a graphic that demonstrates the prevalence of K types in both databases was constructed (**Figure 2**).

Figure 2. Prevalence of *A. baumannii* K types. Information of the K type of the genomes of *A. baumannii* presented in NCBI SRA and NCBI GenBank databases.

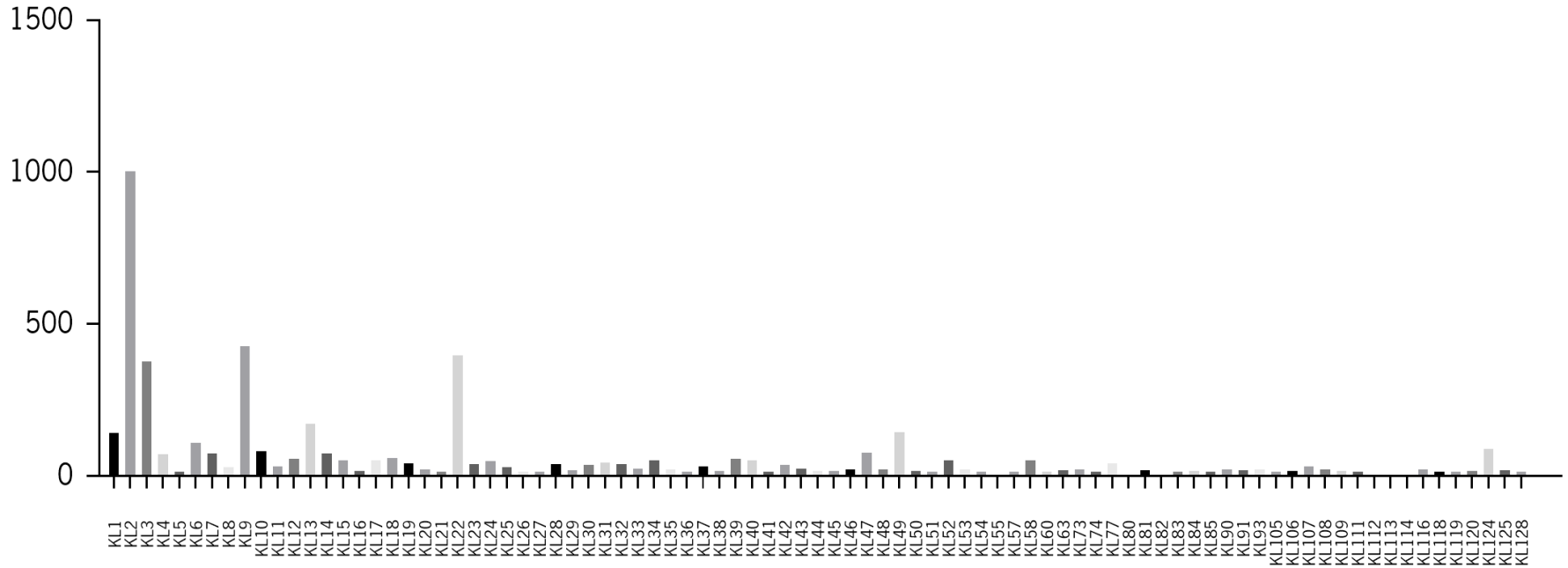

According to **Figure 2**, there are specific prevalent K types. Amongst them, KL2, KL9, KL22, KL3, KL13, KL49 and KL1 can be found following an order of decreased prevalence. This information is very important when developing new strategies to control *A. baumannii* infections since the knowledge about the K type of the strain causing a certain infection is crucial to conduct a specific treatment that affects the target bacterium.

In summary, it is clear that resistance will continue to develop, and novel multidrug-resistant strains will emerge even further. They will eventually culminate in higher mortality, higher costs and decreasing effectiveness of antimicrobial agents to combat those infections. Therefore, it is crucial to develop new approaches to manage and treat the infections caused by antibiotic-resistant bacteria.[4]

1.3. Bacteriophages

Recently, renewed interest in using bacteriophages (phages) to treat infections caused by multidrug-resistant strains has been increasing. Phages are viruses that only infect bacteria, using their cellular machinery to propagate.[38] They are the most abundant entities in the world and exist everywhere their bacterial host is present.[38,39] Phages are composed of at least two components: a nucleic acid and a protein capsid.[40] That capsid, also mentioned as phage head, is icosahedral and shields their genome.[40]

Phage genome replication usually occurs through a lytic or lysogenic cycle.[41] Phages can then be categorized into two main groups: virulent phages and temperate phages.[41] The first replicates strictly through a lytic cycle and the second can enter both lytic and lysogenic cycles.[41] Regarding temperate phages, they can follow a lysogenic cycle, integrating the host's chromosome and remaining dormant as prophages, replicating through generations with the host's genome or, more rarely, by replicating as low-copy-number phage plasmids.[41,42] Under stress conditions, these phages can switch to a lytic life cycle.[42] The lytic part of the phage life cycle is identical for temperate and virulent phages.[42] In the lytic cycle, phage infection induces the reprogramming of the host's genetic functions, resulting in a fast replication and assembly of the virion's genome and functional phage proteins.[42] Lastly, the release of the virion particles is accompanied by the lysis of the bacterial cell.[42] Bacterial cell disruption is accomplished by some phage's lytic enzymes, such as endolysins, holins and spanins.[42]

Currently, phages are being described as an alternative to antibiotics and a potential solution to treat infections caused by multidrug-resistant bacteria worldwide.[43,44] Phage therapy has been used in eastern European countries for medical treatment of those infections, even though in the rest of the world is not as conventional and antibiotics are still the protagonists.[45] However, a consensus on the feasibility of phage therapy under the right conditions has emerged, but it is still necessary to increase research efforts before phage therapy can be implemented worldwide.[46]

Phage mode of action differs from the antibiotics because 1) they are able to self-replicate and grow exponentially in the setting of an infection, which might be more efficient than applying drugs that do not possess that aptitude[2,47] and 2) they have a very high discriminatory nature, as they are highly specific to their target bacteria, reducing negative effects on the rest of the microbiome.[2,47,48] They only bind to bacteria that express specific binding sites, which means that bacteria without those receptors are not affected.[46] So, phage therapy can be envisioned as a personalized treatment to an individual patient.[49] However, this narrow host range is also a significant challenge for phage therapy. A great deal of research is requested in order to have phage cocktails prepared to treat infections caused by different K type strains, instead of using an individual phage, which comes with limitations.[46] Still, phages have an excessive genetic diversity, abundance and there is a limitless source of phages, providing vast resources for this investigation.[7,12]

Concerning *A. baumannii*, phage therapy is still far from clinical use considering that studies with success and consequence predictions are still scarce.[12,50] Nonetheless, several specific virulent phages (that possess lytic activity) against this pathogen have been identified.[12] Additionally, some studies have suggested that these phages can improve clinical outcomes of patients infected with this bacterium.[12] They can reduce the bacterial population, having a direct lytic action upon the bacterium, or they can delay the bacterial growth. Besides that, they can also disrupt biofilms and biofilm formation.[12]

However, as with antibiotics, the major limitation to phage therapy is the inevitable evolution of phage-resistant bacteria, which could decrease the efficacy of phages.[39,44] Any target bacterium that is able to escape phage attack or that encode phage-resistant mechanisms will multiply and most likely establish population levels comparable to those prior to phage administration.[46] According to a recent study, resistance against phages was found a few days after administration.[51] Even though phages may also adapt to that resistance and regain the ability to infect bacteria, this coevolutionary arms race involves many complex mechanisms related to

defense and counter defense. Those mechanisms might not be favorable to enroll inside the human body whilst trying to treat an infection.[8]

Additional concerns with phage therapy include the potential side effects on human flora and the probability of host's inflammatory responses following phage administration. Since they are viruses they might be seen as a potential invader by the immune system and the rapid clearance by human macrophages and the induction of anti-phage antibodies are likely to occur.[12,31] Safety concerns also exist due to the risk of production of some phages that may carry DNA involved in pathogenicity that could be transferred to the target bacterium, since whole phage genomes might contain some genes with unknown function.[46,52]

Not all phages can be suitable for phage therapy.[46] Temperate phages are unfavorable since prophages can possess antibiotic resistance genes, virulence factors or toxins that could be transduced into the host.[49] Therefore, these phages could provide antibiotic-resistant mechanisms to the bacterial host and enable the invasion of eukaryotic cells.[42] Furthermore, temperate phages improve the host's biofilm formation and maintenance.[42] Consequently, virulent phages are more appropriate to use in phage therapy since they lead to relatively fast destruction of the bacterial cell and there are rare occasions for interactions with the bacterial genome.[46,53]

Some virulent phages possess a tail, besides the capsid and nucleic acid, that is responsible for phage adsorption to the host's surface receptors, so as to deliver the phage genome across the bacterial cell envelope.[54] These phages belong to the *Caudovirales* order, which is the most abundant group of lytic phages. Therefore, phage application has focused on three families belonging to that order: *Myoviridae*, *Siphoviridae* and *Podoviridae*.[53]

The typical lytic phage life cycle involves five stages: 1) adsorption to the bacterial cell wall, 2) infection of the phage's DNA inside the cells, 3) expression of viral genes and synthesis of phage's macromolecules, 4) assembly of the phage particle and 5) lysis of the cells to release the phage offspring to the exterior, as it is demonstrated in **Figure 3.**[33,42,54]

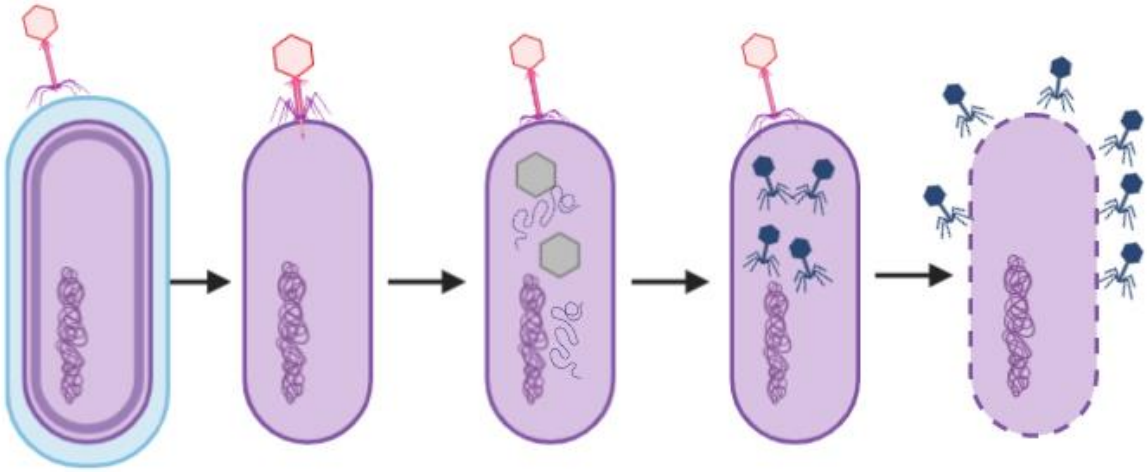

Figure 3. Bacteriophage lytic life cycle. Interaction between phages following a lytic cycle and the bacterial host.

Phage adsorption to the bacterial cell is the crucial step for the infection to occur since it requires a specific recognition of host surface proteins or polysaccharides of the bacterial cell envelope.[42] Therefore, this step dictates the phage host range.[33,38] It is determined by the interaction between the phage tail (spikes or fibers) and a specific host receptor on the surface of the bacterial cell.[31,33] Typically, phages recognize their hosts via binding/degradation of proteins or surface polysaccharides (CPS or lipopolysaccharides (LPS)) using two steps.[38] Phages bind reversibly to a primary receptor to allow a second irreversible recognition, injecting their genome into the bacterial cells.[38] However, bacteria have evolved to protect themselves from phage predation through modification of their surface by masking, mutating or losing the phage receptor proteins.[29,31,36,37] One of the most important mechanisms to avoid phage predation is the presence of a capsule that shields the phage receptors.[31] Bacteria have also evolved to block phage DNA infection, cleave injected DNA, inhibit phage replication and interfere with phage assembly.[56]

Still, phages co-evolved to become infective again by digesting the capsules through specific enzymes, called capsular depolymerases.[38,57] Capsules are then considered the primary receptor of phages and they rely on them to adsorb.[31] The composition of the capsule dictates the ability of phages to infect the strains. Usually, phages infecting *A. baumannii* have a very narrow host range, probably due to the variable composition of the bacterial capsule.[33]

Arguably, phages are the most promising agents that could potentially replace or complement antibiotics.[46] However, the use of intact phages to treat bacterial infections might not be ideal on account of all the reasons mentioned above plus the adversity associated with the

production of a complete virion for mass production and preservation.[52] A better alternative to the use of intact phages is the use of phage encoded antimicrobial enzymes.[46]

1.4. Phage polysaccharide depolymerases

Phage polysaccharide depolymerases are promising antibacterial agents. They are encoded by phages to bind and degrade polysaccharides present in the bacterial surface (e.g., CPS, LPS), allowing phages to reach the secondary host receptors located at the cell wall (**Figure 4**).

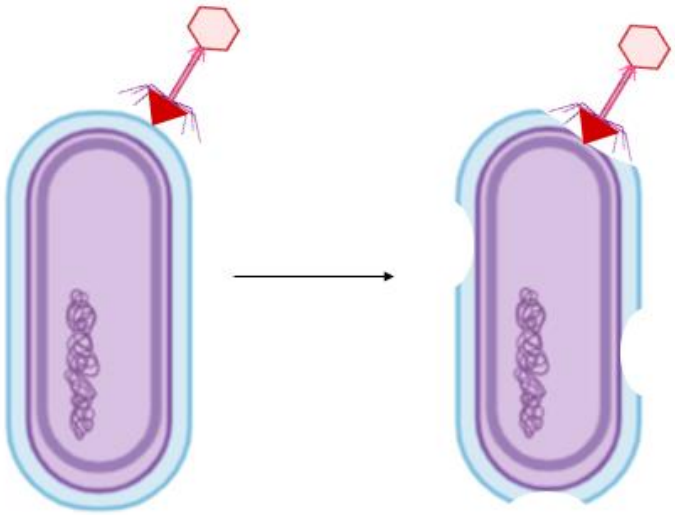

Figure 4. **Interaction between phages with CPS depolymerase activity and bacteria.** Demonstration of phage adsorption and degradation of the CPS by the phage-depolymerase (identified in the red arrow).

While phage therapy is a promising alternative to antibiotics, its success will depend on general public acceptance. As for CPS depolymerases, they are natural enzymes that can be more easily managed and accepted.[34] So, CPS depolymerases are now emerging as a new alternative antimicrobial agent to control infections caused by multidrug-resistant bacteria, such as *A. baumannii*.[30] Since phage-derived CPS depolymerases are able to target and remove bacterial capsules and biofilm structures, which are major virulence factors, they can be seen as an attractive and viable treatment option.[7]

CPS depolymerases were first isolated in the late 1990's from phage solutions.[58] These enzymes not only degrade the CPS, but also remove exopolysaccharides (EPS) involved in biofilm

matrix, facilitating phage adsorption, invasion and disintegration of host bacteria.[59] As mentioned before, it is suggested that CPS act not only as protective barriers from phage predation but also as primary receptors to phages encoding CPS depolymerases.[28,38] As demonstrated by Oliveira et al. (2017), phage adsorption was drastically reduced when cells were previously treated with recombinant CPS depolymerases, demonstrating the vital role of the CPS to enable phage infection.[33]

In *A. baumannii*, CPS depolymerases seem to be predominantly located at the phage tailspikes.[33] According to the literature, *A. baumannii* phages that encode CPS depolymerases are prevalent in specific taxonomic groups of the *Caudovirales* order (*Autographiviridae* family).[38,51] However, phages from other morphologies have also been identified (*Siphoviridae*, *Myoviridae* and *Ackermannviridae* families).[38] These CPS depolymerases were demonstrated to be resistant to high temperatures, and to protease and sodium dodecyl surface denaturation. They have high genetic plasticity, empowering constant adaptation of phages to target new host obstacles. Therefore, they are amongst the most diverse proteins in phages´ genome.[38] These enzymes can be classified in two groups depending on their mode of action, as lyases, that degrade glycosidic bonds, or hydrolases.[38] According to Oliveira et al. (2017), pectin and pectate lyases are the most commonly found CPS depolymerases in *Acinetobacter* phages.[28,33]

Phages encoding CPS depolymerases infect hosts with specific K types.[33] As demonstrated by Oliveira et al. (2017), when recombinantly expressing one CPS depolymerase, it was only active against one K type out of a range of 22 different *A. baumannii* K types, demonstrating that these enzymes are, just as phages, highly specific to certain K types. Furthermore, CPS depolymerases are so specific that they are unable to recognize K types that are close phylogenetically.[33]

There are 17 distinct CPS depolymerases identified and characterized in *Acinetobacter* infecting-phages (K1-2, K9, K19, K27, K30, K32, K37, K44-45, K47-48, K87, K89, K91, K93 and K116). **Table 1** summarizes this information.

Table 1. List of phages encoding characterized CPS depolymerases with the ability to infect certain *Acinetobacter* spp K types. Phages and characterized CPS depolymerases accession numbers are indicated, alongside the published article.

Phage	Accession no.	Capsular type	Reference	CPS depolymerase Accession no.
P1	MF033350	K1	33	ASN73504
B3	MF033348	K2 and K19	30,33	ASN73401
APK2	MK257719	K2 and K93	61	AZU99242.1
Fri1	NC_028848	K19	60	YP_009203055
AS11	KY268296	K19	60	AQN32697
AS12	KY268295	K27	60	APW79830
B9	MH133207	K30 and K45	34	AWD93192
APK32	MK257722	K32	61	AZU99395.1
APK37	MK257723	K37	61	AZU99445.1
APK44	MN604238	K44	61	QGK90444.1
Tapaz	MZ043613	K47	62	QVW53860
APK48	MN294712	K48	61	QFG06960.1
APK87	MN604239	K87	61	QGK90498.1
APK89	MN651570	K89	61	QGK90394.1
APK116	MN807295	K116	61	QHS01530.1

The easiest and most popular technique to detect phage carrying CPS depolymerases is by the presence of plaques surrounded by hazy rings that usually grow over time. This phenotype was first described in 1956 **(Figure 5).**[63] However, the so-called drop test only allows qualitative measurement.[38] The halo is caused by the CPS depolymerases, however, the exact mechanism remains unknown. [57]

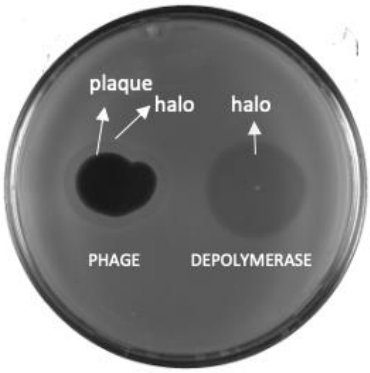

Figure 5. Phage depolymerase activity. Representation of the plaque formation of a phage with depolymerase activity through a second halo (on the left) and the plaque formation of an isolated depolymerase through a surrounding wider second halo (on the right). Adapted from Oliveira et al. (2017).[33]

These enzymes can be heterologously expressed and are able to digest *A. baumannii* capsules, leaving the bacteria susceptible to serum killing or to be eliminated by the host's immune system.[30] Several studies have demonstrated great potential as anti-virulent agents in the treatment of gram-negative bacterial infections *in vitro* and *in vivo*.[28,34 50,52,65] The anti-virulence properties of these enzymes have been established in larvae (*Galleria mellonella)* and mice. It was universally concluded that, when infected with *A. baumannii*, the survival rates were extremely low. However, when pre-treated with these enzymes, their survival rates increased considerably, meaning that the CPS depolymerase therapy was effective against *A. baumannii* infections.[30,34,52]

Additionally, numerous reports have confirmed that bacteria were able to develop resistance to phage but not the CPS depolymerase, probably because the enzyme does not kill the cells but instead is only degrading the extracellular capsule that protects them from the environment. Therefore, as no selective pressure is applied on the bacteria *in vitro* and *in vivo* when injecting only the CPS depolymerase, the development of bacterial resistant strains is unlikely to occur.[30,34]

In summary, these enzymes have demonstrated to be a very powerful anti-virulence weapon with the capability to degrade and strip bacterial cells from their capsule, turning pathogenic bacteria into avirulent forms that can be more easily managed by the host immune system when an infection is present.[38] However, epidemiological studies are necessary to narrow down the most important and frequent bacterial K types present in nosocomial infections, specially caused by *A. baumannii*. Only then, innovative CPS depolymerase-based treatments can become

a reality.[38] Also, there are only a few depolymerases isolated that are able to infect different *A. baumannii* K types, so progress in that area is urgently necessary.

1.5. Aims of this dissertation

One of the aims of this work is to perform an epidemiological study of *A. baumannii* clinical isolates from the Northern Region of Portugal, to understand the genes associated with the resistance to carbapenems, as well as the prevalence of their K types.

Another goal of this work is to expand the current knowledge and collection of CPS depolymerases against *A. baumannii*, by isolating and characterizing novel enzymes against different *A. baumannii* K types and assess their anti-virulence activity against this pathogen through *in vitro* assays and *ex vivo* models.

CHAPTER II

Materials and Methods

2.1. Bacterial strains, phages, clinical isolates, plasmids and media

2.1.1. Bacteria and phages

Acinetobacter spp. strains used to study the phages' lytic spectra are described in **Table 2**. Additionally, ninety-four *A. baumannii* clinical isolates resistant to carbapenems were gathered in the North region of Portugal between 2005 and 2012 (**Table A1**). These isolates were used to uncover the prevalence of resistance genes in the species. These strains were grown at 37°C in trypticase soy broth (TSB) or in trypticase soy agar (TSA, containing 1.2% agar).

Table 2. *Acinetobacter* spp. strains used to study the phage's lytic spectra in this work.

Strain	K type	Accession number
NIPH 290	K1	KB849940
NIPH 2061	K2	KB849309
NIPH 501	K3	KB849970.1
H202	K7	Not available
NIPH 528	K9	KB849906
J9	K11	KF002790
Ab 87	K14	Not available
A85	K15	KC118540
RBH2	K19	KU165787
Ab 93	K22	Not available
NIPH 190	K30	KB849844
Ab 49	K32	Not available
NIPH 67	K33	KB849903.1
LUH5535	K35	KC526896
NIPH 146	K37	APOU01000009
Ab 45	K38	Not available
ANC 4097	K40	KB849962.1
NIPH 60	K43	KB849508.1

NIPH 70	K44	APRC01000043
NIPH 201	K45	KB849844
NIPH 329	K46	KB849871.1
NIPH 601	K47	KB849894.1
NIPH 615	K48	MN166191
NIPH 1734	K49	KB849325.1
BAL_212	K57	KY434631
NIPH76	K67	Not available
SGH0703	K73	MF362178
LUH5538	K83	KC526898
Ab 79	K84	Not available
Ab 100	K85	Not available

E. coli strains **(Table 3)** were used for cloning and protein expression. Strains were grown at 37°C in lysogeny broth (LB) or in LB agar (containing 1.2% agar), supplemented with the appropriate antibiotics.

Table 3. *E. coli* strains used for cloning and recombinant protein expression. The appropriate antibiotics were used when growing these strains, namely, streptomycin (STR, 100 μg/mL) and tetracycline (TET, 10 μg/mL).

Species	Strain	Origin	Known resistance markers
E. coli	Top10	Invitrogen	-
	BL21 (DE3)	Invitrogen	-
	Origami™ 2(DE3)pLysS	Lucigen	STR and TET
	Origami™ B(DE3)	Novagen	TET
	C43 (DE3)	Novagen	-

In collaboration with the Faculty of Biology and Medicine of Lausanne, some *Acinetobacter* spp. infecting phages isolated by them were kindly provided (3048, 3080, 3081, 3042, 3043, 3049, 3072, 3060, 3077, 3083, 3073, 3074 and 3082). In addition, six *Acinetobacter* spp. infecting-phages with CPS depolymerase activity from the LPhage collection were used, namely,

P1 (NC_042006), P2 (NC_042007), B3 (NC_042004), B9 (MH133207), B1 (NC_042003) and F70 (not deposited in GenBank yet).

2.2. Characterization of *A. baumannii*

2.2.1. PCR genotyping

All the clinical isolates (**Table A1**) were grown in TSB plates at 37°C overnight. Afterwards, 1 or 2 colonies of each strain were homogenized in 500 μL of distilled water and boiled at 98°C for 15 minutes. Next, cells were centrifuged (12,000g, 5 min) in order to separate the lysate cells from the DNA.

MBLs, like KPC, IMP, Ndm and Vim, and OXA carbapenemases (subgroups oxa-23, oxa-24, oxa-41 and oxa-58) were subject of study, owning to their historical prevalence in *A. baumannii*.[14,15] Two multiplex-PCR reactions were performed for each strain. Since the annealing temperatures of the primers, built for the amplification of the resistance genes, can be the same, it was possible to group the amplification of four resistance genes in the same PCR reaction, accounting for 2 PCR reactions necessary for each clinical strain in total. The primers designed for these amplifications are displayed in the **Table 4**.

Table 4. List of the primers used to amplify the resistance genes. Main characteristics are indicated.

Target gene		Primer (5' - 3')	Amplicon size	Ref.
Multiplex 1 Class B carbapenemases	**KPC-like**	CGT CTA GTT CTG CTG TCT TG	798 bp	65
		CTT GTC ATC CTT GTT AGG CG		
	IMP-like	GAA GGY GTT TAT GTT CAT AC	587 bp	66
		GTA MGT TTC AAG AGT GAT GC		
	NDM-1-like	TAA AAT ACC TTG AGC GGG C	439 bp	67
		AAA TGG AAA CTG GCG ACC		
	VIM-like	GTT TGG TCG CAT ATC GCA AC	382 bp	66
		AAT GCG CAG CAC CAG GAT AG		
Multiplex 2 OXA carbapenemases	**OXA-58-like**	AAG TAT TGG GGC TTG TGC TG	599 bp	68
		CCC CTC TGC GCT CTA CAT AC		
	OXA-23-like	GAT CGG ATT GGA GAA CCA GA	501 bp	
		ATT TCT GAC CGC ATT TCC AT		
	OXA-51-like	TAA TGC TTT GAT CGG CCT TG	353 bp	
		TGG ATT GCA CTT CAT CTT GG		
	OXA-24-like	GGT TAG TTG GCC CCC TTA AA	246 bp	
		AGT TGA GCG AAA AGG GGA TT		

The PCR amplification mixture and concentrations were the following: 1x reaction buffer (10x, NzyTech), 1.5 mM $MgCl_2$ (50 mM), 0.25 mM dNTPs (dATP, dTTP, dGTP and dCTP, 25 mM), 0.25 μM each of forward and reverse primers (20 mM), 1.25U Supreme NZYTaq II DNA polymerase (NzyTech), DNA template (1 to 10 ng) and distilled water up to 20 μL. The DNA thermal cycler was programed for a PCR reaction of 30 cycles covering: 98°C for 5 min (initial denaturation step), 94°C for 30 seconds (DNA denaturation step), 54°C for 30 sec (primer annealing step), 72°C for 30 sec (extension step), followed by 72°C for 5 min (final extension step).

The amplicons were mixed with 6x NZYDNA loading dye (NzyTech) and subjected to electrophoresis at 100V for 1 hour in a 1.5% agarose gel in TAE buffer (1x) (40 mM Tris-HCl, pH 7.2, 20 mM sodium acetate and 1 mM EDTA), stained with Green Safe Premium (NZYtech), and observed through ultraviolet (UV) illumination using ChemiDocTM (Bio-Rad). These reactions were

performed with positive controls to ensure that the amplification proceeded as expected (**Figure A1**).

2.2.2. Gram staining

Complementary gram staining assays were also performed in *A. baumannii* clinical isolates.[69] Briefly, a drop of water was added onto a slide and a minute amount of one colony was transferred aseptically to the slide. The culture was then spread with an inoculation loop, creating an even thin film. Afterwards, the culture was dried over a gentle flame while moving the slide to avoid overheating. Next, 5 drops of crystal violet stain were added over the culture and allowed to stand for 60 sec, then about 5 drops of the iodine solution were added and allowed to fix the culture for 60 sec. A few drops of decolorizer were added in order to dissolve the lipid layer from the gram-negative cells and dehydrate the thicker gram-positive cell wall. Then, 5 drops of safranin solution were added as a counterstain and allowed to stand for 60 sec. Lastly, the slide was analyzed under an optical microscope.

2.3. Characterization of *A. baumannii* – infecting phages

Novel phages were characterized in order to build a comprehensive collection of phage-encoded CPS depolymerases against different *A. baumannii* K types.

2.3.1. Phage production

Overnight cultures of *Acinetobacter* spp. host strains (NIPH 290 (K1) for phage P1, NIPH 2061 (K2) for phage B3, NIPH 528 (K9) for phage B1, NIPH 70 (K44) for phage F70, NIPH 201 (K30) for phage B9, Ab49 (K32) for phage 3073, Ab45 (K38) for phage 3042 and 3043, Ab79 (K84) for phage 3082, Ab100 (K85) for phage 3060 and NIPH76 (K67) for phage P2) were grown at 37°C in TSB medium. Next day, cultures were diluted in 40 mL of TSB medium and grown at 37°C until an optical density ($OD_{620\ nm}$) of around 0.5. Phage stocks were added and incubated for 4 h at 37°C. Next, the cultures were centrifuged (4,000g, 15 min) and filtered (0.22 µm (Whatman™)).

2.3.2. Lytic spectra

As previously described, first *Acinetobacter* spp. bacterial lawns of each K type were prepared in TSA soft agar overlay plates (TSB with 0.6% agar). After drying, 10^8 plaque forming units (PFU)/mL of phage stocks were spotted on the plates and incubated at 37°C overnight. The presence of lytic activity of the phages was detected by the observation of an opaque double halo on the bacterial lawn.

2.3.3. Extraction of phage DNA

After the lytic spectra, some phages were selected for sequencing (F70, 3042, 3043, 3060, 3073 and 3082), due to their ability to infect novel *A. baumannii* K types.

Phage genomic DNA was extracted using the phenol-chloroform method. After phage production, 1 mL of phage mixture was mixed with 1 M $MgCl_2$. Next, DNase I (10000 mg/mL) and RNase A (100 mg/mL) were added to the mixture. After vortexing, the mixture was incubated at room temperature for 1 h. Next, 0.5 M EDTA, proteinase K (10 mg/mL) and 10% SDS were added to the mixture and incubated overnight at 56°C.

The next day, an equal amount of phenol was added and mixed, followed by a centrifugation (3,000g, 10 min). Next, the aqueous phase was recovered, and an equal amount of phenol and chloroform (1:1) was added, followed by a centrifugation (3,000g,10 min). At last, an equal amount of chloroform was added to the aqueous phase and a centrifugation (3,000g, 10 min) was followed. The DNA was precipitated by adding 100% ethanol and 3 M sodium acetate solution to the aqueous layer and incubated on ice for 30 min. After that, the mixture was centrifuged (13,000g, 15 min, 4°C). The supernatant was discarded, and the pellet was washed with 70% ethanol and the mixture was centrifuged (13,000g, 5 min). Lastly, the pellet was air-dried, dissolved in distilled water and quantified in NanoDrop 1000 Spectrophotometer (ThermoScientific).

2.3.4. Phage sequencing and annotation

Whole genome library was generated by TruSeq® Nano DNA Library Prep Kit, sequenced in Illumina MiSeq with a 300 bp paired-end sequencing read configuration (Stabvida, Portugal). After processing, reads were trimmed and *de novo* assembled in Geneious Prime. The revolved

genome was analysed in PhageTerm[70], and annotated with MyRAST[71], that does automatic *in silico* annotation of genomes, and was used for CDS prediction. Protein encoding-genes homology detection and secondary structure prediction was performed with BLASTP[72] (searches for similarity regions between the biological sequence and the sequence databases and calculates statistical significance) and HHpred[73] (detects homologies and is able to predict protein functions and structures, that was used for protein function prediction), while transfer RNAs (tRNAs) were scanned using tRNAscan-SE v2.0[74] (searches for tRNA and shows their position). The DNA homology comparisons between phages was performed with BLASTN and visualized in EasyFig.

Due to publication purposes, the complete genome sequence of phage 3043 has been deposited on the NCBI database under the accession number MZ593174.

2.4. Cloning and expression of capsular depolymerase genes in *E. coli*

2.4.1. Cloning

CPS depolymerase genes were identified in the phages' genomes by the presence of the "*pectate_lyase_3*" domain (PF12708). One gene was selected for each phage. Genes were cloned into pET28a vectors using two strategies. Genes of phages B1, B9, P2, F70, 3073 and 3082 were directly synthetized in GenScript and cloned in the plasmids. Genes of phages 3042, 3043 and 3060 were amplified from the genomic DNA using the following primers **(Table 5)** and PCR reaction: 1x Green HF buffer, 10 mM dNTP Mix (200 μM each), 0.5 μM each of forward and reverse primers, 1 U Phusion DNA polymerase (Thermo Scientific), DNA template (1 to 10 ng) and distilled water up to 50 μL. The DNA thermal cycler was programed for a PCR reaction of 35 cycles covering: 98°C for 30 sec (initial denaturation step), 98°C for 10 sec (DNA denaturation step), 60°C for 20 sec (primer annealing step), 72°C for 45 sec (extension step), followed by 72°C for 5 min (final extension step).

Table 5. List of primers used to amplify the desired CPS depolymerase genes. Restriction enzymes and main characteristics are specified.

Target tailspike	Primer (5' - 3')	Restriction Enzymes	T (ºC)	Amplicon size (bp)
3042	FW: GGGGGATCCCAATCAACAATTGCTAATAATGTTAATAATCC	BamHI	61	677
	RV: GGGCTCGAGCTATGTTGGGGTAATAGTGGTT	XhoI	61	
3043	FW: GGGGGATCCCAGGAAGTACGTTCGGC	BamHI	63	596
	RV: GGGCTCGAGTTAACTCGGTGTAAGTGTAGTACC	XhoI	63	
3060	FW: GGGGGATCCAAAGGTACATTATTTACAGTGGATTGTA	BamHI	61	821
	RV: GGGCTCGAGTTAAATAATTTTAACTGTTAGGATTGTGGATG	XhoI	61	

The amplicons were subjected to electrophoresis at 90V for 40 min in a 1% agarose gel in TAE buffer (1x), stained with Green Safe Premium (NZYtech), and observed through UV illumination using ChemiDocTM (Bio-Rad).

After, the PCR products were cleaned with the kit DNA Clean & Concentrator ™-5 (Zymo Research) and quantified in NanoDrop 1000 Spectrophotometer (ThermoScientific). Simultaneously, the plasmid pET28a was extracted, after overnight growth of *E. coli* Top10 (Novagen) in LB supplemented with kanamycin (50 μg/mL) at 37°C, through the kit NucleoSpin® Plasmid (Macherey-Nagel) and quantified in NanoDrop 1000 Spectrophotometer (ThermoScientific).

For the cloning, both PCR products and the plasmid were digested using restriction enzymes, that produce compatible sticky ends. The digestion reaction was the following: approximately 1000 to 1500 ng of DNA, 1 μL of both restriction enzymes BamHI and XhoI (Thermo Scientific), 1x of Fast Digest buffer (10x) and distilled water up to 20 μL. After 2h of incubation at 37°C, the enzymes were inactivated for 5 minutes at 80°C and the digested vector and insert were cleaned (kit DNA Clean & Concentrator ™-5 (Zymo Research)). Next, the insert and the vector were ligated overnight at 22°C using approximately 50-100 ng of plasmid, around 300 ng of insert following 7:1 (insert/vector) molar ratio, 2.5 U T4 DNA Ligase (Thermo Scientific), 1x T4 Ligase buffer (10x) and distilled water up to 20 μL. Afterwards, the T4 Ligase was inactivated at 70°C for 5 min. Sometimes, to increase the efficiency of the cloning step, additional steps were added to the protocol. The background of the ligation mixture was cut with the restriction enzyme SacI for 1 h at 37°C with the following reaction: 3 μL Fast Digest buffer (10x) and 1.5 μL of SacI (Thermo

Scientific). Next, a dialysis was performed for 30 min, in order to decrease any salts and impurities that could be present in the reaction.

2.4.2. Electroporation

The ligation mixture was transformed into electrocompetent *E. coli* cells (**Table 3**). Overnight cultures were 100–fold diluted in 100 mL of LB media and grown at 37°C until an optical density ($OD_{620\ nm}$) of around 0.35. Afterwards, the culture was successively centrifuged (4,000g, 4°C, 5 min) and resuspended in 40 mL, 20 mL and 10 mL of ice-cold 10% glycerol. The final centrifugation was made and the culture was resuspended in 500 µL of ice-cold 10% glycerol and the mixture was distributed into eppendorf tubes containing 80 µL of electrocompetent cells. Lastly, the cells were stored at -80°C.

The electroporation was then performed at 1.8 kV using 80 µL of thawed electrocompetent *E. coli* cells and 2 µL of ligation mixture. After the shock, 300 µL of Super Optimal Broth with Catabolite repression (SOC) medium was immediately added to the mixture and the cells were incubated at 37°C for 1 h. After the incubation, the cells were plated onto LB agar plates supplemented with kanamycin (50 µg/mL) and incubated at 37°C overnight.

2.4.3. Colony PCR

The next day, around 10 colonies were picked randomly to screen the recombinant plasmid with Colony PCR using T7 forward and reverse primers. First, colonies were grown in 20 µL of LB supplemented with kanamycin (50 µg/mL) for 1 h at 37°C before the reaction. The PCR amplification mixture and concentrations were the following: 3 µL of Xpert Fast MasterMix, 0.5 µM each of forward and reverse T7 primers (10 µM), 1 µL of the grown colonies as DNA template (1 to 10 ng) and distilled water up to 6 µL. The DNA thermal cycler was programed for a PCR reaction of 35 cycles covering: 95°C for 5 min (initial denaturation step), 95°C for 20 sec (DNA denaturation step), 49°C for 20 sec (primer annealing step), 72°C for 45 sec (extension step), followed by 72°C for 5 min (final extension step).

The amplicons were subjected to electrophoresis at 100V for 1 h in a 1% agarose gel in TAE buffer (1x), stained with Green Safe Premium (NZYtech), and observed through UV illumination using ChemiDocTM (Bio-Rad).

Afterwards, the plasmids were extracted using the kit NucleoSpin® Plasmid (Macherey-Nagel) and confirmed by Sanger sequencing (Stabvida).

2.4.4. Expression and purification

E. coli BL21 (DE3) or C43 (DE3) cells were first made electrocompetent and transformed with the plasmids harboring the depolymerases, as mentioned above. Overnight cultures were incubated at 37°C in 50 mL of LB medium supplemented with kanamycin (50 μg/mL) and were grown until mid-log phase ($OD_{620\ nm}$ of around 0.5-0.6). Protein expression was induced with the addition of Isopropyl-β-D-thiogalactopyranoside (IPTG, 0.5 mM, Fisher Scientific) at 21°C for 18 h. Afterwards, 10 mL of lysis buffer (1x, 100 mM sodium chloride, pH 7.4, 4 mM monosodium phosphate) was added and the cells were freeze-thawed 3 times (-80°C to 37°C) and further disrupted by sonication (Cole-Parmer, Ultrasonic Processors) for 5 cycles (30 sec pulse, 30 sec pause). Lastly, the insoluble cells were removed by centrifugation (9,500g, 15 min) and the supernatant was collected and filtered by 0.22 μm filters (Whatman™).

Proteins were purified using gravity chromatography columns containing Ni^{2+}-NTA resins (Thermo Scientific) through equilibrium and wash steps (25 mM of imidazole), followed by elution of the desired enzymes (250 mM of imidazole).

The purification levels were observed in a sodium dodecyl sulfate polyacrylamide gel electrophoresis (SDS-PAGE) gels using the Bio-Rad system under denaturation conditions. To perform the electrophoresis, a 4% of upper stacking and 12.5% of resolving acrylamide gels were prepared. Then, 10 μL of every sample was added to 10 μL of Blue Loading buffer Pack (2x, New England Biolabs), boiled at 95°C for 5 min and loaded onto the gels. The bands were then separated at 140V for 90 min. Subsequently, the gels were rinsed with water and stained with BlueSafe (NZYTech).

Next, samples were concentrated using Amicon® Ultra Centrifugal Filters (10 kDa cut-off), following the manufacture instructions. Proteins were quantified using the Nanodrop NanoDrop 1000 Spectrophotometer (ThermoScientific; 1 Abs= 1mg/mL), following the **Equation 1**.

(Equation 1) $$\text{Concentration} = \frac{\text{Absorbance}}{\text{Molar attenuation coefficient}} * \frac{1.000.000}{\text{Molecular mass}}$$

Regarding **Equation 1**, the concentration of the proteins is in μM and the molecular mass should be in g/L. Information regarding the molar attenuation coefficient and the molecular masses of the CPS depolymerases are presented in **Table A8**.

2.5. Functional analysis of the capsular depolymerases

2.5.1. Activity spectra

To identify the capsular activity of the phages and cognate recombinant depolymerases, the spot-on-lawn method was used against a panel of 30 different *A. baumannii* K types (K1-3, K7, K9, K11, K14, K15, K19, K22, K30, K32, K33, K35, K37, K38, K40, K43-49, K57, K67, K73, K83-K95). First, lawns of each strain were formed by spreading mid-log phase bacteria in TSA soft agar overlays plates (TSB with 0.6% agar). After drying, 5 μL of the phage (10^8 PFU/mL) or purified enzymes (1 μM) were spotted on the plates and incubated at 37°C overnight. Afterwards, the presence of activity was measured when clear or opaque double halo was formed on the bacterial lawn.

2.5.2. Circular dichroism

The secondary structure of the CPS depolymerases and their melting temperature (T_m) were assessed with circular dichroism in the far-UV region using a Jasco J-1500 circular dichroism spectrometer, equipped with a water-cooled Peltier unit.

The spectra were made using enzymes in 10 mM potassium phosphate buffer (pH 7) between 2 and 5 μM, and using a wavelength from 190 to 250 nm, with 1 nm steps, scanning speed of 50 nm/min, high sensitivity and 16 sec response time. Two consecutive scans were recorded from each sample. The spectrum of the potassium phosphate buffer was used for baseline correction.

Next, T_m were obtained by increasing the protein temperature (1°C per minute from 25 up to 100°C) and monitoring the change in ellipticity of the protein's secondary structure at 217 nm. T_m was plotted as a function of temperature and fitted in Boltzmann sigmoidal function.

2.5.3. Degradation of exopolysaccharides

To further characterize the CPS depolymerase activity, EPS was extracted, digested with the enzymes and analyzed using the 3,5-dinitrosalicylic acid (DNS) test.[57]

The EPS extraction method followed a previously described protocol.[75] Each *Acinetobacter* spp. host strain was grown on 20 thick TSA plates at 37°C for 5 days. Then, cells were harvested by scraping the biomass with 2.5 mL of 0.9% (w/v) NaCl per plate. The suspension was incubated with 5% phenol and agitated with a stir bar for 6 h. Subsequently, the suspension was centrifuged (10,000g, 10 min) and the supernatant, containing the desired EPS, was precipitated with 3 volumes of 95% ethanol overnight at -20°C. The next day, the precipitate was centrifuged (10,000g, 10 min) and suspended in distilled water. Afterwards, the samples were lyophilized.

After the extraction of EPS, 5 mg/mL dissolved in 1 mL of PBS buffer (137 mM sodium chloride, 2.7 mM potassium chloride, 10 mM disodium phosphate, 1.8 mM monopotassium phosphate) were incubated with 1 μM of enzyme or PBS buffer at 37°C for 1 h. The reaction was stopped by heat inactivation at 100°C for 15 min. The mixture was centrifuged (8,000g, 2 min) and the supernatant was added to an equal volume of DNS reagent (10 mg/mL). After, samples were incubated at 100°C for 5 min. Lastly, the absorbance was measured at 535 nm. The experiments were repeated three times.

Additionally, the temperature effect on 3043 CPS depolymerase activity was assessed. EPS was incubated with 1 μM of enzyme or PBS buffer for 1 h at different temperatures (20°C, 30°C, 50°C, 70°C and 90°C). The enzyme was inactivated, and DNS reagent (10 mg/mL) was added. The absorbance was measured at 535 nm. The experiments were repeated three times.

2.5.4. Phage adsorption

Phage adsorption test was performed to identify the bacterial capsules as the phages receptors, as previously described.[34] Overnight cultures grown at 37°C in TSB were diluted to approximately 10^8 colony forming units (CFUs)/mL and incubated with PBS (control) or with the CPS depolymerases (1 μM) to remove the capsule. After 1 h of incubation at 37°C, the cells were incubated with 10^5 PFU/mL of the phage for 5 min at 37°C. Phage was then quantified in the mixture and in the supernatant after centrifugation (10,000g, 1 min). Phage concentrations were determined in bacterial lawns containing the host strain prepared in TSA soft agar overlays plates. The degree of adsorption was calculated by measuring the relative amount of adsorbed or reversibly

adsorbed phages in the supernatants in comparison with total phage titer. The experiments were performed in triplicate and repeated three times.

2.5.5. CPS depolymerase antibiofilm activity

Biofilms were formed on 96-well polystyrene microtiter plates using established protocols.[76] Briefly, *A. baumannii* Ab45 strain (K38) was grown in TSB for 16 h at 37°C and 120 rpm. Each well was inoculated with 200 μL of bacterial suspension and the microtiter plates were incubated for 24 h at 37°C and 120 rpm.

Minimum inhibitory concentration (MIC) detections were performed using microdilution method in Mueller-Hinton broth (MHB). After finding the different MICs for the antibiotics ciprofloxacin, tetracycline and gentamicin against the Ab45 strain (K38), two different concentrations of each antibiotic were tested alongside with 3043 CPS depolymerase, in order to find if there was a synergetic effect of one of the antibiotics with the enzyme.

After biofilm formation, the medium was removed and washed with fresh TSB medium. Afterwards, 200 μL of fresh TSB and the diverse treatments were added to each well. Different treatments were tested, namely, the MIC of each antibiotic (100 μg/mL) with and without the enzyme (at 1 μM), 5MIC of each antibiotic (100 μg/mL) with and without the enzyme (at 1 μM and 5 μM), only the enzyme at 1 μM and 5 μM, and SM buffer (100 mM sodium chloride, 10 mM magnesium sulphate, 50 mM Tris-HCl, pH 7.5, control). The microtiter plates were incubated for 6 and 24 h at 37°C and 120 rpm.

After 6 and 24 h of incubation, the CFUs were evaluated. After the removal of the medium presented in the plates, the wells were washed with 0.9% NaCl. Then, 200 μL of 0.9% NaCl was added to each well. After that, the biofilms were scraped off, and samples were collected and diluted in 0.9% NaCl. Lastly, 10 μL of each dilution was placed on a Petri dish and allowed to run down the plate, in order to obtain single colonies. CFU counts were carried out after overnight incubation at 37°C.

2.5.6. CPS depolymerase activity in planktonic cultures

A. baumannii Ab45 strain (K38) was grown in TSB for 16 h at 37°C and 120 rpm. Then, the culture was 50-fold diluted in 20 mL of TSB and grown at 37°C and 120 rpm until an optical density ($DO_{600\ nm}$) of 0.4 was obtained. After that, a sample was retrieved for later determination of

the CFU counts and 800 μL of the bacterial suspension was mixed with several treatment conditions. The different conditions tested were 0.5MIC of ciprofloxacin, tetracycline or gentamycin (100 μg/mL) with or without the 3043 enzyme (at 1 μM), only the enzyme at 1 μM, and SM buffer (control). The suspensions were incubated at 37°C and 120 rpm. CFU counts were determined after 4 and 24 h of incubation. Unlike the biofilm assays, the CFU counts were evaluated by retrieving samples of the suspension and following the same procedure described above.[76]

2.5.7. CPS depolymerase anti-virulence activity

The anti-virulence activity of the CPS depolymerases was assessed using a human serum model, as previously described.[30] First, human blood was collected from healthy subjects and centrifuged (12,000g, 15 min) to collect sera.

Next, *A. baumannii* mid-exponential phase cultures were diluted to around 10^4 CFU/mL. Then, two reactions were prepared, a control and a test, with 30 μL of serum, 10 μL of cells and 1-5 μL of enzyme (1 μM) or PBS buffer. These reactions were incubated at 37°C for 1 h. Subsequently, the reactions were serial diluted in 0.9% NaCl and CFUs were counted by spotting 10 μL on TSA plates. Similar samples supplemented with decomplemented serum (at 56°C for 30 min) were used as controls.

CHAPTER III

Results and Discussion

3.1. Characterization of *A. baumannii*

To describe the epidemiology of multidrug-resistant *A. baumannii* strains, a retrospective analysis of carbapenem-resistant isolates from 2005 and 2012 in the Northern region of Portugal was performed (**Figure 6**). The DNA of all clinical isolates was extracted, and their resistance genes were amplified by PCR. *Acinetobacter* spp. is known to have a wide range of resistance genes, that diverge from strain to strain. The *oxa-51* gene is specific to the *A. baumannii* chromosome, being present in most strains, consequently considered as a landmark in the identification of the species.[24,68] Usually, about 94-100% of *A. baumannii* strains are *oxa-51* positive.[23,68,77,78]

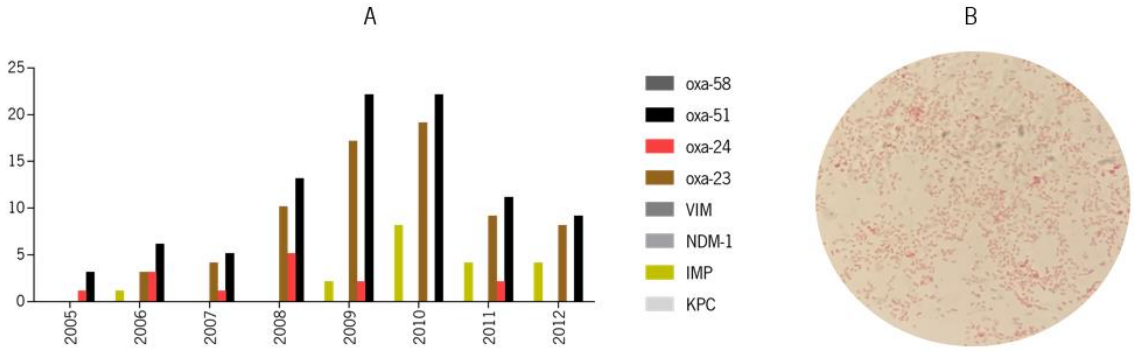

Figure 6. **Characterization of *A. baumannii* clinical isolates**. Prevalence of resistance genes over time (between 2005 and 2012) (**A**) and coccobacillus bacterial morphology using gram staining (**B**).

The results show that the *oxa-51* and *oxa-23* genes were found throughout the years, while *oxa-24* gene was found in most years, except for 2010 and 2012, and *Imp-like* gene was found in 2006 and from 2009 to 2012 (**Figure 6.A.**). *Oxa-51* was the prevalent gene (96% of the isolates) (**Figure 6.A.**). The fact that this intrinsic gene was absent in 3 clinical isolates suggests that these isolates possibly belong to another species within the *Acinetobacter* genus.[68] Since species from the ACB complex are difficult to distinguish, they are usually mistaken for *A. baumannii*. Nevertheless, without a more specific analysis to confirm this suspicion, they were still considered in this study, since they possess clinically relevant genes (other *oxa*-genes) that are most likely to be responsible for the carbapenem resistances. In these situations, the typical *A. baumannii* coccobacillus gram-negative morphology was confirmed under gram staining (**Figure 6.B.**).

Besides the intrinsic gene, *oxa-23*, *Imp-like* and *oxa-24* genes can be found following an order of decreased prevalence. *Oxa-23* gene was found in 76% of the isolates, while *Imp-like* gene was found in 20% and *oxa-24* gene was found in 16% of the cases. The *Imp-like* gene was found in a similar percentage previously described, alongside with the *oxa-24* gene. *Vim-like*, *Pdm1-like* and *KPC* genes were not found within the isolates. Contrary to previous studies, the *oxa-58* gene was also absent within the isolates. However, this could be due to the presence of other carbapenemase genes in the chosen sampling. It should be noted that the referenced percentages regarding the prevalence of the resistance genes have changed throughout the years and diverge from region to region. In the Mediterranean countries, between 1999 and 2009, the predominant gene was the *oxa-58*, and it transitioned to the *oxa-23* gene since 2009.[77]

In previous studies, *oxa-23* was found to be the dominant resistance gene in *A. baumannii* clinical isolates.[23] It is recurring to find this gene presented in several clinical isolates recovered from all over the world (Saudi Arabia, Turkey, Kuwait, Thailand and India), ranging from 49%-100%.[23,77–80] This prevalence can be explained by the easy spread of the *oxa-23* gene via transposons and conjugative plasmids.[77] On the contrary, the absence of *Imp-like*, *Ndm-1-like*, *KPC* and *Vim-like* genes is common among clinical isolates.[23,78] However, in some studies, *Imp-like* gene was found in 13-15% of the clinical isolates recovered in Kuwait, while *Vim-like* gene has been found in 4% of the isolates recovered from a lake in Brazil.[78,81] Also, in one study, *Ndm-1-like* gene was found in 21% of the clinical isolates in India.[80] The *oxa-58* gene is frequently found in around 1-15% of the strains and *oxa-24* gene is usually in 0-13% of the isolates.[77–80]

Overall, the results from this study are in line with previous reports. Regarding the oxa-enzymes, only oxa-58 was absent from the sampling, while oxa-51, oxa-23 and oxa-24 were uncovered following an order of decreased prevalence. Concerning the MBLs, only *Imp-like* was found in the sampling. These results are according to the expectations set by previous studies.

In epidemiologic studies, co-occurences of carbapenemase genes have been found.[82] In this study, *oxa-51* - *oxa23* was the most recurring co-occurrence (55%), followed by *oxa-51* – *oxa-23* – *Imp-like* (18%), *oxa-51* – *oxa-24* (10%) and *oxa-51* – *oxa-24* – *Imp-like* (3%). Also, one incidence of *oxa-23* – *oxa-24* was found. These co-occurrences can exist due to the presence of different genes in the same strain, or due to the presence of polyclonal populations of *A. baumanii* from the same isolate.[82]

For further insight of the clinical isolates, cells were analyzed by optical microscopy (**Figure 6.B.**). The results show coccobacillus gram-negative bacteria, which is the expected and most common morphology within the *Acinetobacter* genus.

Regarding the assessment of the prevalence of the K types among these clinical isolates, according to the isolation date and antibiotic resistances, 25 isolates were chosen to be whole-genome sequenced. Samples were sent to Charles Franz at the Max Rubner-Institut in Germany for Next-Generation Sequencing. This would allow the first epidemiological study of the most prevalent K types needed to strategically isolate the corresponding CPS depolymerases, performing as an alternative treatment of *A. baumannii* infections. Unfortunately, the Next-Generation Sequencing results did not arrive during the period of this thesis. Therefore, the assessment of the most prevalent *A. baumannii* K types in these clinical isolates shall be done in the near future.

3.2. Characterization of *A. baumannii* – infecting phages

Phages B1, B3, B9, P1, P2, F70, 3042, 3043, 3060, 3073 and 3082 were isolated prior to this work with bacterial strains of *Acinetobacter* spp. from sewage and environmental samples using an enrichment procedure.[83] Additionally, phages B1, B3, B9, P1 and P2 were characterized formerly.[30,33,34] All these phages were selected to be further characterized for their ability to produce phage plaques surrounded by hazy haloes, hallmark of viruses encoding CPS depolymerases.

3.2.1. Lytic spectra

To identify the CPS depolymerase activity of the phages B1, B3, B9, P1, P2, F70, 3042, 3043, 3060, 3073 and 3082, the spot-on-lawn method was used against a panel of 30 different *A. baumannii* K types. The phages lytic spectra can be consulted in **Table 6**. Results demonstrate that phages P1, B3, B1, B9, 3073, 3042/3043, F70, P2, 3082 and 3073 infected K1, K3/K19, K9, K30/K45, K32, K38, K44, K67, K84 and K85 *A. baumannii* K types respectively.

Table 6. Phages host range of activity. 11 phages were tested against a panel of 30 different *A. baumannii* K types. "+" means activity and "-" means absence of activity.

K type	*Acinetobacter* spp. strains	Phages with CPS depolymerase										
		B1	**B3**	**B9**	**P1**	**P2**	**F70**	**3042**	**3043**	**3060**	**3073**	**3082**
K1	NIPH 290	-	-	-	+	-	-	-	-	-	-	-
K2	NIPH 2061	-	+	-	-	-	-	-	-	-	-	-
K3	NIPH 501	-	-	-	-	-	-	-	-	-	-	-
K7	H202	-	-	-	-	-	-	-	-	-	-	-
K9	NIPH 528	+	-	-	-	-	-	-	-	-	-	-
K11	J9	-	-	-	-	-	-	-	-	-	-	-
K14	Ab 87	-	-	-	-	-	-	-	-	-	-	-
K15	A85	-	-	-	-	-	-	-	-	-	-	-
K19	RBH2	-	+	-	-	-	-	-	-	-	-	-
K22	Ab 93	-	-	-	-	-	-	-	-	-	-	-
K30	NIPH 190	-	-	+	-	-	-	-	-	-	-	-
K32	Ab 49	-	-	-	-	-	-	-	-	-	+	-
K33	NIPH 67	-	-	-	-	-	-	-	-	-	-	-
K35	LUH5535	-	-	-	-	-	-	-	-	-	-	-
K37	NIPH 146	-	-	-	-	-	-	-	-	-	-	-
K38	Ab 45	-	-	-	-	-	-	+	+	-	-	-
K40	ANC 4097	-	-	-	-	-	-	-	-	-	-	-
K43	NIPH 60	-	-	-	-	-	-	-	-	-	-	-
K44	NIPH 70	-	-	-	-	-	+	-	-	-	-	-
K45	NIPH 201	-	-	+	-	-	-	-	-	-	-	-
K46	NIPH 329	-	-	-	-	-	-	-	-	-	-	-
K47	NIPH 601	-	-	-	-	-	-	-	-	-	-	-
K48	NIPH 615	-	-	-	-	-	-	-	-	-	-	-
K49	NIPH 1734	-	-	-	-	-	-	-	-	-	-	-
K57	BAL_212	-	-	-	-	-	-	-	-	-	-	-
K67	NIPH 76	-	-	-	-	+	-	-	-	-	-	-
K73	SGHO703	-	-	-	-	-	-	-	-	-	-	-
K83	LUH5538	-	-	-	-	-	-	-	-	-	-	-
K84	Ab 79	-	-	-	-	-	-	-	-	-	-	+
K85	Ab 100	-	-	-	-	-	-	-	-	+	-	-

All phages produced clear plaques surrounded by haloes that increased over time. As mentioned, this indicates the presence of CPS depolymerase (**Figure 7**).[61]

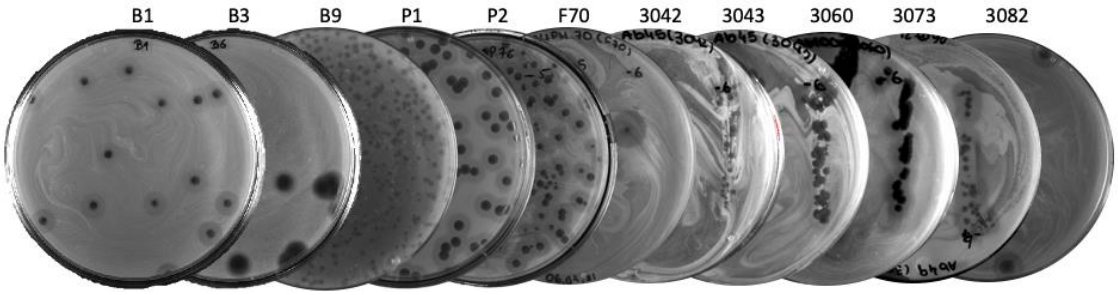

Figure 7. Isolated *Acinetobacter*-infecting phages plaque characteristics. Plaque morphologies of phages B1, B3, B9, P1, P2, F70, 3042, 3043, 3060, 3073 and 3082 on TSB with 1.2% agar plates. The morphologies feature plaques surrounded by a second translucent halo that increases over time.

The formed halo is caused by the action of the CPS depolymerases. The precise mechanism remains unknown. One theory hypothesized that, given the fact that all CPS depolymerases are encoded in structural genes (i.e. are not secreted during infection), the enzyme is released due to an overproduction of the CPS depolymerases during the phage lytic cycle, that was not assembled into the phage particle, or a free CPS depolymerase domain resulting of the synthesis of an alternative codon.[31] This would make a free enzyme able to diffuse through the agar more rapidly than the phage.[63]

Phages P1, B1 and P2 infect only one *A. baumannii* K type (K1, K9 and K67) and phages B3 and B9 infect two *A. baumannii* K types (K2/K19 and K30/K45). Phages 3073, 3082 and 3060 also infect only one *A. baumannii* K type (K32, K84 and K85), while phages 3042 and 3043 share an equal spectrum of activity, lysing one *A. baumannii* K type (K38).

In summary, these 11 phages recognize 12 *A. baumannii* different K types (K1-2, K9, K19, K30, K32, K38, K44-45, K67 and K84-85). A very narrow host range was observed, as previously observed by other phages carrying CPS depolymerases.[30,33,34,57,61,62,84]

3.2.2. Phage sequencing and annotation

The genomes of phages F70, 3042, 3043, 3060, 3073 and 3082 were sequenced, annotated (**Annex II**) and screened in order to find the CPS depolymerase enzymes. The phages linear genomes ranged from 40,593 to 44,851-bp in size, containing between 48 and 84 Open Reading Frames (ORFs). ORFs were encoded in the same DNA strand.

Interestingly, phages were highly similar, sharing substantial nucleotide identity (80%) and (>85%) genes among each other (**Figure 8**) and with several other *Acinetobacter* phages, such as vB_AbaP_APK128 (MW459163) and vB_AbaP_APK116 (MN807295), that belong to the *Autographiviridae* family and *Friunavirus* genus. Intriguingly, all genomes were highly similar, but varying the region encoding the tailspike genes. This information confirms previous observations that *Friunavirus* have evolved to maintain their genetic structure but varying the C-terminal of the tailspike genes encoding CPS depolymerases to be able to modulate its host range. The ability of the CPS depolymerases to recognize the host receptors has been previously reported.[30,33,34,85,86]

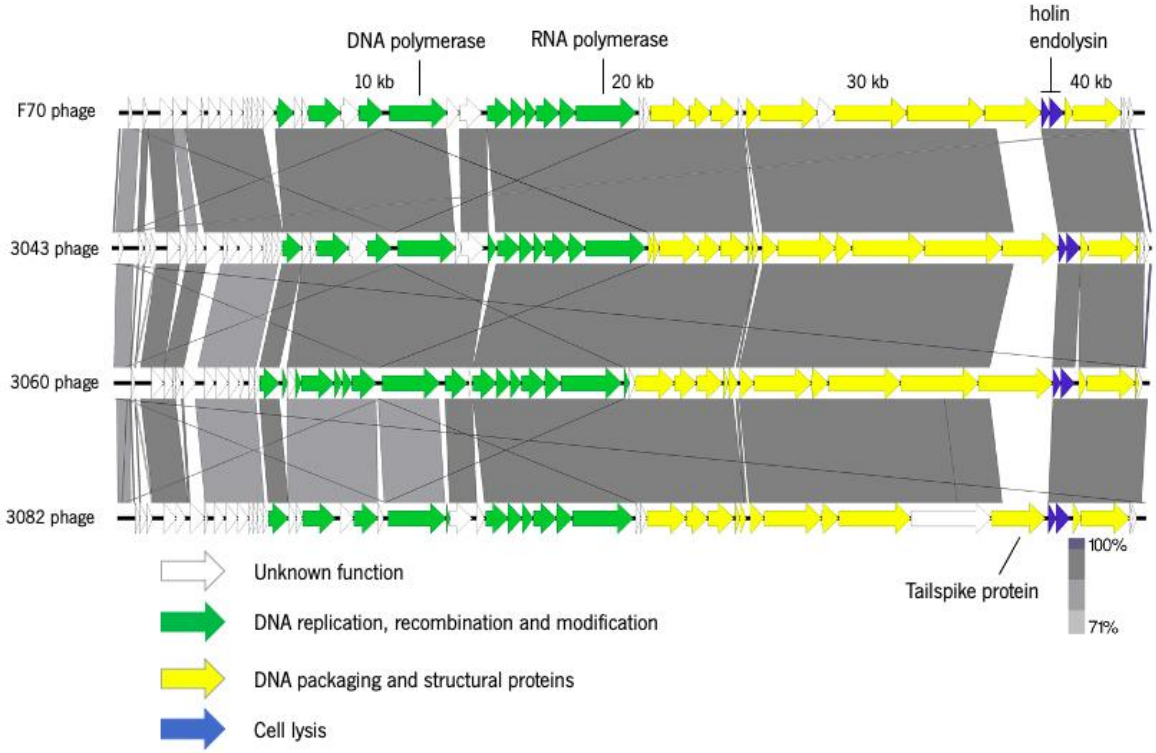

Figure 8. Genomic map of phages F70, 3043, 3060 and 3082. The predicted proteins are colored according to their function.

3.2.3. *In silico* uncovering of CPS depolymerase genes

CPS depolymerases belonging to phages B1, B3, B9, P1 and P2 were screened prior to this work.[30,33,34] In this study, it was possible to identify additional CPS depolymerases in newly isolated phage genomes: F70gp41, 3042gp48, 3043gp46, 3060gp42, 3073gp72 and 3082gp44. They are all present at the phage tailspikes. All had a N-terminal anchor domain and a center depolymerase domain (pectate_lyase_3) identified (**Figure 9**). This domain is envisaged to degrade the bacterial CPS and has been associated with β-helix enzymes with CPS depolymerase activity.[33,64,87,88] These domains have been found in many other *Acinetobacter* phage taispikes. However, sometimes, an additional C-terminal chaperone can be identified.[89]

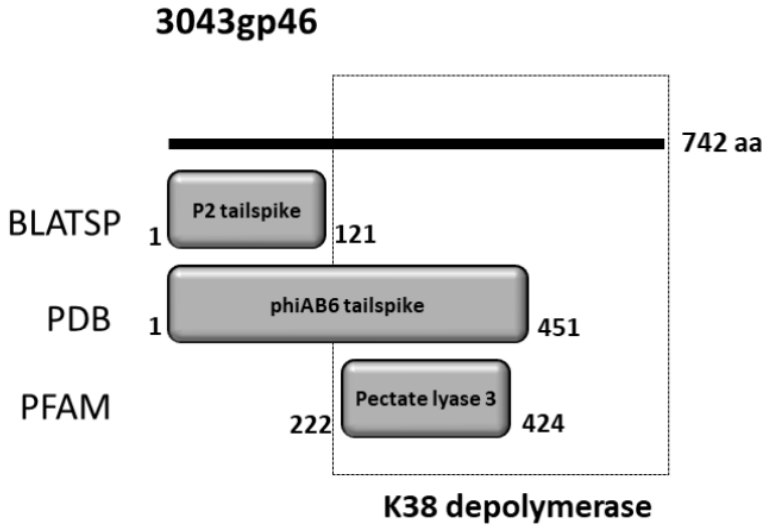

Figure 9. 3043 CPS depolymerase schematic representation. Bioinformatics analysis of 3043 tailspike gene (gp46), with a CPS depolymerase region identified and a C-terminal "pectate_lyase_3" domain, inferred by HHpred. Adapted from Domingues et al. (2021).[90]

BLASTP search demonstrated moderate homology (E-value<1^{-68} and >52% identity) between F70, 3043, 3060 and 3082 CPS depolymerases and other tailspike proteins from *Acinetobacter* phages APK44 (MN604238), APK32 (MK257722) and APK87 (MN604239). The N-terminal was highly conserved, while the C-terminal and center part was highly variable. The C-terminal part is usually related to the ability of these enzymes to degrade bacterial capsules.[30,61] Similarly, BLASTP search showed a high homology (E-value<4^{-65} and >75% identity) of 3042 and

3073 CPS depolymerase domains with tail fiber proteins from *Acinetobacter* phages IME285 (MH853786) and AP22 (HE806280).

Overall, F70, 3042, 3043, 3060, 3073 and 3082 CPS depolymerases are between 260 and 985 amino-acid proteins with predicted molecular weights ranging 54 and 90 kDa. The CPS tailspike/tail fiber middles and the C-terminal regions were recombinantly expressed in *E. coli*, predicted to encode the CPS depolymerase domain and its putative chaperone.

3.3. Cloning and expression of CPS depolymerase genes in *E. coli*

As mentioned above, F70, 3073 and 3082 CPS depolymerase genes were cloned in GenScript. As for B1, B9 and P2 CPS depolymerase genes, they were previously cloned. These protein-encoding genes were also expressed during the period of this master thesis. As for B3 and P1 CPS depolymerase genes, they were previously cloned and expressed.

E. coli Top10 strain is usually used for a higher success in cloning, while BL21 (DE3) strain is usually used in expressions. At first, 3042, 3043 and 3060 CPS depolymerase genes were amplified by PCR, ligated to pET28a plasmid and cloned directly in *E. coli* BL21(DE3) strain (**Figure 10.A** and **Figure A2**). However, only 3042 and 3043 CPS depolymerases were successfully cloned and expressed.

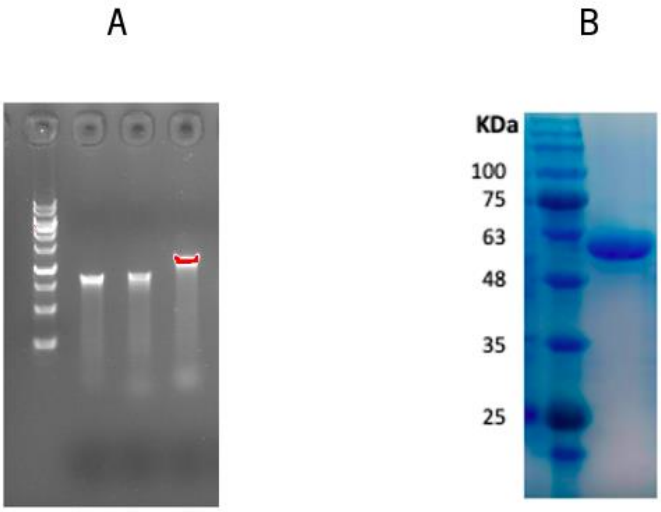

Figure 10. Agarose and SDS-PAGE gels. 1.0% Agarose separation gel of the amplified 3042, 3043 and 3060 CPS depolymerase genes (left to right) using GeneRuler 100 bp DNA ladder (Thermo Scientific) (**A**). 12.5% SDS-PAGE separation gel of the purified 3043 CPS depolymerase using Nzycolour Protein Marker II (NZYTech) (**B**).

Overexpression of protein yielded a soluble protein of 46 μM (for 3042 depolymerase) and 288 μM (for 3043 depolymerase) with 95% purity, as judged by densitometric analysis of SDS-PAGE gels (**Figure 10.B** and **Figure A2**). Molecular masses obtained by electrophoresis met the theoretical value calculated from the protein amino-acid sequence (approximately 55 kDa). 3060 CPS depolymerase gene was first cloned in *E. coli* Top10 strain and later expressed in *E. coli* BL21 (DE3), with a concentration of 34 μM and molecular mass of 85 kDa, as determined by electrophoresis of the polyacrylamide gel (**Figure A2**).

B1, B9, P2, F70, 3073 and 3082 were firstly expressed into *E. coli* BL21 (DE3) strain. However, only B1, B9 and 3073 CPS depolymerases were successfully expressed at first, with concentrations of 109 μM, 103 μM, and 204 μM and molecular masses of 63, 70 and 50kDa, as determined by electrophoresis of the polyacrylamide gel (**Figure A2**). Since the expression in *E. coli* BL21 (DE3) strain was being challenging for the remaining constructions, different *E. coli* strains were used, namely, Origami™ 2 (DE3)pLysS, Origami™ B (DE3) and C43 (DE3). C43 (DE3) strain is usually used for proteins that can be toxic for cells and Origami strains are used to increase disulfide bond formation. P2, F70 and 3082 genes were then successfully expressed in *E. coli* C43 (DE3), resulting in protein yields ranging from 17 μM and 56 μM, and molecular masses of, approximately, 60 and 70 kDa, as determined by electrophoresis of the polyacrylamide gel (**Figure A2**).

3.4. Functional analysis of the CPS depolymerases

3.4.1. Activity spectra

To identify the CPS depolymerases activity spectra, the spot-on-lawn method was used against a panel of 30 different *A. baumannii* K types. Drop tests showed that the enzymes activity spectra matched their parental phage. These results reinforce the idea that CPS depolymerases play a vital role in the recognition of specific host capsular receptors.

This goes in line with other described CPS depolymerases.[30,33,34,57,61,62,84] All CPS depolymerases produced haloes that increased over time on susceptible strains. **Figure A3** presents a visual example of the activity of one CPS depolymerase.

CPS depolymerases 3060 and 3082 did not demonstrate activity against any strain, including the strains susceptible to their parental phage. This could be due to the cloning strategy.

It is important to mention that, for this approach, deletion mutants lacking the N-terminal were created in all CPS depolymerases in order to facilitate solubility and expression. In this case, the selected truncated region of 3060 and 3082 CPS depolymerases might not have included the whole enzymatic part, explaining the lack of activity observed. To confirm that suspicion, it would be necessary to clone the entire gene and assess their lytic activity. Another explanation could be an unsuccessful expression, leading to an inadequate folding of the proteins and a consequent lack of enzymatic activity. Therefore, the optimization of the expression conditions could potentially enhance their activity.

Henceforth, B1, B3, B9, P1, P2, F70, 3042, 3043 and 3073 CPS depolymerases are mentioned as K9, K2/K19, K30/K45, K1, K67, K44, K38-1, K38-2 and K32 depolymerases, respectively.

3.4.2. Circular dichroism

The secondary structure of the CPS depolymerases was assessed with CD spectroscopy. The CD spectra demonstrated negative dichroic minimums around 216-220 nm and positive maximum peaks between 190 nm and 210 nm (**Figure 11**). These CD spectra demonstrate that the proteins are rich β -structures, similar to the secondary content described in other phage CPS depolymerases.[30,64,85,87,88,91–93]

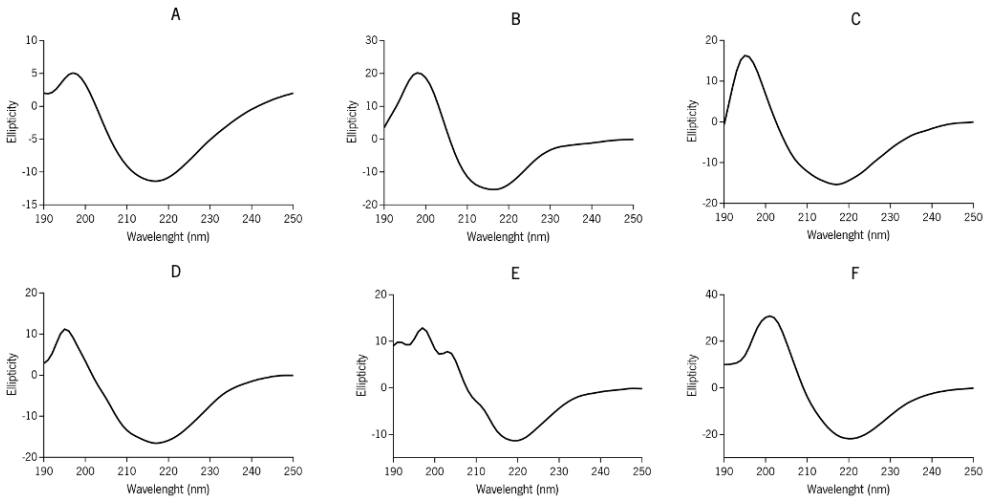

Figure 11. Circular dichroism spectra of CPS depolymerases. CD spectrum of K9 (**A**) K32 (**B**), K38-1 (**C**), K38-2 (**D**), K44 (**E**) and K67 (**F**) depolymerases. Both display a β-sheet structure. Measurements were performed in potassium phosphate at pH 7.

Additionally, the secondary structure stability was measured using the CD, by monitoring transitions in function of temperature (**Table 7** and **Figure A4**).

Table 7. Estimated T_m of CPS depolymerases. Melting temperature curves were performed in potassium phosphate at pH 7, with heating rates 1ºC/min and temperature range from 25ºC to 100 ºC. The wavelengths used in these measurements were selected based on the negative dichroic minimum of their CD spectra (ranging from 216 to 220 nm).

Depolymerase	T_m (ºC)
K9	60
K32	95
K38-1	No structural denaturation
K38-2	85
K44	75
K67	95

All CPS depolymerases demonstrated a very high structural stability, correlating with their ability to remain active at high temperatures. The T_m of these enzymes ranged between 60 and 95ºC. K38-1 depolymerase is a peculiar case, since it did not demonstrate a structure denaturation within the temperature range tested (25-100ºC). The CD equipment could only be used within that range, so it was not possible to determine the T_m of this enzyme. However, it is the CPS depolymerase with the highest melting temperature (above 100ºC) reported until this day.[30,52,85–87,91–95] This thermostability has been described before and it could be related with the evolution of phages to endure in unfavorable conditions and remain infective.[30,52] As reported by other studies and in this thesis, CPS depolymerases are encoded in tailspikes, which are vital phage structural proteins, needed to recognize the host prior to infection. This high-thermal stability is supposed to be determined by the beta-sheet structures that characteristically highly interweave.[54,96]

3.4.3. Degradation of exopolysaccharides

In order to assess the degrading activity of the CPS depolymerases, the EPS of the bacterial hosts were extracted and incubated with the enzymes. Upon incubation, the enzymes are supposed to cleave the EPS, synthetizing reducing sugars in the process. So, a DNS test was performed in

order to quantify the produced sugars, therefore accessing the CPS depolymerases degrading activity.[39] The results are represented in **Figure 12.**

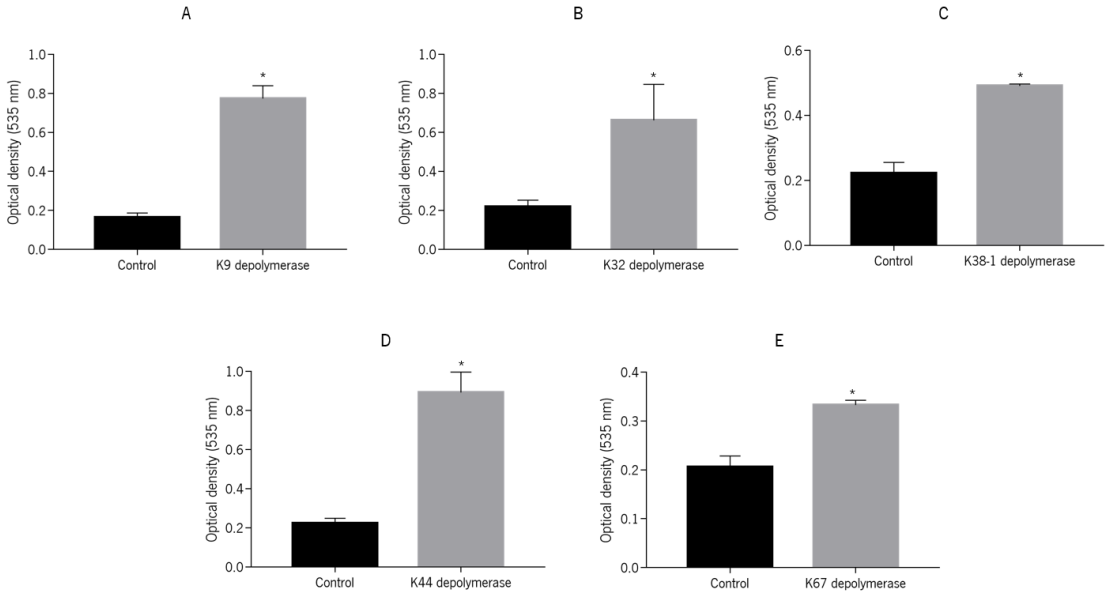

Figure 12. CPS depolymerases degrading activity against the EPS of the bacterial hosts. K9 (**A**), K32 (**B**), K38-1 (**C**), K38-2 (**D**), K44 (**E**) and K67 (**F**) depolymerases degrading activity was assessed using the extracted EPS from the respective *Acinetobacter* strains (K9, K32, K38, K44 and K67). Control assays were performed with PBS buffer. Evaluation was performed by the quantification of reducing ends produced with DNS reagent, measuring the absorbance at 535 nm. Error bars represent standard deviation for three repeated experiments. Significance was determined by a Student *t* test between untreated and treated samples. * Statistically different ($P < 0.01$).

Overall, the control samples (with PBS buffer) displayed lower values compared to the test samples (with CPS depolymerase). $OD_{535\ nm}$ between 0.15±0.02 and 0.22±0.03 for the control samples, against $OD_{535\ nm}$ between 0.33±0.01 and 0.89±0.10 for the test samples (**Figure 12**). Additionally, the results between untreated and treated samples with CPS depolymerase exhibit statistical difference ($P < 0.01$). The increase of the $OD_{535\ nm}$ of EPS incubated with the enzymes demonstrates the presence of reducing sugars, indicating enzymatic degradation.

In short, all CPS depolymerases exhibit degrading activity against the EPS of the respective bacterial hosts. Incubation with the EPS was performed with 1 μM of enzyme. Still, it was possible to observe that some enzymes produced more reducing ends than others (**Figure 12**). K9, K32 and K44 depolymerases displayed higher values compared to K38-2 and K67 depolymerases. This can be associated with the extraction of the EPS, since its success deviates from strain to strain.

So, even though some enzymes seem to have a higher degrading capacity than others, that could be related to the EPS and not to the enzyme's activity.

Temperature effect

As an example, the temperature effect on CPS depolymerase activity was assessed in K38-2 depolymerase. This protein was incubated with EPS at different temperatures (20°C, 30°C, 50°C, 70°C and 90°C). The results are displayed in **Figure 13**.

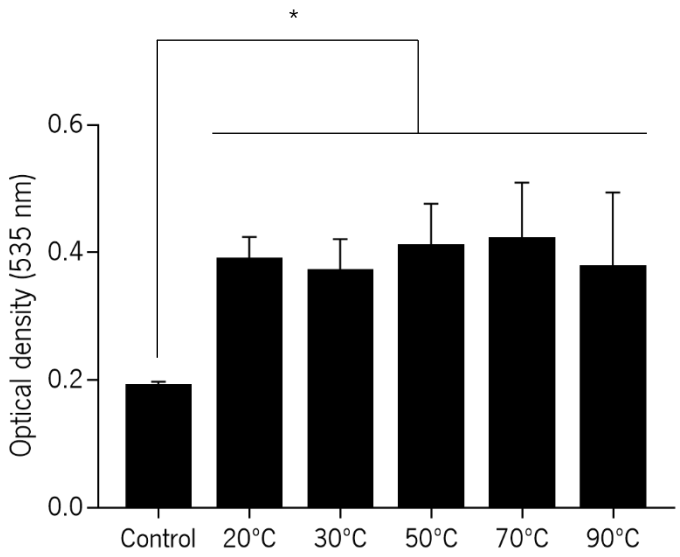

Figure 13. K38-2 depolymerase activity under different temperatures. K38-2 depolymerase degrading activity was assessed using extracted EPS from K38 strain. The activity was analyzed at different temperatures (20°C, 30°C, 50°C, 70°C and 90°C). Control assays were performed with PBS buffer at room temperature. The evaluation was performed by the quantification of reducing ends produced with DNS reagent, measuring the absorbance at 535 nm. Error bars represent standard deviation for three repeated experiments. Significance between control and each tested temperature was determined by Two-way ANOVA and Dunnett's multiple comparisons test. Significance between each tested temperature was determined by One-way ANOVA and Turkey's multiple comparison test. *Statistically different ($P < 0.05$).

The results between the control samples and test samples with K38-2 depolymerase are statistically different ($P < 0.05$), meaning that K38-2 protein remained active in all tested temperatures (**Figure 13**). Also, there was no statistical difference between each tested temperature (**Figure 13**). Therefore, K38-2 depolymerase displayed an optimal temperature

range of 20°C to 90°C. This information correlates with the melting temperature for this protein (T_m = 95°C).

Besides maintaining a secondary structure up to very high temperatures, it was also proved that bellow that temperature, the protein always upholds an optimal activity. These optimal ranges of temperature make these enzymes desirable to be used as a therapeutic option, since they retain their activity through challenging conditions.

3.4.4. Role of CPS depolymerases in phage adsorption

The role of CPS depolymerases in phage adsorption was assessed in order to identify the CPS as the phage receptor. Experiments were conducted using K9, K32, K38, K44 and K67 host cells after incubation with and without the respective CPS depolymerases. Then, phages were added, and the degree of adsorption was calculated by measuring the relative number of adsorbed phages in the supernatants in comparison with total phage titer. The expected results are adsorbed phages when the cells are treated with PBS only, and no adsorption when the cells are treated with the enzymes. Results are displayed in **Figure 14.**

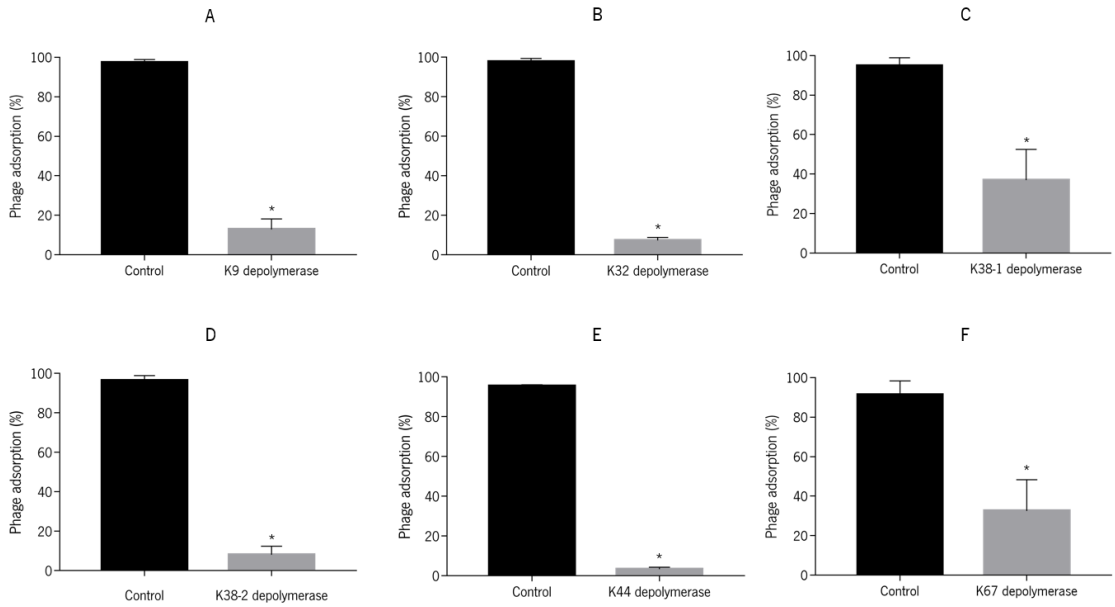

Figure 14. Phage adsorption on *Acinetobacter* host cells. B1 (**A**), 3073 (**B**), 3042 (**C**), 3043 (**D**), F70 (**E**) and P2 (**F**) phage adsorption to the respective K9, K32, K38, K44 and K67 *Acinetobacter* strains after treatment with the corresponding CPS depolymerases was assessed. The results are presented in PFU percentages in comparison with the adsorption of untreated cells. Error bars represent standard deviation for three repeated experiments. Significance was determined by a Student *t* test between untreated and treated samples. * Statistically different ($P < 0.01$).

Overall, for untreated host cells, phage adsorption rates were higher than 91% (**Figure 14**). For CPS depolymerase–treated cells, phage adsorption rates were much lower, decreasing to a range of 3.25%±0.87% and 36.93%±13.93% (**Figure 14**). Results between the control samples and the test samples are statistically different ($P<0.01$).

These results are in line with what was formerly described.[30,33,34,85,86] Like previously clarified, phage adsorption is the initial step of the infection cycle. Phages use tailspike or tail fiber proteins to recognize specific receptors on the bacterial surface and allow phage adsorption to the cells.[30,33,34,50,59,91] As demonstrated by the present results, when bacteria are striped from their capsule, phages carrying CPS depolymerases lose the ability to effectively attach to the cells. Therefore, the results demonstrate that the bacterial capsule is necessary for the adsorption of these phages.

These interactions demonstrate the evolution arms-race between bacteria and phages. Bacteria have evolved to develop a capsule in order to prevent predation from phages.[33,93] However, some phages co-evolved to produce CPS depolymerases that are able to recognize and strip the bacterial capsule.[33,34,91,93] So, these phages not only use CPS as the bacterial receptor for the phage

adsorption, but they are dependent of its recognition and degradation to maintain the ability to infect the bacteria.

Further phage adsorption assays were performed using non-sensitive strains. Results show that CPS depolymerases are not able to infect untreated and CPS depolymerase-treated non-sensitive strains (data not shown). In summary, CPS depolymerases are able to adsorb to the untreated host strains, that possess the CPS, and are not able to effectively infect the host strain when the capsule is removed. Moreover, they are not able to successively adsorb to a non-sensitive strain with or without the CPS as the receptor, proving that phages are only able to adsorb to sensitive strains.

3.4.5. K38-2 CPS depolymerase activity in biofilms and planktonic cultures

A. baumannii possesses the ability to form biofilms.[61,62] Biofilm formation occurs to surpass unfavorable conditions and allow a higher survival rate of bacteria enclosed in the extracellular matrix.[86] Additionally, biofilm communities are surrounded by EPS that act as a barrier to phage penetration.[59] When compared to planktonic cells, biofilms require a higher dosage of antimicrobials in order to disrupt them (higher MIC).[97] Moreover, antibiotics have trouble diffusing through the matrix and exerting their antimicrobial effect.[98] Therefore, the ability of K38-2 depolymerase to support the disruption of 24h-old biofilms alongside different antibiotics was tested under different conditions. Biofilms were formed using K38 strain and treated with K38-2 depolymerase (1 μM and 5 μM) and/or with the antibiotic (MIC or 5 MIC) for 6h and 24h. Additionally, a potential synergetic effect of K38-2 depolymerase (1 μM) and the antibiotic (0.5MIC) on planktonic cells was assessed. The results are displayed in **Figure 15** and **Figure A5**.

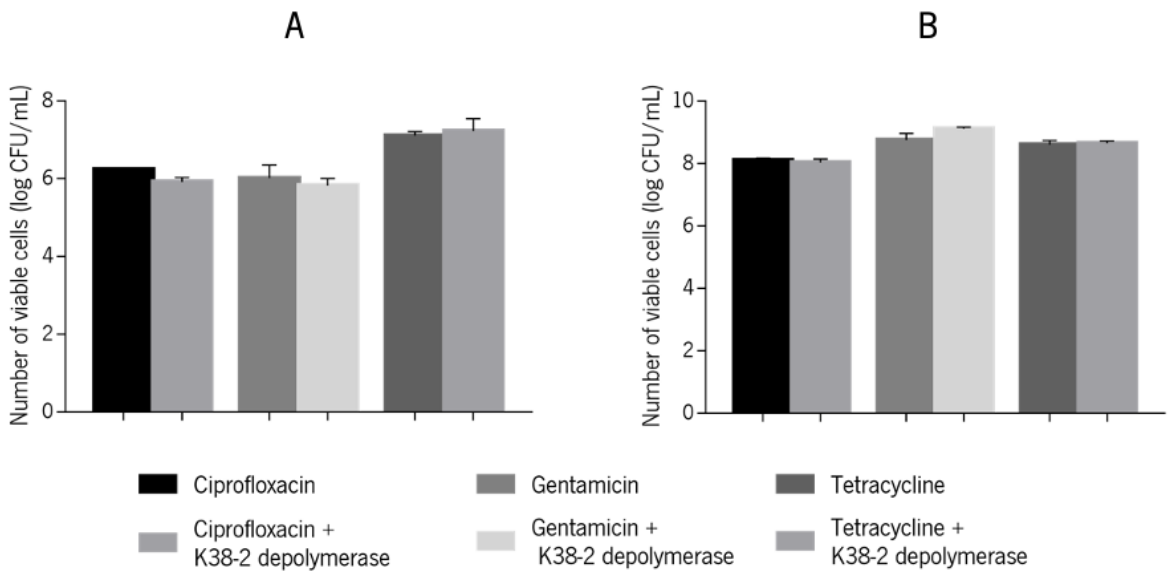

Figure 15. Synergetic effect of K38-2 depolymerase and ciprofloxacin, gentamicin and tetracycline antibiotics on 24h-old biofilm and planktonic cells. Potential 24h-old K38 biofilm disruption was assessed by quantification of viable cells after 24h of infection using 5 μM of K38-2 depolymerase and/or 5MIC of different antibiotics (**A**) Potential synergetic effect of K38-2 depolymerase (1 μM) and antibiotics (0.5MIC) after 24h of infection on K38 planktonic cells (**B**). Error bars represent standard deviation for two repeated experiments. Significance was determined by a Student *t* test between untreated and treated samples. * Statistically different ($P < 0.01$).

As previously proved, CPS depolymerases degrade the EPS of their respective bacterial host. Therefore, it was expected that K38-2 depolymerase would disrupt the K38 biofilm matrix and allow an easier diffusion of the antibiotic, which would kill the cells.[52,85] However, based on the obtained results, a synergetic action between the three tested antibiotics and the CPS depolymerase in the disruption of biofilms was not observed regardless of the concentration of enzyme (1 μM or 5 μM), concentration of antibiotic (MIC or 5MIC) and time of infection (6h and 24h) (**Figure 15.A, Figure A5.A**). Some data is not shown. The lack of disruption of biofilm matrix by K38-2 depolymerase could be related to a low content of EPS, which is strain-dependent.[99] Moreover, the EPS from the biofilm matrix could be different enough from the CPS that the enzyme recognizes and degrades. Then, the lack of activity of K38-2 enzyme would be expected, since it would not be able to recognize the EPS and disrupt the matrix. Furthermore, K38-2 depolymerase could prevent biofilms instead of removing them, since some studies have reported that aptitude.[64,94] Lastly, there are few reports on the effects of CPS depolymerases on biofilms, but some studies have established the efficiency of a recombinant CPS depolymerase in releasing the matrix EPS,

even though synergy with antibiotics is usually not observed.[42,86,94] However, two studies demonstrated that a recombinant CPS depolymerase improved *K. pneumoniae* biofilm sensitivity to gentamicin and polymyxin.[94,100]

After observing no synergetic effect between K38-2 depolymerase and the antibiotics on the disruption of biofilms, a synergetic effect was tested on K38 planktonic cells. K38-2 depolymerase alone does not possess the ability to kill the cells, since it only removes the CPS, leaving the bacteria less virulent. Therefore, only using the enzyme does not reduce the number of viable cells (data not shown). On the other hand, antibiotics have the ability to kill the bacteria, however, bacteria are able to resist to most antibiotics, canceling their therapeutic effect. So, a synergetic effect between CPS depolymerases and antibiotics is desirable. CPS depolymerases leave bacteria less virulent and antibiotics are able to kill the microorganisms more efficiently. However, no synergy was achieved on planktonic cells (**Figure 15.B** and **Figure A5.B**).

3.4.6. CPS depolymerase anti-virulence activity in human serum

The therapeutic effect of the CPS depolymerases was further assessed using a human serum model. These assays were performed in order to assess the anti-virulence activity of these enzymes in combination with the host's immune system. Previously, it has been proven that, when treated with an isolated phage-derived CPS depolymerase in a human serum model, *A. baumannii* became more susceptible to serum killing.[30,34,52,98] Experiments were conducted using K9, K32, K38, K44 and K67 strains incubated with serum and the respective CPS depolymerases or PBS (control). Complement killing was measured in CFUs. Results are displayed in **Figure 16.**

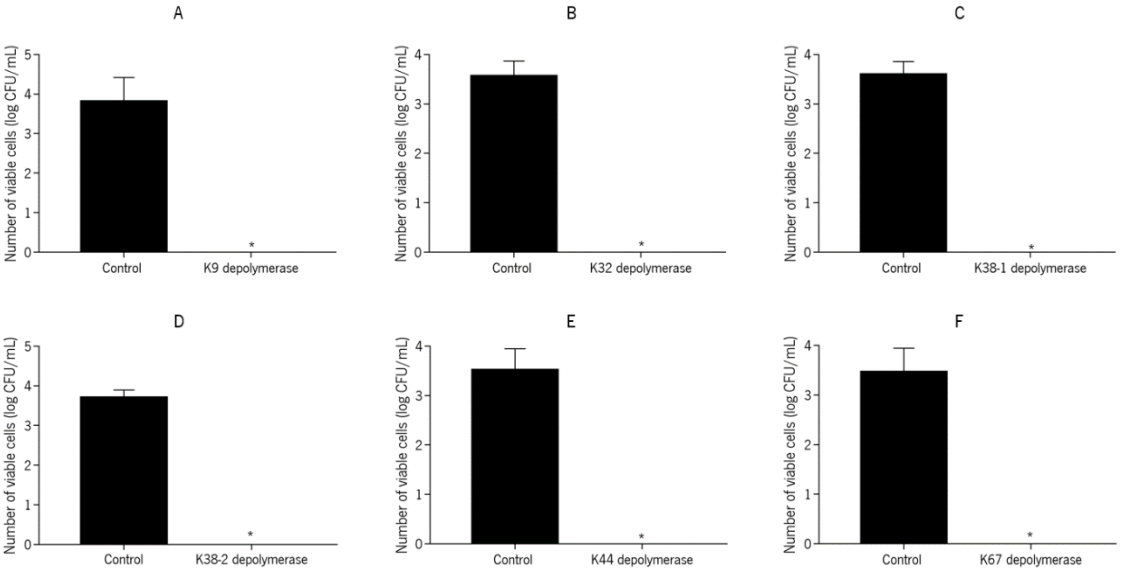

Figure 16. Serum assay on *Acinetobacter* host cells. K9 (**A**), K32 (**B**), K38-1 (**C**), K38-2 (**D**), K44 (**E**) and K67 (**F**) depolymerases anti-virulence activity alongside with the serum complement (collected from healthy human subjects) against the respective K9, K32, K38, K44 and K67 *Acinetobacter* strains was assessed. PBS buffer was used as a control or the enzymes at 1 μM. Error bars represent standard deviation for three repeated experiments. Significance was determined by a Student *t* test between untreated and treated samples. * Statistically different ($P < 0.01$).

Overall, all CPS depolymerases could counterpart the serum's complement killing activity against host cells, that otherwise were resistant (**Figure 16**). The 4-log bacterial load was reduced below detection limit (**Figure 16**). These results are in line with what was previously described. Even though there has not been numerous progress in the dissolution of biofilms and a synergetic effect with antibiotics has not been completely established, these outcomes on human serum are very promising. These results demonstrate that when the enzymes are added to the human serum, they are able to remove the CPS, leaving bacteria less virulent and more susceptible to be easily eliminated by the complement system.

Further serum killing assays were performed in non-sensitive strains. Results demonstrate that CPS depolymerases could not make a non-sensitive strain susceptible to serum killing (data not shown). These results corroborate that CPS depolymerases are only able to affect a very narrow host range and have no anti-virulence effect on non-sensitive strains. Therefore, these enzymes are able to make host cells susceptible to serum killing but are not able to do the same with a non-sensitive strain. Additionally, the same test was performed with heat-inactivated serum together with CPS depolymerase and no antibacterial effect was observed (data not shown). This goes in

line with what was previously explained. Since CPS depolymerases are only able to remove the capsule, and not kill the bacteria, when the serum is inactivated, the cells are still able to survive without the capsule. However, when the serum is intact, they become susceptible to be eliminated, since they become less virulent without their capsule.

In summary, when the serum is active and CPS depolymerase is present, susceptible strains lose their capsule, becoming less virulent and being more easily eliminated by the serum's complement system. CPS depolymerases decapsulate bacteria and the immune system is able to remove the infection.

Phage-derived CPS depolymerases are a very promising therapeutic option since they can complement the serum killing activity and remove the infection. Additionally, these enzymes have been proven to possess the same anti-virulence activity in *in vivo* models.[30] In larvae (*G. mellonella*), it was found that bacteria-infected larvae had a very low survival rate, which decreased throughout the incubation time. In opposition, when bacteria-infected larvae were pre-treated with the enzyme, their survival rates increased considerably with an increasing concentration of CPS depolymerase (up to 100% survival rate). To further evaluate anti-virulence properties of the isolated enzyme, the authors tested it in mice infected with *A. baumannii*. After 20 h post-infection, 90% of the mice survived when treated with depolymerase decreasing to 60% after 42 h post-infection.[30] However, Liu et al. (2019) were able to isolate a CPS depolymerase capable of rescuing 100% of immunocompromised mice infected with *A. baumannii* after 2 h post-infection, while all the untreated immunocompromised mice died within 24 h of infection.[48] Additionally, Wang et al. (2020) were also able to isolate a CPS depolymerase that is able to rescue 100% of mice infected with *A. baumannii*, while untreated mice died within 26 h of infection.[98] In short, all the authors from the papers described above concluded that the CPS depolymerases therapy was effective against *A. baumannii* infections.[26,48,53]

CHAPTER IV

Conclusions and Future perspectives

4.1. General conclusions

Antibiotic resistance is the major mishap in the efficient treatment of *Acinetobacter spp*. infections. Phages have emerged as a new alternative to antimicrobials due to their lytic activity against bacteria. However, there are still many difficulties related to phage therapy. Therefore, phage-derived CPS depolymerases display a great potential in combating *Acinetobacter* infections.

The purpose of this work was to perform an epidemiological study of *A. baumannii* clinical isolates, in order to understand the genes associated with the resistance to carbapenems and the prevalence of K types. The goal was also to expand the collection of phage-derived CPS depolymerases that are able to infect different *A. baumannii* K types and also characterize these enzymes.

Resistance genes of 94 *A. baumannii* clinical isolates collected from the Northern Region of Portugal during 2005 and 2012 were assessed. In this study, *oxa-51* and *oxa-23* β-lactamases were the most predominant within the tested strains, followed by *Imp-like* and *oxa-24* genes. As for the prevalence of K types, selected strains were sent to be sequenced through an international collaboration, however, the results were not obtained in time. Therefore, *in silico* assessment of the K types of the clinical isolates shall be done in the near future.

Currently, 17 distinct ACB complex K-specific depolymerases have been identified in phage proteomes (K1-2, K9, K19, K27, K30, K32, K37, K44-45, K47-48, K87, K89, K91, K93 and K116).[30,33,34,61,62,63] In this study, 6 novel phage-derived CPS depolymerases were identified (F70, 3042, 3043, 3060, 3073 and 3082). These CPS depolymerases were cloned and expressed in *E. coli* and further characterized alongside with previously identified CPS depolymerases (B1, B3, B9, P1 and P2). After testing their lytic activity against a panel of 30 different *Acinetobacter* K types, only CPS depolymerases belonging to phages 3060 and 3082 did not demonstrate any activity against any strain. CPS depolymerases B1, B3, B9, P1, P2, F70, 3042, 3043 and 3073 were found to affect K9, K3/K19, K30/K45, K1, K67, K38 and K32 *A. baumannii* K types. Now, the collection increased to 19 different ACB complex K-specific depolymerases, since K38 and K67 depolymerases target novel K types.

Collectively, this work demonstrates that CPS depolymerases are highly stable proteins that degrade the bacterial capsular polysaccharides, thereby turning them into less virulent forms, more easily managed by the host's immune system. Hence, CPS depolymerases may be used as anti-virulence agents against multidrug-resistant pathogens, such as *A. baumannii*.

4.2. Future perspectives

By isolating novel CPS depolymerases, this work contributed to unpuzzle the potential application of these enzymes to control bacterial infections. However, due to the high specificity of these CPS depolymerases for a given K type, epidemiological studies are required to have a comprehensive knowledge of the most prevalent ACB complex K types circulating in human clinical isolates. Only then, the anti-virulence therapy based on CPS depolymerases could be implemented and potentially become an alternative to current antimicrobial options, which are becoming less effective against drug-resistant infections, such as the ones caused by ACB species. Accordingly, when the Next-Generation Sequencing results arrive, the prevalence of K types of the *A. baumannii* clinical isolates analyzed in this thesis shall be assessed through Kaptive software.

As the preliminary results in this study show no benefits in combining these enzymes with antibiotics, additional testing is required to assay its possible synergy with other antibiotics. Likewise, the ability to control biofilms may be ultimately related with the prevalence of capsule polysaccharides in the extracellular matrix, which will be strain dependent. Therefore, further testing is required. Also, the prevention of biofilms instead of their disruption should also be tested.

Although this work proved the great potential of these enzymes, further *in vivo* testing is required in order to establish even further their prospective as a therapeutic option. In this work, it was demonstrated that these enzymes are able to complement serum killing in an *ex vivo* model. As abovementioned, similar tests were performed in *in vivo* models and demonstrated astonishing results. Therefore, the isolated enzymes in this work will most likely possess a similar anti-bacterial effect *in vivo*.

Also, since 3060 and 3082 CPS depolymerases did not possess degrading activity against the panel of tested *A. baumannii* K types, further optimization of cloning and expression of these enzymes is required. The continuous deposition of novel structures would enable a more efficient mapping of the CPS depolymerase coding region within the tailspike genes, that would then facilitate the isolation of novel proteins. Future efforts shall be made in the future to characterize these two novel depolymerases targeting 2 different *A. baumannii* K types (K84 and K85).

In a complex new direction, since CPS depolymerases have a natural ability to bind to capsules, they could also be explored in the future as a novel tool to conjugate vaccines.

REFERENCES

1. Hancock REW. Peptide antibiotics. *Lancet*. 1997;349(9049):418-422. doi:10.1016/S0140-6736(97)80051-7
2. Kortright KE, Chan BK, Koff JL, Turner PE. Phage Therapy: A Renewed Approach to Combat Antibiotic-Resistant Bacteria. *Cell Host Microbe*. 2019;25(2):219-232. doi:10.1016/j.chom.2019.01.014
3. Dodds DR. Antibiotic resistance: A current epilogue. *Biochem Pharmacol*. 2017;134(6):139-146. doi:10.1016/j.bcp.2016.12.005
4. Alanis AJ. Resistance to antibiotics: Are we in the post-antibiotic era? *Arch Med Res*. 2005;36(6):697-705. doi:10.1016/j.arcmed.2005.06.009
5. Walsh C. Molecular mechanisms that confer antibacterial drug resistance. *Nature*. 2000;406(6797):775-781. doi:10.1038/35021219
6. Guillemot D. Antibiotic use in humans and bacterial resistance. *Curr Opin Microbiol*. 1999;2(5):494-498. doi:10.1016/S1369-5274(99)00006-5
7. Gordillo Altamirano FL, Barr JJ. Phage therapy in the postantibiotic era. *Clin Microbiol Rev*. 2019;32(2):1-25. doi:10.1128/CMR.00066-18
8. Chen LK, Kuo SC, Chang KC, Cheng CC, Yu PY, Chang CH, Chen TY, Tseng CC. Clinical Antibiotic-resistant *Acinetobacter baumannii* Strains with Higher Susceptibility to Environmental Phages than Antibiotic-sensitive Strains. *Sci Rep*. 2017;7(1):1-10. doi:10.1038/s41598-017-06688-w
9. Harding CM, Hennon SW, Feldman MF. Uncovering the mechanisms of *Acinetobacter baumannii* virulence. *Nat Rev Microbiol*. 2018;16(2):91-102. doi:10.1038/nrmicro.2017.148
10. Perez F, Hujer AM, Hujer KM, Decker BK, Rather PN, Bonomo RA. Global challenge of multidrug-resistant *Acinetobacter baumannii*. *Antimicrob Agents Chemother*. 2007;51(10):3471-3484. doi:10.1128/AAC.01464-06
11. Bergogne-Bé E, Zin RÉ, Towner KJ. *Acinetobacter* ssp. as nosocomial Pathogens : Microbiological, Clinical, and Epidemiological Features. *Clin Microbiol Rev*. 1996;9(2):148-165. doi:10.1128/CMR.9.2.148
12. Wong D, Nielsen TB, Bonomo RA, Pantapalangkoor P, Luna B, Spellberg B. Clinical and pathophysiological overview of *Acinetobacter* infections: A century of challenges. *Clin Microbiol Rev*. 2017;30(1):409-447. doi:10.1128/CMR.00058-16
13. Zeidler S, Müller V. Coping with low water activities and osmotic stress in *Acinetobacter baumannii*: significance, current status and perspectives. *Environ Microbiol*. 2019;21(7):2212-2230. doi:10.1111/1462-2920.14565
14. Lee CR, Lee JH, Park M, Park KS, Bae IK, Kim YB, Cha CJ, Jeong BC, Lee SH. Biology of *Acinetobacter baumannii*: Pathogenesis, antibiotic resistance mechanisms, and prospective treatment options. *Front Cell Infect Microbiol*. 2017;7(3):1-35. doi:10.3389/fcimb.2017.00055
15. Lupo A, Haenni M, Madec J-Y. Antimicrobial resistance in *Acinetobacter* spp. and *Pseudomonas* spp. *Microbiol Spectr*. 2018;6(3):243-264. doi:10.1128/microbiolspec.ARBA -0007-2017.
16. Bartual SG, Seifert H, Hippler C, Luzon MAD, Wisplinghoff H, Rodríguez-Valera F. Development of a multilocus sequence typing scheme for characterization of clinical isolates of *Acinetobacter baumannii*. *J Clin Microbiol*. 2005;43(9):4382-4390. doi:10.1128/JCM.43.9.4382-4390.2005
17. Weber BS, Kinsella RL, Harding CM, Feldman MF. The Secrets of *Acinetobacter* Secretion. *Trends Microbiol*. 2017;25(7):532-545. doi:10.1016/j.tim.2017.01.005
18. Saipriya K, Swathi CH, Ratnakar KS, Sritharan V. Quorum-sensing system in

Acinetobacter baumannii: a potential target for new drug development. *J Appl Microbiol*. 2020;128(1):15-27. doi:10.1111/jam.14330

19. Nie D, Hu Y, Chen Z, Li M, Hou Z, Luo X, Mao X, Xue X. Outer membrane protein A (OmpA) as a potential therapeutic target for *Acinetobacter baumannii* infection. *J Biomed Sci*. 2020;27(1):1-8. doi:10.1186/s12929-020-0617-7
20. Shin B, Park C, Park W. Stress responses linked to antimicrobial resistance in *Acinetobacter* species. *Appl Microbiol Biotechnol*. 2020;104(4):1423-1435. doi:10.1007/s00253-019-10317-z
21. Li F-J, Starrs L, Burgio G. Tug-of-war between *Acinetobacter baumannii* and host immune responses. *Pathog Dis*. 2018;76(9):1-51. doi:10.1093/femspd/ftz004
22. Skariyachan S, Taskeen N, Ganta M, Venkata Krishna B. Recent perspectives on the virulent factors and treatment options for multidrug-resistant *Acinetobacter baumannii*. *Crit Rev Microbiol*. 2019;45(3):315-333. doi:10.1080/1040841X.2019.1600472
23. Ibrahim ME. Prevalence of *Acinetobacter baumannii* in Saudi Arabia: Risk factors, antimicrobial resistance patterns and mechanisms of carbapenem resistance. *Ann Clin Microbiol Antimicrob*. 2019;18(1):1-12. doi:10.1186/s12941-018-0301-x
24. Ramirez MS, Bonomo RA, Tolmasky ME. Carbapenemases: Transforming *Acinetobacter baumannii* into a yet more dangerous menace. *Biomolecules*. 2020;10(5):1-31. doi:10.3390/biom10050720
25. Farrow JM, Wells G, Pesci EC. Desiccation tolerance in *Acinetobacter baumannii* is mediated by the two-component response regulator BfmR. *PLoS One*. 2018;13(10):1-25. doi:10.1371/journal.pone.0205638
26. Bravo Z, Orruño M, Navascues T, Ogayar E, Ramos-Vivas J, Kaberdin VR, Arana I. Analysis of *Acinetobacter baumannii* survival in liquid media and on solid matrices as well as effect of disinfectants. *J Hosp Infect*. 2019;103(1):e42-e52. doi:10.1016/j.jhin.2019.04.009
27. Wood CR, Mack LE, Actis LA. An Update on the *Acinetobacter baumannii* Regulatory Circuitry. *Trends Microbiol*. 2018;26(7):560-562. doi:10.1016/j.tim.2018.05.005
28. Hsieh PF, Lin HH, Lin TL, Chen YY, Wang JT. Two T7-like Bacteriophages, K5-2 and K5-4, Each Encodes Two Capsule Depolymerases: Isolation and Functional Characterization. *Sci Rep*. 2017;7(1):1-13. doi:10.1038/s41598-017-04644-2
29. Russo TA, Luke NR, Beanan JM, Olson R, Sauberan SL, MacDonald U, Schultz LW, Umland TC, Campagnari AA. The K1 capsular polysaccharide of *Acinetobacter baumannii* strain 307-0294 is a major virulence factor. *Infect Immun*. 2010;78(9):3993-4000. doi:10.1128/IAI.00366-10
30. Oliveira H, Mendes A, Fraga AG, Ferreira A, Pimenta AI, Mil-Homens D, Fialho AM, Pedrosa J, Joana Azeredo. K2 capsule depolymerase is highly stable, is refractory to resistance, and protects larvae and mice from *Acinetobacter baumannii* sepsis. *Appl Environ Microbiol*. 2019;85(17):e00934-19. doi:10.1128/AEM.00934-19
31. Knecht LE, Veljkovic M, Fieseler L. Diversity and Function of Phage Encoded Depolymerases. *Front Microbiol*. 2020;10(1):2949. doi:10.3389/fmicb.2019.02949
32. Kenyon JJ, Notaro A, Hsu LY, De Castro C, Hall RM. 5,7-Di-N-acetyl-8-epiacinetaminic acid: A new non-2-ulosonic acid found in the K73 capsule produced by an *Acinetobacter baumannii* isolate from Singapore. *Sci Rep*. 2017;7(1):6-11. doi:10.1038/s41598-017-11166-4
33. Oliveira H, Costa AR, Konstantinides N, Ferreira A, Akturk E, Sillankorva S, Nemec A, Shneider M, Dötsch A, Azeredo J. Ability of phages to infect *Acinetobacter calcoaceticus-Acinetobacter baumannii* complex species through acquisition of different pectate lyase

depolymerase domains. *Environ Microbiol*. 2017;19(12):5060-5077. doi:10.1111/1462-2920.13970

34. Oliveira H, Costa AR, Ferreira A, Konstantinides N, Santos SB, Boon M, Noben JP, Lavigne R, Azeredo J. Functional Analysis and Antivirulence Properties of a New Depolymerase from a Myovirus That Infects *Acinetobacter baumannii* Capsule K45. *J Virol*. 2019;93(4):1-16. doi:10.1128/jvi.01163-18
35. Kasimova AA, Kenyon JJ, Arbatsky NP, Shashkov AS, Popova AV, Shneider MM, Knirel YA, Hall RM. *Acinetobacter baumannii* K20 and K21 Capsular Polysaccharide Structures Establish Roles for UDP-Glucose Dehydrogenase Ugd2, Pyruvyl Transferase Ptr2 and Two Glycosyltransferases. *Glycobiology*. 2018; 28(11):876-884. doi:10.1093/glycob/cwy074
36. Kenyon JJ, Kasimova AA, Shashkov AS, Hall RM, Knirel YA. *Acinetobacter baumannii* isolate BAL_212 from vietnam produces the K57 capsular polysaccharide containing a rarely occurring amino sugar N-acetylviosamine. *Microbiol (United Kingdom)*. 2018;164(2):217-220. doi:10.1099/mic.0.000598
37. Wyres KL, Cahill SM, Holt KE, Hall RM, Kenyon JJ. Identification of *Acinetobacter baumannii* loci for capsular polysaccharide (KL) and lipooligosaccharide outer core (OCL) synthesis in genome assemblies using curated reference databases compatible with kaptive. *Microb Genomics*. 2020;6(3):e000339. doi:10.1099/mgen.0.000339
38. Santos SB, Melo LDR, Oliveira H. Phage Structural Antimicrobial Proteins. In: *Bacterial Viruses: Exploitation for Biocontrol and Therapeutics*. ; 2020:419-476. doi:10.21775/9781913652517.12
39. Wittebole X, De Roock S, Opal SM. A historical overview of bacteriophage therapy as an alternative to antibiotics for the treatment of bacterial pathogens. *Virulence*. 2014;5(1):226-235. doi:10.4161/viru.25991
40. Campbell A. The future of bacteriophage biology. *Nat Rev Genet*. 2003;4(6):1-7. doi:10.1038/nrg1089
41. Kim M, Ryu S. Antirepression System Associated with the Life Cycle Switch in the Temperate Podoviridae Phage SPC32H. *J Virol*. 2013;87(21):11775-11786. doi:10.1128/jvi.02173-13
42. Olszak T, Shneider MM, Latka A, Maciejewska B, Browning C, Sycheva LV, Cornelissen A, Danis-Wlodarczyk K, Senchenkova SN, Shashkov AS, Gula G, Arabski M, Wasik S, Miroshnikov KA, Lavigne R, Leiman PG, Knirel YA, Drulis-Kawa Z. The O-specific polysaccharide lyase from the phage LKA1 tailspike reduces *Pseudomonas* virulence. *Sci Rep*. 2017;7(1):1-14. doi:10.1038/s41598-017-16411-4
43. Kakasis A, Panitsa G. Bacteriophage therapy as an alternative treatment for human infections. A comprehensive review. *Int J Antimicrob Agents*. 2019;53(1):16-21. doi:10.1016/j.ijantimicag.2018.09.004
44. Labrie SJ, Samson JE, Moineau S. Bacteriophage resistance mechanisms. *Nat Rev Microbiol*. 2010;8(5):317-327. doi:10.1038/nrmicro2315
45. García R, Latz S, Romero J, Higuera G, García K, Bastías R. Bacteriophage production models: An overview. *Front Microbiol*. 2019;10(1187):1-7. doi:10.3389/fmicb.2019.01187
46. Joerger RD. Alternatives to antibiotics: Bacteriocins, antimicrobial peptides and bacteriophages. *Poult Sci*. 2003;82(4):640-647. doi:10.1093/ps/82.4.640
47. Aslam S, Schooley RT. What's old is new again: Bacteriophage Therapy in the 21st Century. *Antimicrob Agents Chemother*. 2020;64(1):1-9. doi:10.1128/AAC.01987-19
48. Langdon A, Crook N, Dantas G. The effects of antibiotics on the microbiome throughout development and alternative approaches for therapeutic modulation. *Genome Med*.

2016;8(39):1-16. doi:10.1186/s13073-016-0294-z
49. Pelfrene E, Willebrand E, Cavaleiro Sanches A, Sebris Z, Cavaleri M. Bacteriophage therapy: A regulatory perspective. *J Antimicrob Chemother*. 2016;71(8):2071-2074. doi:10.1093/jac/dkw083
50. Lai MJ, Chang KC, Huang SW, Luo CH, Chiou PY, Wu CC, Lin NT. The tail associated protein of *Acinetobacter baumannii* phage qab6 is the host specificity determinant possessing exopolysaccharide depolymerase activity. *PLoS One*. 2016;11(4):1-14. doi:10.1371/journal.pone.0153361
51. Schooley RT, Biswas B, Gill JJ, Hernandez-Morales A, Lancaster J, Lessor L, Barr JJ, Reed SL, Rohwer F, Benler S, Segall AM, Taplitz R, Smith DM, Kerr K, Kumaraswamy M, Nizet V, Lin L, McCauley MD, Strathdee SA, Benson CA, Pope RK, Leroux BM, Picel AC, Mateczun AJ, Cilwa KE, Regeimbal JM, Estrella LA, Wolfe DM, Henry MS, Quinones J, Salka S, Bishop-Lilly KA,Young R, Hamilton T. Development and use of personalized bacteriophage-based therapeutic cocktails to treat a patient with a disseminated resistant *Acinetobacter baumannii* infection. *Antimicrob Agents Chemother*. 2017;61(10):e00954-17. doi:10.1128/AAC.00954-17
52. Liu Y, Leung SSY, Guo Y, Zhao L, Jiang N, Mi L, Li P, Wang C, Qin Y, Mi Z, Bai C, Gao Z. The capsule depolymerase Dpo48 rescues *Galleria mellonella* and mice from *Acinetobacter baumannii* systemic infections. *Front Microbiol*. 2019;10(545):1-9. doi:10.3389/fmicb.2019.00545
53. Drulis-Kawa Z, Majkowska-Skrobek G, Maciejewska B. Bacteriophages and Phage-Derived Proteins – Application Approaches. *Curr Med Chem*. 2015;22(14):1757-1773. doi:10.2174/0929867322666150209152851
54. Yan J, Mao J, Xie J. Bacteriophage polysaccharide depolymerases and biomedical applications. *BioDrugs*. 2014;28(3):265-274. doi:10.1007/s40259-013-0081-y
55. Safari F, Sharifi M, Farajnia S, Akbari B, Ahmadi MKB, Negahdaripour M, Ghasemi Y. The interaction of phages and bacteria: the co-evolutionary arms race. *Crit Rev Biotechnol*. 2020;40(2):119-137. doi:10.1080/07388551.2019.1674774
56. Azam AH, Tanji Y. Bacteriophage-host arm race: an update on the mechanism of phage resistance in bacteria and revenge of the phage with the perspective for phage therapy. *Appl Microbiol Biotechnol*. 2019;103(5):2121-2131. doi:10.1007/s00253-019-09629-x
57. Lee IM, Tu IF, Yang FL, Ko TP, Liao JH, Lin NT, Wu CY, Ren CT, Wang AHJ, Chang CM, Huang KF, Wu SH. Structural basis for fragmenting the exopolysaccharide of *Acinetobacter baumannii* by bacteriophage ΦaB6 tailspike protein. *Sci Rep*. 2017;7(2):1-13. doi:10.1038/srep42711
58. Hughes D, Andersson DI. Evolutionary Trajectories to Antibiotic Resistance. *Annu Rev Microbiol*. 2017;71(1):579-596. doi:10.1146/annurev-micro-090816-093813
59. Pires DP, Oliveira H, Melo LDR, Sillankorva S, Azeredo J. Bacteriophage-encoded depolymerases: their diversity and biotechnological applications. *Appl Microbiol Biotechnol*. 2016;100(5):2141-2151. doi:10.1007/s00253-015-7247-0
60. Popova A V., Lavysh DG, Klimuk EI, Edelstein MV, Bogun AG, Shneider MM, Goncharov AE, Leonov SV, Severinov KV. Novel Fri1-like viruses infecting *Acinetobacter baumannii*—vB_AbaP_AS11 and vB_AbaP_AS12—characterization, comparative genomic analysis, and host-recognition strategy. *Viruses*. 2017;9(7):1-15. doi:10.3390/v9070188
61. Popova A V., Shneider MM, Arbatsky NP, Kasimova AA, Senchenkova SN, Shashkov AS, Dmitrenok AS, Chizhov AO, Mikhailova YV, Shagin DA, Sokolova OS, Timoshina OY, Kozlov, Miroshnikov KA, Knirel YA. Specific Interaction of Novel Friunavirus Phages Encoding Tailspike Depolymerases with Corresponding *Acinetobacter baumannii* Capsular

Types. *J Virol*. 2021;95(5):1-23. doi:10.1128/jvi.01714-20
62. Shchurova AS, Shneider MM, Arbatsky NP, Shashkov AS, Chizhov AO, Skryabin YP, Mikhaylova YV, Sokolova OS, Shelenkov AA, Miroshnikov KA, Knirel YA, Popova A. Novel *Acinetobacter baumannii* myovirus tapaz encoding two tailspike depolymerases: Characterization and host-recognition strategy. *Viruses*. 2021;13(6):1-14. doi:10.3390/v13060978
63. Adams MH, Park BH. An Enzyme Produced by a Phage-Host Cell System. II. The Properties of the Polysaccharide Depolymerase. *Virology*. 1956;2(6):719-736. doi:10.1016/0042-6822(56)90054-x
64. Guo Z, Huang J, Yan G, Lei L, Wang S, Yu L, Zhou L, Gao A, Feng X, Han W, Gu J, Yang J. Identification and characterization of Dpo42, a novel depolymerase derived from the *Escherichia coli* phage vB_EcoM_ECO078. *Front Microbiol*. 2017;8(1460):1-12. doi:10.3389/fmicb.2017.01460
65. Poirel L, Walsh TR, Cuvillier V, Nordmann P. Multiplex PCR for detection of acquired carbapenemase genes. *Diagn Microbiol Infect Dis*. 2011;70(1):119-123. doi:10.1016/j.diagmicrobio.2010.12.002
66. Pitout JDD, Gregson DB, Poirel L, McClure JA, Le P, Church DL. Detection of *Pseudomonas aeruginosa* producing metallo-β-lactamases in a large centralized laboratory. *J Clin Microbiol*. 2005;43(7):3129-3135. doi:10.1128/JCM.43.7.3129-3135.2005
67. Mlynarcik P, Roderova M, Kolar M. Primer evaluation for PCR and its application for detection of carbapenemases in *Enterobacteriaceae*. *Jundishapur J Microbiol*. 2016;9(1):e29314. doi:10.5812/jjm.29314
68. Woodford N, Ellington MJ, Coelho JM, Turton JF, Ward ME, Brown S, Amyes SGB, Livermore DM. Multiplex PCR for genes encoding prevalent OXA carbapenemases in *Acinetobacter* spp. *Int J Antimicrob Agents*. 2006;27(4):351-353. doi:10.1016/j.ijantimicag.2006.01.004
69. Gregersen T. Rapid method for distinction of gram-negative from gram-positive bacteria. *Eur J Appl Microbiol Biotechnol*. 1978;5(2):123-127. doi:10.1007/BF00498806
70. Garneau JR, Depardieu F, Fortier LC, Bikard D, Monot M. PhageTerm: A tool for fast and accurate determination of phage termini and packaging mechanism using next-generation sequencing data. *Sci Rep*. 2017;7(1):1-10. doi:10.1038/s41598-017-07910-5
71. Aziz RK, Bartels D, Best A, DeJongh M, Disz T, Edwards RA, Formsma K, Gerdes S, Glass EM, Kubal M, Meyer F, Olsen GJ, Olson R, Osterman AL, Overbeek RA, McNeil LK, Paarmann D, Paczian T, Parrello B, Pusch GD, Reich C, Stevens R, Vassieva O, Vonstein V, Wilke A, Zagnitka O. The RAST Server: Rapid annotations using subsystems technology. *BMC Genomics*. 2008;9(2):1-15. doi:10.1186/1471-2164-9-75
72. Altschul SF, Gish W, Miller W, Myers EW, Lipman DJ. Basic local alignment search tool. *J Mol Biol*. 1990;215(3):403-410. doi:10.1016/S0022-2836(05)80360-2
73. Söding J, Biegert A, Lupas AN. The HHpred interactive server for protein homology detection and structure prediction. *Nucleic Acids Res*. 2005;33(7):244-248. doi:10.1093/nar/gki408
74. Lowe TM, Eddy SR. TRNAscan-SE: A program for improved detection of transfer RNA genes in genomic sequence. *Nucleic Acids Res*. 1996;25(5):955-964. doi:10.1093/nar/25.5.0955
75. Migl DD. Expression, Purification, and Characterization of a Polysaccharide Depolymerase from *Acinetobacter baumannii* Bacteriophage AbauYa1. [Master's Thesis]. 2012.
76. Pires DP, Dötsch A, Anderson EM, Hao Y, Khursigara CM, Lam JS, Sillankorva S, Azeredo

J. A genotypic analysis of five *P. aeruginosa* strains after biofilm infection by phages targeting different cell surface receptors. *Front Microbiol*. 2017;8(6):1-14. doi:10.3389/fmicb.2017.01229

77. Boral B, Unaldi Ö, Ergin A, Durmaz R, Eser OK. A prospective multicenter study on the evaluation of antimicrobial resistance and molecular epidemiology of multidrug-resistant *Acinetobacter baumannii* infections in intensive care units with clinical and environmental features. *Ann Clin Microbiol Antimicrob*. 2019;18(1):1-9. doi:10.1186/s12941-019-0319-8
78. Al-Hashem G, Rotimi VO, Albert MJ. Antimicrobial Resistance of Serial Isolates of *Acinetobacter baumannii* Colonizing the Rectum of Adult Intensive Care Unit Patients in a Teaching Hospital in Kuwait. *Microb Drug Resist*. 2021;27(1):64-72. doi:10.1089/mdr.2020.0106
79. Leungtongkam U, Thummeepak R, Tasanapak K, Sitthisak S. Acquisition and transfer of antibiotic resistance genes in association with conjugative plasmid or class 1 integrons of *Acinetobacter baumannii*. *PLoS One*. 2018;13(12):1-12. doi:10.1371/journal.pone.0208468
80. Chatterjee S, Datta S, Roy S, Ramanan L, Saha A, Viswanathan R, Som T, Basu S. Carbapenem resistance in *Acinetobacter baumannii* and other *Acinetobacter* spp. causing neonatal sepsis: Focus on NDM-1 and its linkage to ISAba125. *Front Microbiol*. 2016;7(8):1-13. doi:10.3389/fmicb.2016.01126
81. Alves J, Dias L, Mateus J, Marques J, Graças D, Ramos R, Seldin L, Henriques I, Silva A, Folador A. Resistome in Lake Bolonha, Brazilian Amazon: Identification of Genes Related to Resistance to Broad-Spectrum Antibiotics. *Front Microbiol*. 2020;11(2):1-13. doi:10.3389/fmicb.2020.00067
82. Hadjadj L, Bakour S, Rolain JM. Co-occurrence of carbapenemase encoding genes in *Acinetobacter baumannii*, a dream or reality? *BMC Microbiol*. 2018;18(1):4-9. doi:10.1186/s12866-018-1252-2
83. Leshkasheli L, Kutateladze M, Balarjishvili N, Bolkvadze D, Save J, Oechslin F, Que YA, Resch G. Efficacy of newly isolated and highly potent bacteriophages in a mouse model of extensively drug-resistant *Acinetobacter baumannii* bacteraemia. *J Glob Antimicrob Resist*. 2019;19:255-261. doi:10.1016/j.jgar.2019.05.005
84. Popova A V., Shneider MM, Myakinina VP, Bannov VA, Edelstein MV, Rubalskii EO, Aleshkin AV, Fursova NK, Volozhantsev NV. Characterization of myophage AM24 infecting *Acinetobacter baumannii* of the K9 capsular type. *Arch Virol*. 2019;164(5):1493-1497. doi:10.1007/s00705-019-04208-x
85. Oliveira H, Pinto G, Mendes B, Dias O, Hendrix H, Akturk E, Noben JP, Gawor J, Lobocka M, Lavigne R, Azeredo J. A tailspike with exopolysaccharide depolymerase activity from a new *Providencia stuartii* phage makes multidrug-resistant bacteria susceptible to serum-mediated killing. *Appl Environ Microbiol*. 2020;86(13):e00073-20. doi:10.1128/AEM.00073-20
86. Chen Y, Li X, Wang S, Guan L, Li X, Hu D, Gao D, Song J, Chen H, Qian P. A novel tail-associated O91-specific polysaccharide depolymerase from a podophage reveals lytic efficacy of Shiga Toxin-producing *Escherichia coli*. *Appl Environ Microbiol*. 2020;86(9):e00145-20. doi:10.1128/AEM.00145-20
87. Majkowska-Skrobek G, Łątka A, Berisio R, Maciejewska B, Squeglia F, Romano M, Lavigne R, Struve C, Drulis-Kawa Z. Capsule-targeting depolymerase, derived from *Klebsiella* KP36 phage, as a tool for the development of anti-virulent strategy. *Viruses*. 2016;8(12):324. doi:10.3390/v8120324

88. Mitraki A, Miller S, Van Raaij MJ. Review: Conformation and folding of novel beta-structural elements in viral fiber proteins: The triple beta-spiral and triple beta-helix. *J Struct Biol*. 2002;137(1-2):236-247. doi:10.1006/jsbi.2002.4447
89. Latka A, Leiman PG, Drulis-Kawa Z, Briers Y. Modeling the Architecture of Depolymerase-Containing Receptor Binding Proteins in *Klebsiella* Phages. *Front Microbiol*. 2019;10(November):2649. doi:10.3389/fmicb.2019.02649
90. Domingues R, Barbosa A, Santos SB, Pires DP, Save J, Resch G, Azeredo J, Oliveira H. Unpuzzling Friunavirus-Host Interactions One Piece at a Time : Phage Recognizes *Acinetobacter pittii* via a New K38 Capsule Depolymerase. *Antibiotics*. 2021;10(11):1304. doi:10.3390/antibiotics10111304
91. Greenfield J, Shang X, Luo H, Zhou Y, Heselpoth RD, Nelson DC, Herzberg O. Structure and tailspike glycosidase machinery of ORF212 from *E. coli* O157:H7 phage CBA120 (TSP3). *Sci Rep*. 2019;9(1):1-11. doi:10.1038/s41598-019-43748-9
92. Greenfield J, Shang X, Luo H, Zhou Y, Linden SB, Heselpoth RD, Leiman PG, Nelson DC, Herzberg O. Structure and function of bacteriophage CBA120 ORF211 (TSP2), the determinant of phage specificity towards *E. coli* O157:H7. *Sci Rep*. 2020;10(1):1-14. doi:10.1038/s41598-020-72373-0
93. Majkowska-Skrobek G, Latka A, Berisio R, Squeglia F, Maciejewska B, Briers Y, Drulis-Kawa Z. Phage-borne depolymerases decrease *Klebsiella pneumoniae* resistance to innate defense mechanisms. *Front Microbiol*. 2018;9(10):1-12. doi:10.3389/fmicb.2018.02517
94. Wu Y, Wang R, Xu M, Liu Y, Zhu X, Qiu J, Liu Q, He P Li Q. A Novel Polysaccharide Depolymerase Encoded by the Phage SH-KP152226 Confers Specific Activity Against Multidrug-Resistant *Klebsiella pneumoniae* via Biofilm Degradation. *Front Microbiol*. 2019;10(12):2768. doi:10.3389/fmicb.2019.02768
95. Liu Y, Leung SSY, Huang Y, Guo Y, Jiang N, Li P, Chen J, Wang R, Bai C, Mi Z, Gao Z. Identification of Two Depolymerases From Phage IME205 and Their Antivirulent Functions on K47 Capsule of *Klebsiella pneumoniae*. *Front Microbiol*. 2020;11(2):1-11. doi:10.3389/fmicb.2020.00218
96. Latka A, Maciejewska B, Majkowska-Skrobek G, Briers Y, Drulis-Kawa Z. Bacteriophage-encoded virion-associated enzymes to overcome the carbohydrate barriers during the infection process. *Appl Microbiol Biotechnol*. 2017;101(8):3103-3119. doi:10.1007/s00253-017-8224-6
97. Latka A, Drulis-Kawa Z. Advantages and limitations of microtiter biofilm assays in the model of antibiofilm activity of *Klebsiella* phage KP34 and its depolymerase. *Sci Rep*. 2020;10(1):1-12. doi:10.1038/s41598-020-77198-5
98. Wang C, Li P, Zhu Y, Huang Y, Gao M, Yuan X, Niu W, Liu H, Fan H, Qin Y, Tong Y, Mi Z, Bai C. Identification of a Novel *Acinetobacter baumannii* Phage-Derived Depolymerase and Its Therapeutic Application in Mice. *Front Microbiol*. 2020;11(7):1-11. doi:10.3389/fmicb.2020.01407
99. Gutiérrez D, Briers Y, Rodríguez-Rubio L, Martinez B, Rodriguez A, Lavigne R, Garcia P. Role of the pre-neck appendage protein (Dpo7) from phage vB_SepiS-phiIPLA7 as an anti-biofilm agent in staphylococcal species. *Front Microbiol*. 2015;6(11):1-10. doi:10.3389/fmicb.2015.01315
100. Bansal S, Harjai K, Chhibber S. *Aeromonas punctata* derived depolymerase improves susceptibility of *Klebsiella pneumoniae* biofilm to gentamicin Microbial biochemistry, physiology and metabolism. *BMC Microbiol*. 2015;15(1):1-10. doi:10.1186/s12866-015-0455-z

ANNEXES

Annex I. Information regarding the clinical isolates used in this study

Table A1. *A. baumannii* clinical isolates used in the epidemiological study.

ID	Origin	Date
MJH47	Urine	16/05/05
MJH58	Sputum	31/10/05
MJH62	Urine	03/11/05
MJH74	Swab from non-specified origin	06/02/06
MJH75	Swab from non-specified origin	08/02/06
MJH78	Swab from surgical wound	11/03/06
MJH85	Bronchial secretion / Tracheal aspiration	08/05/06
MJH86	Sputum	12/05/06
MJH97	Sputum	Not specified
MJH105	Sputum	14/03/07
MJH107	Urine	20/03/07
MJH122	Swab from surgical wound	28/05/07
MJH134	Urine	09/07/07
MJH152	Swab from non-specified origin	26/12/07
MJH156	Urine	07/02/08
MJH158	Sputum	14/04/08
MJH169	Sputum	15/04/08
MJH170	Sputum	24/04/08
MJH173	Bronchial secretion / Tracheal aspiration	17/06/08
MJH174	Bronchial secretion / Tracheal aspiration	24/06/08
MJH176	Sputum	01/07/08
MJH177	Urine	29/09/08
MJH181	Urine	27/10/08
MJH183	Superficial pus	30/10/08
MJH184	Swab from decubitus ulcer	03/11/08
MJH185	Bronchial secretion / Tracheal aspiration	04/11/08
MJH190	Sputum	27/11/08
MJH191	Bronchial aspiration	22/12/08
MJH193	Sputum	26/12/08
MJH195	Bronchial secretion / Tracheal aspiration	09/01/09
MJH196	Urine	12/01/09
MJH206	Bronchial secretion / Tracheal aspiration	04/03/09
MJH212	Bronchial secretion / Tracheal aspiration	03/04/09
MJH218	Bronchial secretion / Tracheal aspiration	22/05/09
MJH219	Hemoculture	24/05/09
MJH220	Bronchial secretion / Tracheal aspiration	29/05/09

MJH222	Bronchial aspiration	19/06/09
MJH224	Sputum	06/07/09
MJH229	Swab from decubitus ulcer	27/08/09
MJH230	Bronchial secretion / Tracheal aspiration	31/08/09
MJH231	Hemoculture	04/09/09
MJH232	Urine	25/09/09
MJH233	Sputum	06/10/09
MJH235	Sputum	14/10/09
MJH236	Bronchial secretion / Tracheal aspiration	14/10/09
MJH238	Hemoculture	03/11/09
MJH239	Sputum	04/11/09
MJH240	Urine	15/12/09
MJH242	Sputum	23/12/09
MJH243	Bronchial secretion / Tracheal aspiration	23/12/09
MJH244	Bronchial secretion / Tracheal aspiration	28/12/09
MJH245	Bronchial secretion / Tracheal aspiration	30/12/09
MJH246	Hemoculture	07/01/10
MJH247	Sputum	11/01/10
MJH250	Bronchial secretion / Tracheal aspiration	26/01/10
MJH252	Bronchial secretion / Tracheal aspiration	03/02/10
MJH253	Sputum	04/02/10
MJH254	Bronchial secretion / Tracheal aspiration	11/02/10
MJH255	Urine	15/02/10
MJH257	Drainage of abscesse and hematoma	24/02/10
MJH258	Bronchial secretion / Tracheal aspiration	25/02/10
MJH259	Urine	26/02/10
MJH262	Sputum	08/03/10
MJH265	Sputum	17/03/10
MJH266	Bronchial secretion / Tracheal aspiration	23/03/10
MJH276	Swab from decubitus ulcer	02/06/10
MJH277	Swab from pustule	04/06/10
MJH280	Sputum	29/07/10
MJH283	Swab from non-surgical wound	17/09/10
MJH285	Urine	22/10/10
MJH288	Bronchial secretion / Tracheal aspiration	02/11/10
MJH291	Urine	27/11/10
MJH294	Sputum	20/12/10
MJH295	Swab from non-specified origin	21/12/10
MJH299	Urine	07/03/11
MJH300	Urine	18/03/11
MJH301	Swab from non-specified origin	28/03/11
MJH302	Swab from non-specified origin	28/03/11

MJH303	Urine	31/03/11
MJH306	Sputum	11/04/11
MJH307	Bronchial secretion	04/05/11
MJH309	Bronchial secretion	30/05/11
MJH317	Bronchial secretion	03/10/11
MJH320	Sputum	21/11/11
MJH321	Bronchial secretion	22/11/11
MJH324	Bronchial aspiration	27/01/12
MJH326	Urine	23/02/12
MJH327	Urine	23/02/12
MJH331	Sputum	14/05/12
MJH333	Urine	11/07/12
MJH334	Urine	21/09/12
MJH335	Bronchial secretion	13/10/12
MJH336	Urine	17/10/12
MJH337	Bronchial secretion	17/11/12

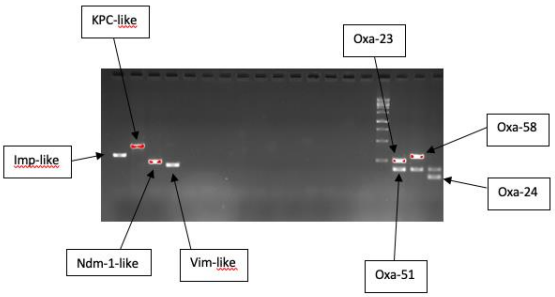

Figure A1. 1.5% agarose gel that translates the size of the desired resistance genes using GRS Ladder 1 kb (Grisp). Positive controls were used to ensure a correct amplification.

Annex II. *In silico* annotation of phages

Table A2. Annotation of phage F70. For each ORF, the transcription start and stop position. The corresponding gene product size and putative predicted function based on the best hit obtained in BLASTP and the E-value are indicated.

ORF	Start (bp)	Stop (bp)	Predicted proteins			
			Size (aa)	Best Species Hit	Putative function (Accession number)	E-value
gp01	380	541	54	-	-	-
gp02	982	1164	60	*Acinetobacter* phage vB_ApiP_P1	hypothetical protein (YP_009610440.1)	1E-35
gp03	1656	2165	169	*Acinetobacter* phage vB_AbaP_APK128	hypothetical protein (QVD48847.1)	8E-119
gp04	2167	2541	124	*Acinetobacter* phage vB_AbaP_B09_Aci08	hypothetical protein (YP_009814018.1)	3E-79
gp05	2720	3316	198	*Acinetobacter* phage vB_AbaP_APK2	hypothetical protein (AZU99204.1)	5E-146
gp06	3304	3417	38	*Acinetobacter* phage vB_AbaP_B1	hypothetical protein (YP_009610294.1)	5E-18
gp07	3576	3974	132	*Acinetobacter* phage Paty	hypothetical protein (QQM15047.1)	1E-93
gp08	4045	4524	159	*Acinetobacter* phage vB_AbaP_IME546	hypothetical protein (QFR59019.1)	3E-113
gp09	4526	4963	145	*Acinetobacter* phage vB_AbaP_APK89	hypothetical protein (QGK90359.1)	2E-100
gp10	4974	5141	55	*Acinetobacter* phage WCHABP5	hypothetical protein (YP_009604596.1)	3E-29
gp11	5128	5316	62	*Acinetobacter* phage vB_AbaP_APK48	hypothetical protein (QFG06928.1)	5E-38
gp12	5313	5540	75	*Acinetobacter* phage vB_AbaP_B09_Aci08	hypothetical protein (YP_009814028.1)	1E-42
gp13	5530	5754	74	*Acinetobacter* phage AbKT21phiIII	hypothetical protein (YP_009818731.1)	6E-47
gp14	5776	6225	149	*Acinetobacter* phage Pipo	hypothetical protein (QQO92942.1)	2E-104
gp15	6303	7010	235	*Acinetobacter* phage SWH-Ab-1	DNA primase (YP_009949031.1)	4E-175
gp16	7010	7330	106	*Acinetobacter* phage Fri1	hypothetical protein (YP_009203025.1)	3E-69
gp17	7330	7566	79	*Acinetobacter* phage vB_AbaP_APK128	hypothetical protein (QVD48859.1)	3E-46
gp18	7579	8877	432	*Acinetobacter* phage vB_AbaP_APK128	DNA helicase (QVD48860.1)	0
gp19	8880	9617	245	*Acinetobacter* phage vB_AbaP_APK128	hypothetical protein (QVD48861.1)	2E-169
gp20	9614	10570	318	*Acinetobacter* phage vB_AbaP_B1	ATP-dependent DNA ligase (YP_009610306.1)	0
gp21	10820	13132	770	*Acinetobacter* phage vB_AbaP_APK37	DNA polymerase I (AZU99423.1)	0

gp22	13141	13620	160	*Siphoviridae sp.*	hypothetical protein (QHJ81729.1)	7E-59
gp23	13638	14528	296	*Acinetobacter* phage vB_AbaP_APK37	hypothetical protein (AZU99425.1)	0
gp24	14739	15692	318	*Acinetobacter* phage vB_AbaP_APK116	5'-3'-exonuclease (QHS01512.1)	0
gp25	15682	16251	189	*Acinetobacter* phage vB_AbaP_APK26	tRNA nucleotidyltransferase (QQO96985.1)	1E-125
gp26	16248	16688	147	*Acinetobacter* phage phiAB1	DNA endonuclease VII (YP_009189364.1)	4E-105
gp27	16692	17627	311	*Acinetobacter* phage vB_AbaA_fBenAci001	phosphodiestherase (QOV07734.1)	0
gp28	17627	18277	216	*Acinetobacter* phage vB_AbaP_AS12	dNMP kinase (YP_009599215.1)	3E-155
gp29	18286	20703	805	*Acinetobacter* phage vB_AbaP_APK128	DNA-directed RNA-polymerase (QVD48875.1)	0
gp30	20807	21004	65	*Acinetobacter* phage vB_AbaP_IME200	hypothetical protein (YP_009216529.1)	8E-40
gp31	21001	21252	84	*Acinetobacter* phage vB_AbaP_IME200	hypothetical protein (YP_009216530.1)	2E-53
gp32	21261	22817	518	*Acinetobacter* phage AB3	head-tail connector protein (YP_008060145.1)	0
gp33	22826	23686	286	*Acinetobacter* phage vB_AbaP_B09_Aci08	scaffold protein (YP_009814051.1)	0
gp34	23702	24733	343	*Acinetobacter* phage SWH-Ab-1	major capsid protein (YP_009949051.1)	0
gp35	24786	24971	61	*Acinetobacter* phage Fri1	hypothetical protein (YP_009203048.1)	1E-32
gp36	25099	25659	186	*Acinetobacter* phage vB_AbaP_AS12	tail tubular protein A (YP_009599224.1)	1E-133
gp37	25668	27959	763	*Acinetobacter* phage vB_AbaP_IME200	tail tubular protein B (YP_009216537.1)	0
gp38	27959	28633	225	*Acinetobacter* phage vB_AbaP_IME546	hypothetical protein (QFR58987.1)	1E-149
gp39	28646	31531	961	*Acinetobacter* phage vB_AbaP_PD-AB9	internal virion protein B (YP_009189832.1)	0
gp40	31541	34639	1032	*Acinetobacter* phage vB_AbaP_APK128	internal virion protein C (QVD48887.1)	0
gp41	34646	36904	752	*Acinetobacter* phage vB_AbaP_APK44	tail spike protein (QGK90444.1)	0
gp42	36915	37250	111	*Acinetobacter* phage vB_AbaP_AS11	holin (YP_009599282.1)	6E-71
gp43	37237	37794	186	*Acinetobacter* phage vB_AbaP_PMK34	endolysin (QGF20176.1)	4E-129
gp44	37854	38162	102	*Acinetobacter* phage vB_AbaA_fBenAci002	DNA maturase A (QOV07803.1)	1E-65
gp45	38172	40109	645	*Acinetobacter* phage SH-Ab 15519	DNA maturase B (YP_009598264.1)	0
gp46	40106	40243	45	*Acinetobacter* phage vB_AbaP_APK14	hypothetical protein (AYR04399.1)	5E-22
gp47	40200	40403	67	*Acinetobacter* phage vB_AbaP_APK2	hypothetical protein (AZU99248.1)	2E-35
gp48	40414	40593	59	*Acinetobacter* phage SH-Ab 15519	hypothetical protein (YP_009598261.1)	5E-34

Table A3. Annotation of phage 3042. For each ORF, the transcription start and stop position. The corresponding gene product size and putative predicted function based on the best hit obtained in BLASTP and the E-value are indicated.

ORF	Start (bp)	Stop (bp)	Predicted proteins			
			Size (aa)	Best Species Hit	Putative function (Accession number)	E-value
gp01	165	404	79	*Acinetobacter* phage vB_AbaM_B9	hypothetical protein (AWD93298.1)	7E-11
gp02	463	1233	256	*Acinetobacter* phage WCHABP12	putative head protein (YP_009600560.1)	3E-172
gp03	1234	1404	56	*Thermovibrio guaymasensis*	hypothetical protein (WP_170137400.1)	1E-14
gp04	1391	2812	473	*Acinetobacter* phage IME-AB2	putative phage head portal protein (YP_009592177.1)	0
gp05	2805	4112	435	*Acinetobacter* phage IME-AB3	putative phage terminase large subunit (YP_009592178.1)	0
gp06	4204	4644	146	*Acinetobacter baumannii*	DNA-packaging protein (EGY7252758.1)	6E-15
gp07	4699	4863	54	*Acinetobacter* phage WCHABP12	hypothetical protein (YP_009600556.1)	5E-28
gp08	4853	5095	80	*Acinetobacter* phage vB_AbaM_IME284	hypothetical protein (AYP68940.1)	3E-48
gp09	5092	5520	142	*Acinetobacter calcoaceticus/ baumannii* complex	hypothetical protein (WP_000005732.1)	4E-37
gp10	5517	5867	116	*Acinetobacter baumannii*	hypothetical protein (WP_140968383.1)	3E-46
gp11	5867	6193	108	*Acinetobacter* phage YMC-13-01-C62	hypothetical protein (YP_009055427.1)	5E-66
gp12	6190	6342	50	*Acinetobacter bereziniae*	hypothetical protein (KAF1026162.1)	4E-07
gp13	6339	6557	72	*Acinetobacter* phage AP22	hypothetical protein (YP_006383755.1)	1E-43
gp14	6736	6975	79	*Acinetobacter* phage vB_AbaM_IME284	hypothetical protein (AYP68947.1)	4E-45
gp15	7116	7397	93	*Acinetobacter* phage YMC-13-01-C62	hypothetical protein (YP_009055432.1)	3E-60
gp16	7394	7672	92	*Acinetobacter* phage LZ35	hypothetical protein (YP_009291935.1)	3E-27
gp17	7665	8198	177	*Acinetobacter* phage IME-AB2	hypothetical protein (YP_009592193.1)	1E-47
gp18	8195	8359	54	*Acinetobacter* phage IME-AB3	hypothetical protein (YP_009592194.1)	5E-28
gp19	8356	8931	191	*Acinetobacter* phage YMC-13-01-C62	hypothetical protein (YP_009055437.1)	1E-138
gp20	8928	9725	265	*Acinetobacter* phage AB1	hypothetical protein (YP_009613812.1)	4E-85
gp21	9835	10017	60	*Acinetobacter* phage LZ35	hypothetical protein (YP_009291929.1)	2E-34
gp22	10119	10409	96	*Acinetobacter* phage AB1	hypothetical protein (YP_009613815.1)	2E-65
gp23	10406	10672	88	*Acinetobacter* phage YMC-13-01-C62	hypothetical protein (YP_009055442.1)	8E-54

gp24	10713	11423	236	*Acinetobacter* phage vB_AbaM_IME285	hypothetical protein (AYP68878.1)	2E-167
gp25	11425	12738	437	*Acinetobacter* phage vB_AbaM_IME285	replicative DNA helicase (AYP68879.1)	0
gp26	12735	13508	257	*Acinetobacter* phage vB_AbaM_IME285	hypothetical protein (AYP68880.1)	0
gp27	13508	13705	65	*Acinetobacter* phage vB_AbaM_IME285	hypothetical protein (AYP68881.1)	2E-39
gp28	13828	14151	107	*Acinetobacter* phage vB_AbaM_IME285	hypothetical protein (AYP69065.1)	5E-64
gp29	14148	14393	81	*Acinetobacter* phage AB1	hypothetical protein (YP_009613822.1)	2E-51
gp30	14390	14629	79	*Acinetobacter* phage vB_AbaM_IME284	hypothetical protein (AYP68965.1)	2E-23
gp31	14626	14877	83	*Acinetobacter bereziniae*	hypothetical protein (KAF1026215.1)	3E-42
gp32	14960	15154	64	*Acinetobacter* phage YMC-13-01-C62	hypothetical protein (YP_009055450.1)	3E-37
gp33	15254	15967	237	*Acinetobacter* phage AB1	hypothetical protein (YP_009613827.1)	3E-82
gp34	16090	16299	69	*Acinetobacter* phage AP22	hypothetical protein (YP_006383758.1)	6E-32
gp35	16392	16724	110	*Acinetobacter* phage AP22	hypothetical protein (YP_006383816.1)	3E-71
gp36	16724	16906	60	*Acinetobacter* phage AP22	hypothetical protein (YP_006383815.1)	5E-30
gp37	16903	17076	57	*Acinetobacter* phage vB_AbaM_IME284	hypothetical protein (AYP68971.1)	2E-28
gp38	17073	17972	299	*Acinetobacter* phage AB1	hypothetical protein (YP_009613831.1)	0
gp39	18008	18724	238	*Acinetobacter* phage AB1	hypothetical protein (YP_009613832.1)	6E-172
gp40	18725	19018	97	*Acinetobacter* phage vB_AbaM_IME284	hypothetical protein (AYP68974.1)	3E-63
gp41	19030	19176	48	*Acinetobacter* phage WCHABP1	hypothetical protein (YP_009604579.1)	3E-25
gp42	19179	19685	168	*Acinetobacter* phage vB_AbaM_IME284	deoxyuridine 5'-triphosphate nucleotidohydrolase (AYP68977.1)	1E-09
gp43	19678	19908	76	*Acinetobacter* phage YMC-13-01-C62	hypothetical protein (YP_009055462.1)	3E-47
gp44	19905	20105	66	-	-	-
gp45	20198	20806	202	*Acinetobacter* phage AB1	hypothetical protein (YP_009613838.1)	3E-145
gp46	20793	21068	91	*Acinetobacter* phage WCHABP12	hypothetical protein (YP_009600512.1)	2E-51
gp47	21052	21387	111	*Acinetobacter* phage LZ35	hypothetical protein (YP_009291903.1)	2E-69
gp48	21447	23480	677	*Acinetobacter* phage vB_AbaM_IME285	tail fiber protein (AYP68900.1)	4E-65
gp49	23482	24318	278	*Acinetobacter* phage AbP2	putative tail fiber protein (YP_009609871.1)	1E-129
gp50	24311	24937	208	*Acinetobacter* phage IME-AB2	hypothetical protein (YP_009592224.1)	6E-149
gp51	24937	26121	394	*Acinetobacter* phage WCHABP1	putative baseplate J-like protein (YP_009604499.1)	0
gp52	26118	26471	117	*Acinetobacter* phage AB1	hypothetical protein (YP_009613845.1)	7E-80

gp53	26468	26614	48	*Acinetobacter* phage AbP2	hypothetical protein (YP_009609875.1)	4E-23
gp54	26617	27261	214	*Acinetobacter* phage WCHABP1	putative baseplate assembly protein (YP_009604501.1)	2E-152
gp55	27242	28132	296	*Acinetobacter* phage vB_AbaM_IME512	hypothetical protein (AYP69091.1)	0
gp56	28241	28516	91	*Acinetobacter* phage AbP2	hypothetical protein (YP_009609880.1)	2E-58
gp57	28513	29130	205	*Acinetobacter* phage AbP2	hypothetical protein (YP_009609881.1)	1E-140
gp58	29138	31186	682	*Acinetobacter* phage vB_AbaM_IME284	hypothetical protein (AYP68992.1)	0
gp59	31189	31401	70	*Acinetobacter* phage LZ35	putative tail-fiber protein (YP_009291892.1)	3E-44
gp60	31431	31856	141	*Acinetobacter* phage Abp9	hypothetical protein (QEA11038.1)	2E-98
gp61	31902	32351	149	*Acinetobacter* phage YMC-13-01-C62	hypothetical protein (YP_009055478.1)	7E-104
gp62	32364	33827	487	*Acinetobacter* phage Bphi-R1888	hypothetical protein (QGH74121.1)	0
gp63	33817	34311	164	*Acinetobacter* phage IME-AB2	hypothetical protein (YP_009592155.1)	7E-115
gp64	34308	34721	137	*Acinetobacter* phage AB1	hypothetical protein (YP_009613770.1)	2E-96
gp65	34718	35221	167	*Acinetobacter* phage IME-AB2	hypothetical protein (YP_009592156.1)	3E-118
gp66	35261	35962	233	*Acinetobacter* phage BS46	hypothetical protein (QEP53318.1)	3E-142
gp67	36030	36215	61	*Acinetobacter* phage vB_AbaM_IME284	hypothetical protein (AYP69000.1)	3E-34
gp68	36212	36649	145	*Acinetobacter* phage Bphi-R2919	hypothetical protein (QGH74036.1)	1E-100
gp69	36640	36939	99	-	-	-
gp70	37075	37527	150	*Acinetobacter* phage vB_AbaM_IME284	hypothetical protein (AYP69004.1)	3E-105
gp71	37530	37880	116	*Acinetobacter* phage AB1	hypothetical protein (YP_009613778.1)	6E-74
gp72	37960	38952	330	*Acinetobacter* phage AB1	hypothetical protein (YP_009613780.1)	0
gp73	38963	39457	164	*Acinetobacter* phage AB1	hypothetical protein (YP_009613781.1)	4E-112
gp74	39457	40809	450	*Acinetobacter* phage AB1	hypothetical protein (YP_009613782.1)	0
gp75	40809	40973	54	*Acinetobacter* phage YMC-13-01-C62	hypothetical protein (YP_009055492.1)	2E-30
gp76	41023	41229	68	*Acinetobacter* phage YMC-13-01-C62	hypothetical protein (YP_009055493.1)	5E-43
gp77	41219	41485	88	*Acinetobacter* phage vB_AbaM_IME284	hypothetical protein (AYP69011.1)	1E-56
gp78	41563	41739	58	-	.	-
gp79	41736	42092	118	*Acinetobacter* sp. 723929	hypothetical protein (EXI19295.1)	1E-47
gp80	42094	42423	109	*Acinetobacter* sp. ANC 4558	hypothetical protein (WP_086182742.1)	5E-32
gp81	42472	42654	60	*Acinetobacter* phage AB1	hypothetical protein (YP_009613789.1)	2E-36

Table A4. Annotation of phage 3043. For each ORF, the transcription start and stop position. The corresponding gene product size and putative predicted function based on the best hit obtained in BLASTP and the E-value are indicated.

ORF	Start (bp)	Stop (bp)	Predicted proteins			
			Size (aa)	Best Species Hit	Putative function (Accession number)	E-value
gp01	268	447	59	*Acinetobacter* phage vB_AbaP_B3	hypothetical protein (YP_009610338.1)	3E-09
gp02	1069	1251	60	*Acinetobacter* phage vB_ApiP_P1	hypothetical protein (YP_009610440.1)	1E-36
gp03	1320	1532	70	*Acinetobacter* phage vB_ApiP_P1	hypothetical protein (YP_009610441.1)	3E-41
gp04	1540	1755	71	*Acinetobacter* phage vB_ApiP_P2	hypothetical protein (YP_009610490.1)	1E-41
gp05	2197	2706	169	*Acinetobacter* phage vB_AbaP_APK87	hypothetical protein (QGK90454.1)	2E-119
gp06	2708	2983	91	*Acinetobacter* phage vB_ApiP_P2	hypothetical protein (YP_009610493.1)	4E-60
gp07	2985	3359	124	*Acinetobacter* phage vB_ApiP_P1	hypothetical protein (YP_009610444.1)	1E-87
gp08	3350	3679	109	*Acinetobacter* phage vB_AbaP_PD-AB9	hypothetical protein (YP_009189868.1)	5E-54
gp09	3764	4360	198	*Acinetobacter* phage phiAB6	hypothetical protein (YP_009288635.1)	2E-146
gp10	4448	4618	56	*Acinetobacter* phage vB_ApiP_P1	hypothetical protein (YP_009610448.1)	9E-29
gp11	4627	5025	132	*Acinetobacter* phage vB_AbaP_APK87	hypothetical protein (QGK90460.1)	1E-93
gp12	5097	5576	159	*Acinetobacter* phage vB_ApiP_P2	hypothetical protein (YP_009610501.1)	8E-114
gp13	5578	6015	145	*Acinetobacter* phage vB_AbaP_APK87	hypothetical protein (QGK90462.1)	8E-92
gp14	6026	6193	55	*Acinetobacter* phage vB_ApiP_P1	hypothetical protein (YP_009610452.1)	6E-30
gp15	6180	6374	64	*Acinetobacter* phage vB_ApiP_P2	hypothetical protein (YP_009610504.1)	1E-36
gp16	6371	6601	76	*Acinetobacter* phage vB_AbaP_APK87	hypothetical protein (QGK90465.1)	7E-49
gp17	6591	6815	74	*Acinetobacter* phage vB_AbaP_AS12	DNA binding protein (YP_009599198.1)	3E-32
gp18	6805	7605	266	*Acinetobacter* virus vB_AbaP_AGC01	DNA primase/helicase (QIW86333.1)	0
gp19	7605	7922	105	*Acinetobacter* phage IME200	hypothetical protein (YP_009216513.1)	9E-66
gp20	7922	8158	78	*Acinetobacter* phage vB_AbaP_APK32	hypothetical protein (AZU99369.1)	9E-46
gp21	8171	9469	432	*Acinetobacter* phage vB_AbaP_APK87	DNA helicase (QGK90471.1)	0
gp22	9472	10209	245	*Acinetobacter* phage vB_AbaP_B09_Aci08	hypothetical protein (YP_009814035.1)	5E-160
gp23	10206	11177	323	*Acinetobacter* phage Pipo	DNA ligase (QQO92947.1)	0
gp24	11426	13753	775	*Acinetobacter* phage vB_AbaP_AS12	DNA polymerase I (YP_009599206.1)	0

gp25	13743	13976	77	*Acinetobacter* phage Fri1	hypothetical protein (YP_009203033.1)	5E-44
gp26	13973	14863	296	*Acinetobacter* phage vB_ApiP_P2	hypothetical protein (YP_009610515.1)	0
gp27	15036	15371	111	*Acinetobacter* phage vB_AbaP_B09_Aci08	putative DNA binding protein (YP_009814041.1)	5E-53
gp28	15415	16317	300	*Acinetobacter* phage vB_ApiP_P2	exonuclease (YP_009610518.1)	0
gp29	16298	16873	191	*Acinetobacter* phage vB_ApiP_P1	tRNA nucleotidyltransferase (YP_009610466.1)	3E-124
gp30	16870	17310	146	*Acinetobacter* phage phiAB1	putative DNA endonuclease VII (YP_009189364.1)	5E-104
gp31	17314	18249	311	*Acinetobacter* phage SWH-Ab-3	DNA-directed RNA polymerase (YP_009949093.1)	0
gp32	18249	18923	224	*Acinetobacter* phage vB_AbaP_APK116	dNMP kinase (QHS01516.1)	9E-144
gp33	18932	21349	805	*Acinetobacter* phage vB_AbaP_APK87	RNA polymerase (QGK90485.1)	0
gp34	21451	21648	65	*Acinetobacter* virus vB_AbaP_AGC01	head-to-tail connector protein (QIW86352.1)	6E-38
gp35	21645	21896	83	*Acinetobacter* phage vB_ApiP_P1	structural protein (YP_009610472.1)	5E-53
gp36	21905	23461	518	*Acinetobacter* phage Abp1	head-to-tail joining protein (YP_008058229.1)	0
gp37	23470	24330	286	*Acinetobacter* virus vB_AbaP_AGC01	tail tubular protein A (QIW86355.1)	0
gp38	24346	25383	345	*Acinetobacter* phage vB_AbaP_CEB2	capsid protein (ALR87465.1)	0
gp39	25439	25624	61	*Acinetobacter* phage vB_ApiP_P1	tail tubular protein A (YP_009610476.1)	2E-31
gp40	25636	25845	69	*Acinetobacter* phage vB_AbaP_B5	chromosome segregation ATPase-like protein (YP_009610427.1)	9E-29
gp41	26007	26633	208	*Acinetobacter* phage SH-Ab 15519	tail tubular protein A (YP_009598273.1)	5E-149
gp42	26642	28933	763	*Acinetobacter* phage vB_ApiP_P2	tail tubular protein B (YP_009610532.1)	0
gp43	28933	29607	224	*Acinetobacter* phage vB_ApiP_P2	internal virion protein B (YP_009610533.1)	2E-157
gp44	29620	32505	961	*Acinetobacter* virus vB_AbaP_AGC01	tail fiber protein (QIW86362.1)	0
gp45	32515	35613	1032	*Acinetobacter* phage vB_AbaA_fBenAci003	internal virion protein C (QOV07847.1)	0
gp46	35619	37847	742	*Acinetobacter* phage vB_AbaP_APK32	tailspike protein (AZU99395.1)	1E-68
gp47	37863	38198	111	*Acinetobacter* phage vB_AbaP_APK14	holin (AYR04395.1)	8E-71
gp48	38185	38742	185	*Acinetobacter* phage vB_ApiP_P1	endolysin (YP_009610484.1)	1E-127
gp49	38751	39059	102	*Acinetobacter* phage vB_ApiP_P1	DNA maturase A (YP_009610485.1)	3E-65
gp50	39069	41006	645	*Acinetobacter* phage vB_AbaA_fBenAci003	DNA maturase B (QOV07852.1)	0
gp51	41003	41140	45	*Acinetobacter* phage vB_AbaP_AS12	DNA binding protein (YP_009599234.1)	1E-18
gp52	41097	41300	67	*Acinetobacter* phage phiAB1	hypothetical protein (YP_009189385.1)	2E-36
gp53	41310	41501	63	-	-	-

Table A5. Annotation of phage 3060. For each ORF, the transcription start and stop position. The corresponding gene product size and putative predicted function based on the best hit obtained in BLASTP and the E-value are indicated.

ORF	Start (bp)	Stop (bp)	Predicted proteins			
			Size (aa)	Best Species Hit	Putative function (Accession number)	E-value
gp01	699	842	47	*Acinetobacter* phage vB_AbaA_fBenAci003	hypothetical protein (QOV07809.1)	8E-23
gp02	1496	1999	167	*Acinetobacter* phage Abp1	hypothetical protein (YP_008058195.1)	6E-119
gp03	2007	2381	124	*Acinetobacter* phage vB_AbaP_AS12	hypothetical protein (YP_009599190.1)	3E-71
gp04	2372	2485	37	*Acinetobacter* phage vB_AbaA_fBenAci002	hypothetical protein (QOV07757.1)	3E-16
gp05	2472	2696	74	*Acinetobacter* phage Fri1	hypothetical protein (YP_009203013.1)	7E-45
gp06	2782	3276	164	*Acinetobacter* phage vB_AbaP_Acibel007	structural protein (YP_009103214.1)	2E-76
gp07	3620	4018	132	*Acinetobacter* phage vB_AbaP_B09_Aci08	hypothetical protein (YP_009814022.1)	1E-88
gp08	4089	4583	164	*Acinetobacter* phage vB_AbaP_APK26	hypothetical protein (QQO96964.1)	4E-117
gp09	4585	5022	145	*Acinetobacter* phage vB_AbaP_APK14	hypothetical protein (AYR04357.1)	7E-97
gp10	5033	5200	55	*Acinetobacter* phage IME200	hypothetical protein (YP_009216508.1)	7E-30
gp11	5390	5638	82	*Acinetobacter* phage vB_AbaP_46-62_Aci	hypothetical protein (YP_009813407.1)	9E-34
gp12	5628	5837	69	*Acinetobacter* phage vB_AbaP_AS11	DNA binding protein (YP_009599250.1)	6E-36
gp13	5848	6633	261	*Acinetobacter* phage WCHABP5	putative DNA primase (YP_009604600.1)	0
gp14	6737	6943	68	*Acinetobacter* virus vB_AbaP_AGC01	hypothetical protein (QIW86334.1)	1E-35
gp15	6943	7284	113	*Acinetobacter* phage vB_AbaP_APK48-3	DNA primase (QGH71539.1)	3E-54
gp16	7259	7504	81	*Acinetobacter* phage vB_AbaP_AS11	DNA/RNA binding protein (YP_009599253.1)	4E-45
gp17	7513	8811	432	*Acinetobacter* virus vB_AbaP_AGC01	DNA helicase (QIW86337.1)	0
gp18	8814	9128	104	*Acinetobacter* phage vB_AbaP_AS12	DNA binding protein (YP_009599204.1)	1E-61
gp19	9152	9526	124	*Acinetobacter* phage vB_AbaP_AS12	DNA binding protein (YP_009599204.1)	1E-75
gp20	9523	10497	324	*Acinetobacter* phage vB_AbaP_APK48-3	ATP-dependent DNA ligase (QGH71543.1)	0
gp21	10735	13038	767	*Acinetobacter* phage vB_AbaP_AS12	DNA polymerase I (YP_009599206.1)	0
gp22	13258	14148	296	*Acinetobacter* phage vB_AbaP_AS12	hypothetical protein (YP_009599208.1)	0
gp23	14205	14324	39	*Acinetobacter* phage vB_AbaP_APK	deoxynucleoside monophosphate kinase (AYR04374.1)	8E-20
gp24	14357	15310	317	*Acinetobacter* phage vB_AbaP_AS12	5'-3' exonuclease (YP_009599211.1)	0

gp25	15291	15866	191	*Acinetobacter* phage vB_AbaP_AS11	tRNA nucleotidyltransferase (YP_009599264.1)	5E-128
gp26	15863	16303	146	*Acinetobacter* phage IME200	DNA endonuclease (YP_009216525.1)	7E-105
gp27	16307	17242	311	*Acinetobacter* phage WCHABP5	putative phosphodiesterase (YP_009604614.1)	0
gp28	17242	17892	216	*Acinetobacter* phage vB_AbaP_APK2-2	dNMP kinase (AZU99278.1)	1E-153
gp29	17901	20318	805	*Acinetobacter* phage AbKT21phiIII	RNA polymerase (YP_009818746.1)	0
gp30	20421	20618	65	*Acinetobacter* phage phiAB1	hypothetical protein (YP_009189368.1)	7E-40
gp31	20615	20866	83	*Acinetobacter* phage vB_AbaP_PD-AB9	structural protein (YP_009189841.1)	5E-53
gp32	20875	22431	518	*Acinetobacter* phage vB_AbaP_B09_Aci08	putative head-tail connector protein (YP_009814050.1)	0
gp33	22440	23300	286	*Acinetobacter* phage vB_AbaA_fBenAci001	scaffolding protein (QOV07740.1)	0
gp34	23316	24347	343	*Acinetobacter* phage vB_AbaP_B09_Aci08	putative capsid and scaffold (YP_009814052.1)	0.01
gp35	24401	24586	61	*Acinetobacter* virus vB_AbaP_AGC01	tail tubular protein B (QIW86357.1)	1E-30
gp36	24605	24955	116	*Acinetobacter* phage vB_AbaP_AS11	tail needle protein (YP_009599275.1)	3E-30
gp37	25052	25612	186	*Acinetobacter* phage AbKT21phiIII	tail fiber protein (YP_009818752.1)	7E-132
gp38	25621	27912	763	*Acinetobacter* phage AbKT21phiIII	tail fiber protein (YP_009818753.1)	0
gp39	27912	28586	224	*Acinetobacter* phage vB_AbaP_B1	internal virion protein B (YP_009610328.1)	3E-154
gp40	28599	31484	961	*Acinetobacter* phage vB_AbaA_fBenAci001	putative internal virion protein C (QOV07746.1)	0
gp41	31494	34592	1032	*Acinetobacter* phage vB_AbaP_APK26	putative internal virion protein C (QQO97000.1)	0
gp42	34599	37556	985	*Acinetobacter* phage vB_AbaP_APK87	tailspike protein (QGK90498.1)	5E-75
gp43	37566	37901	111	*Acinetobacter* phage IME200	putative holin (YP_009216490.1)	1E-73
gp44	37888	38445	185	*Acinetobacter* phage vB_AbaP_B3	endolysin (YP_009610381.1)	8E-127
gp45	38615	38923	102	*Acinetobacter* phage vB_AbaP_AS12	DNA maturase A (YP_009599232.1)	3E-65
gp46	38933	40870	645	*Acinetobacter* phage vB_AbaA_fBenAci002	DNA maturase B (QOV07804.1)	0
gp47	40867	41004	45	*Acinetobacter* phage vB_AbaP_AS12	DNA binding protein (YP_009599234.1)	5E-22
gp48	40961	41164	67	*Acinetobacter* phage vB_AbaP_AS11	hypothetical protein (YP_009599287.1)	5E-36

Table A6. Annotation of phage 3073. For each ORF, the transcription start and stop position. The corresponding gene product size and putative predicted function based on the best hit obtained in BLASTP and the E-value are indicated.

ORF	Start (bp)	Stop (bp)	Predicted proteins			
			Size (aa)	Best Species Hit	Putative function (Accession number)	E-value
gp01	16	441	141	*Acinetobacter* phage WCHABP1	hypothetical protein (YP_009604507.1)	4E-99
gp02	487	936	149	*Acinetobacter* phage YMC-13-01-C62	hypothetical protein (YP_009055478.1)	3E-103
gp03	949	2412	487	*Acinetobacter* phage AB1	hypothetical protein (YP_009613768.1)	0
gp04	2402	2896	164	*Acinetobacter* phage AB1	hypothetical protein (YP_009613769.1)	3E-111
gp05	2893	3306	137	*Acinetobacter* phage AB1	hypothetical protein (YP_009613770.1)	7E-93
gp06	3303	3806	167	*Acinetobacter phage Bphi-R2919*	hypothetical protein (QGH74040.1)	5E-121
gp07	3844	4770	308	*Thermovibrio guaymasensis*	DNA (cytosine-5-)-methyltransferase (WP_170137398.1)	2E-155
gp08	4825	5013	62	*Acinetobacter* phage AB1	hypothetical protein (YP_009613773.1)	2E-09
gp09	5028	5465	145	*Acinetobacter* phage IME-AB2	putative RNA polymerase (YP_009592159.1)	1E-95
gp10	5740	6021	93	*Acinetobacter* phage WCHABP12	hypothetical protein (YP_009600579.1)	1E-56
gp11	6037	6489	150	*Acinetobacter* phage AB1	hypothetical protein (YP_009613777.1)	2E-93
gp12	6492	6842	116	*Acinetobacter* phage AB1	hypothetical protein (YP_009613778.1)	8E-65
gp13	6922	7914	330	*Acinetobacter* phage AB1	hypothetical protein (YP_009613780.1)	0
gp14	7925	8419	164	*Acinetobacter* phage AB1	hypothetical protein (YP_009613781.1)	3E-113
gp15	8419	9771	450	*Acinetobacter* phage AB1	hypothetical protein (YP_009613782.1)	0
gp16	9780	9965	61	-	-	-
gp17	10211	10477	88	*Acinetobacter* phage AB1	hypothetical protein (YP_009613785.1)	3E-51
gp18	10575	10937	120	*Acinetobacter nosocomialis*	hypothetical protein (AZC08656.1)	3E-81
gp19	10934	11371	145	*Acinetobacter sp. 39-4*	hypothetical protein (OJU54552.1)	7E-26
gp20	11373	11627	84	*Acinetobacter pittii*	hypothetical protein (WP_068550348.1)	1E-54
gp21	11823	12014	63	*Thermovibrio guaymasensis*	hypothetical protein (WP_121171932.1)	2E-04
gp22	12015	12224	69	*Acinetobacter* phage WCHABP12	hypothetical protein (YP_009600564.1)	0.027
gp23	12221	12415	64	*Acinetobacter* phage BS46	hypothetical protein (QEP53345.1)	9E-31
gp24	12427	12585	52	-	-	-

gp25	13205	13921	238	*Acinetobacter* phage WCHABP1	putative head protein (YP_009604534.1)	8E-152
gp26	13987	14163	58	*Acinetobacter sp.* ANC 3813	hypothetical protein (WP_086214221.1)	9E-09
gp27	14135	15577	480	*Acinetobacter* phage YMC-13-01-C62	putative portal protein (YP_009055503.1)	0
gp28	15581	16741	386	*Acinetobacter phage AP22*	putative phage terminase large subunit (YP_006383766.1)	0
gp29	16863	17294	143	*Acinetobacter phage AP22*	putative phage terminase small subunit (YP_006383765.1)	3E-98
gp30	17360	17521	53	*Acinetobacter* phage AbP2	hypothetical protein (YP_009609912.1)	0.002
gp31	17511	17753	80	*Acinetobacter* phage AbP2	hypothetical protein (YP_009609913.1)	7E-45
gp32	17750	17947	65	*Acinetobacter* phage Bphi-R1888	DNA-binding protein (QGH74172.1)	3E-32
gp33	17944	18153	69	*Acinetobacter baumannii*	hypothetical protein (WP_032057375.1)	2E-41
gp34	18150	18374	74	*Acinetobacter baumannii*	hypothetical protein (WP_140947163.1)	4E-47
gp35	18361	18720	119	*Acinetobacter baumannii*	hypothetical protein (KQK45630.1)	5E-73
gp36	18823	19185	120	*Acinetobacter* phage WCHABP12	hypothetical protein (YP_009600549.1)	1E-76
gp37	19249	19488	79	*Acinetobacter* phage AB1	hypothetical protein (YP_009613805.1)	5E-44
gp38	19543	20145	200	*Chitinophagaceae* bacterium	KilA-N domain-containing protein (MBK6382040.1)	7E-110
gp39	20306	20668	120	*Acinetobacter* phage WCHABP12	putative endodeoxyribonuclease (YP_009600547.1)	3E-77
gp40	20693	21217	174	*Acinetobacter* phage IME-AB2	hypothetical protein (YP_009592193.1)	1E-53
gp41	21214	21378	54	*Acinetobacter* phage WCHABP12	hypothetical protein (YP_009600543.1)	3E-28
gp42	21375	21950	191	*Acinetobacter* phage YMC-13-01-C62	hypothetical protein (YP_009055437.1)	1E-138
gp43	21947	22744	265	*Acinetobacter* phage WCHABP12	hypothetical protein (YP_009600541.1)	3E-77
gp44	22904	23494	196	*Acinetobacter* phage BS46	HNH family homing endonuclease (QEP53257.1)	7E-46
gp45	23566	23856	96	*Acinetobacter* phage AbP2	hypothetical protein (YP_009609930.1)	2E-57
gp46	23853	24119	88	*Acinetobacter* phage YMC-13-01-C62	hypothetical protein (YP_009055442.1)	1E-53
gp47	24130	25473	447	*Acinetobacter* phage Bphi-R2919	replicative DNA helicase (QGH74077.1)	0
gp48	25479	26210	243	*Acinetobacter* phage LZ35	primosomal protein I (YP_009291925.1)	2E-162
gp49	26223	26435	70	*Acinetobacter* phage AB1	hypothetical protein (YP_009613819.1)	3E-43
gp50	26446	26619	57	*Acinetobacter* phage AB1	hypothetical protein (YP_009613820.1)	6E-33
gp51	26762	27205	147	*Acinetobacter* phage LZ35	hypothetical protein (YP_009291921.1)	4E-101
gp52	27202	27444	80	*Acinetobacter* phage AB1	hypothetical protein (YP_009613824.1)	1E-08
gp53	27441	27680	79	*Thermovibrio guaymasensis*	hypothetical protein (RKQ59915.1)	8E-47
gp54	27783	28208	141	*Acinetobacter* phage AbP2	hypothetical protein (YP_009609854.1)	3E-99

gp55	28310	29071	253	*Acinetobacter* phage AbP2	putative transcriptional regulator (YP_009609855.1)	5E-94
gp56	29138	29395	85	*Acinetobacter* phage AB1	hypothetical protein (YP_009613828.1)	2E-53
gp57	29488	29823	111	*Acinetobacter* phage AP22	hypothetical protein (YP_006383816.1)	1E-58
gp58	29820	30038	72	*Acinetobacter* phage AbP2	hypothetical protein (YP_009609913.1)	3E-06
gp59	30028	30270	80	*Acinetobacter* sp. GWC1_38_13	hypothetical protein (OFW44131.1)	8E-14
gp60	30274	30954	226	*Acinetobacter* phage AP22	putative ERF family protein (YP_006383814.1)	9E-150
gp61	30951	31577	208	*Acinetobacter* phage WCHABP1	hypothetical protein (YP_009604576.1)	7E-104
gp62	31556	31849	97	*Acinetobacter* phage YMC-13-01-C62	hypothetical protein (YP_009055457.1)	3E-28
gp63	31846	32034	62	*Acinetobacter bereziniae*	hypothetical protein (KAF1026206.1)	7E-04
gp64	32024	32215	63	*Acinetobacter* phage vB_AbaM_B9	hypothetical protein (AWD93323.1)	7E-18
gp65	32212	32370	52	*Acinetobacter* phage AP22	hypothetical protein (YP_006383811.1)	8E-17
gp66	32367	32858	163	*Acinetobacter* phage vB_AbaM_IME284	deoxyuridine 5'-triphosphate nucleotidohydrolase (AYP68977.1)	1E-87
gp67	32851	33081	76	*Acinetobacter* phage AP22	hypothetical protein (YP_006383809.1)	5E-45
gp68	33078	33299	73	*Thermovibrio guaymasensis*	hypothetical protein (WP_121172014.1)	5E-42
gp69	33453	34007	184	*Acinetobacter* phage YMC-13-01-C62	putative endolysin/autolysin (YP_009055463.1)	3E-129
gp70	34019	34159	46	*Acinetobacter* phage WCHABP12	hypothetical protein (YP_009600512.1)	1E-25
gp71	34278	34613	111	*Acinetobacter* phage AB1	hypothetical protein (YP_009613840.1)	2E-67
gp72	34674	36533	619	*Acinetobacter* phage vB_AbaM_IME285	tail fiber protein (AYP68900.1)	2E-63
gp73	36535	37317	260	*Acinetobacter* phage AP22	putative tail fiber protein (YP_006383803.1)	1E-137
gp74	37310	37936	208	*Thermovibrio guaymasensis*	DUF2612 domain-containing protein (WP_121171876.1)	8E-147
gp75	37936	39120	394	*Acinetobacter* phage WCHABP1	putative baseplate J-like protein (YP_009604499.1)	0
gp76	39117	39470	117	*Acinetobacter* phage AB1	hypothetical protein (YP_009613845.1)	5E-81
gp77	39467	39613	48	*Acinetobacter* phage AP22	hypothetical protein (YP_006383799.1)	2E-23
gp78	39616	40260	214	*Acinetobacter* phage WCHABP1	putative baseplate assembly protein (YP_009604501.1)	1E-151
gp79	40241	41131	296	*Acinetobacter* phage LZ35	hypothetical protein (YP_009291896.1)	0
gp80	41177	41677	166	*Acinetobacter* phage WCHABP12	hypothetical protein (YP_009600503.1)	3E-64
gp81	41708	41986	92	Acinetobacter phage WCHABP12	hypothetical protein (YP_009600502.1)	1E-59
gp82	41988	42584	198	*Acinetobacter* phage AP22	hypothetical protein (YP_006383795.1)	3E-139
gp83	42592	44640	682	*Acinetobacter* phage YMC-13-01-C62	lysozyme like domain protein (YP_009055475.1)	0
gp84	44633	44851	72	*Acinetobacter* phage *WCHABP1*	putative tail-fiber/lysozyme protein (YP_009604506.1)	1E-44

Table A7. Annotation of phage 3082. For each ORF, the transcription start and stop position. The corresponding gene product size and putative predicted function based on the best hit obtained in BLASTP and the E-value are indicated.

ORF	Start (bp)	Stop (bp)	Predicted proteins			
			Size (aa)	Best Species Hit	Putative function (Accession number)	E-value
gp01	715	897	60	*Acinetobacter* phage vB_ApiP_P1	hypothetical protein (YP_009610440.1)	2E-35
gp02	897	1178	94	*Acinetobacter* phage vB_ApiP_P1	hypothetical protein (YP_009610441.1)	7E-42
gp03	1186	1401	71	*Acinetobacter* phage vB_AbaP_APK37	hypothetical protein (AZU99403.1)	1E-41
gp04	1845	2354	169	*Acinetobacter* phage vB_AbaP_IME546	hypothetical protein (QFR59027.1)	2E-120
gp05	2356	2730	0	*Acinetobacter* phage vB_AbaP_APK87	hypothetical protein (QGK90456.1)	8E-73
gp06	2909	3505	198	*Acinetobacter* phage phiAB6	hypothetical protein (YP_009288635.1)	2E-147
gp07	3493	3609	38	-	-	-
gp08	3869	4267	133	*Acinetobacter* phage vB_AbaP_APK37	hypothetical protein (AZU99408.1)	1E-92
gp09	4339	4818	159	*Acinetobacter* phage vB_ApiP_P2	hypothetical protein (YP_009610501.1)	7E-114
gp10	4820	5257	145	*Acinetobacter* phage IME-200	hypothetical protein (YP_009216507.1)	2E-89
gp11	5268	5435	55	*Acinetobacter* phage Fri1	hypothetical protein (YP_009203020.1)	1E-29
gp12	5422	5616	64	*Acinetobacter* phage vB_AbaP_APK87	hypothetical protein (QGK90464.1)	2E-26
gp13	5613	5843	76	*Acinetobacter* phage vB_AbaP_APK87	hypothetical protein (QGK90465.1)	5E-45
gp14	5833	6057	75	*Acinetobacter* phage vB_AbaP_APK87	hypothetical protein (QGK90466.1)	1E-38
gp15	6047	6847	266	*Acinetobacter* phage vB_AbaP_APK89	DNA primase (QGK90365.1)	0
gp16	6847	7164	105	*Acinetobacter* phage vB_AbaP_APK87	hypothetical protein (QGK90469.1)	4E-66
gp17	7164	7406	80	*Acinetobacter* phage vB_AbaP_APK87	hypothetical protein (QGK90470.1)	1E-46
gp18	7419	8717	432	*Acinetobacter* phage vB_AbaP_APK87	DNA helicase (QGK90471.1)	0
gp19	8912	9457	181	*Acinetobacter* phage vB_AbaP_APK14	hypothetical protein (AYR04368.1)	2E-121
gp20	9454	10425	323	*Acinetobacter* phage Pipo	DNA ligase (QQO92947.1)	0
gp21	10418	10642	74	*Acinetobacter* phage vB_AbaP_APK87	hypothetical protein (QGK90474.1)	5E-44
gp22	10830	13148	772	*Acinetobacter* phage vB_ApiP_P2	DNA polymerase I (YP_009610513.1)	0
gp23	13157	13279	40	*Acinetobacter* phage vB_ApiP_P2	HNH endonuclease (YP_009610514.1)	2E-18
gp24	13297	14187	296	*Acinetobacter* phage vB_AbaP_WU2001	hypothetical protein (QVQ34712.1)	0

gp25	14360	14695	111	*Acinetobacter* phage vB_ApiP_P1	hypothetical protein (YP_009610464.1)	1E-73
gp26	14739	15641	300	*Acinetobacter* phage vB_ApiP_P2	exonuclease (YP_009610518.1)	0
gp27	15631	16200	189	*Acinetobacter* phage vB_AbaP_APK81	tRNA nucleotidyltransferase (QNO11401.1)	7E-127
gp28	16197	16637	146	*Acinetobacter* phage phiAB1	DNA endonuclease VII (YP_009189364.1)	2E-104
gp29	16641	17576	311	*Acinetobacter* phage vB_AbaP_APK26	phosphoesterase (QQO96987.1)	0
gp30	17576	18214	212	*Acinetobacter* phage vB_AbaP_APK48	dNMP kinase (QFG06946.1)	2E-152
gp31	18223	20640	805	*Acinetobacter* phage vB_AbaP_APK87	RNA polymerase (QGK90485.1)	0
gp32	20741	20938	65	*Acinetobacter* phage phiAB6	hypothetical protein (YP_009288659.1)	5E-40
gp33	20935	21186	83	*Acinetobacter* phage vB_AbaP_APK128	hypothetical protein (QVD48877.1)	4E-52
gp34	21195	22751	518	*Acinetobacter* phage vB_AbaP_APK87	head-tail connector protein (QGK90488.1)	0
gp35	22760	23620	286	*Acinetobacter* phage vB_ApiP_P1	scaffolding protein (YP_009610474.1)	0
gp36	23636	24667	343	*Acinetobacter* phage Pipo	major capsid protein (QQO92965.1)	0
gp37	24723	24908	61	*Acinetobacter* phage phiAB6	hypothetical protein (YP_009288664.1)	2E-32
gp38	24920	25150	76	*Acinetobacter* phage vB_ApiP_P2	hypothetical protein (YP_009610530.1)	1E-41
gp39	25321	25881	186	*Acinetobacter* phage vB_ApiP_P1	tail tubular protein A (YP_009610477.1)	3E-132
gp40	25890	28181	763	*Acinetobacter* phage vB_ApiP_P2	tail tubular protein B (YP_009610532.1)	0
gp41	28181	28855	224	*Acinetobacter* phage vB_ApiP_P2	internal virion protein (YP_009610533.1)	5E-158
gp42	28868	31753	961	*Acinetobacter* phage vB_AbaP_APK26	internal virion protein (QQO96999.1)	0
gp43	31763	34969	1065	*Acinetobacter* phage Paty	hypothetical protein (QQM15082.1)	0
gp44	34967	37123	718	*Acinetobacter* phage vB_AbaP_APK87	tailspike protein (QGK90498.1)	5E-153
gp45	37238	37573	111	*Acinetobacter* phage Fri1	holin (YP_009203056.1)	3E-72
gp46	37560	38117	185	*Acinetobacter* phage vB_AbaA_fBenAci003	endolysin (QOV07850.1)	2E-130
gp47	38237	38545	103	*Acinetobacter* phage vB_AbaP_APK32	DNA maturase (AZU99398.1)	6E-66
gp48	38555	40492	645	*Acinetobacter* phage vB_AbaP_B1	DNA maturase B (YP_009610335.1)	0
gp49	40489	40626	46	*Acinetobacter* phage vB_AbaP_APK81	hypothetical protein (QNO11423.1)	3E-22
gp50	40583	40786	67	*Acinetobacter* phage phiAB1	hypothetical protein (YP_009189385.1)	9E-36

Annex III. Expression of CPS depolymerase proteins

Table A8. Additional information regarding the CPS depolymerases. Information regarding the molar attenuation coefficient and the molecular masses (in g/L) of the CPS depolymerases.

CPS depolymerase	Molar attenuation coefficent	Molecular mass
B1	1.010	63,253.2
B9	1.391	72,100.83
P2	0.882	69,978.48
F70	1.492	62,013.56
3042	1.218	62,235.75
3043	1.133	63,348.28
3060	1.535	90,241.77
3073	1.327	54,445.03
3082	1.187	62,584.02

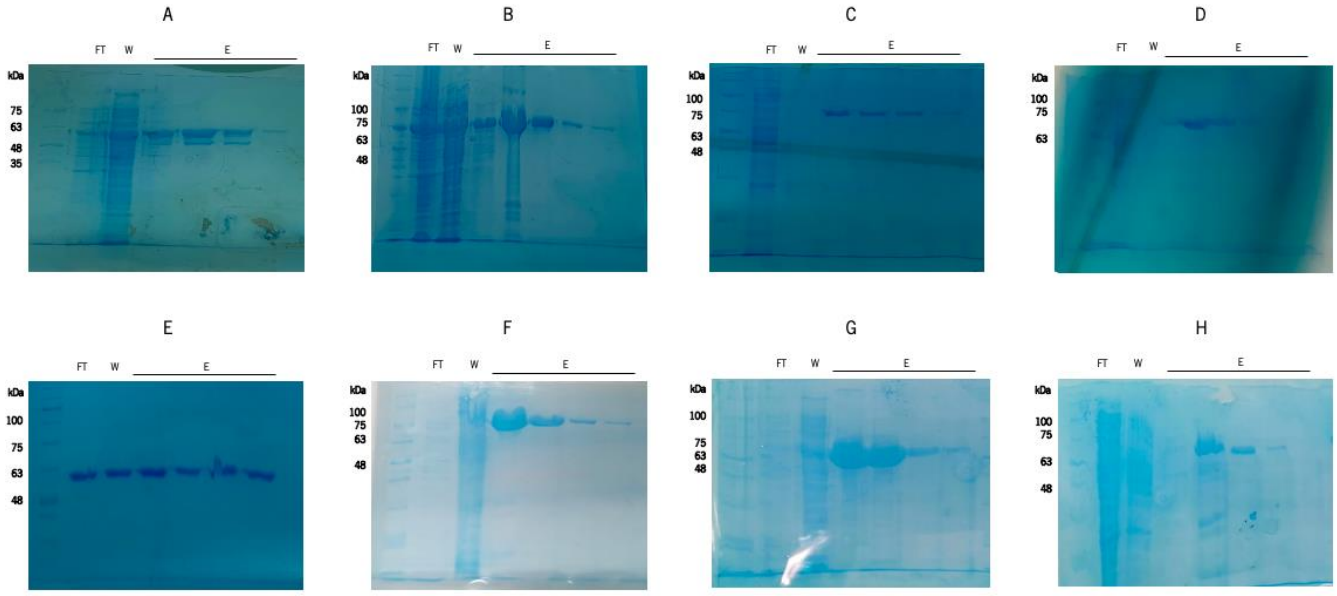

Figure A2. SDS-PAGE gels. 12.5% SDS-PAGE separation gel of the purified B1 (**A**), B9 (**B**), P2 (**C**), F70 (**D**), 3042 (**E**), 3060 (**F**), 3073 (**G**) and 3082 (**H**) CPS depolymerases using Nzycolour Protein Marker II (NZYTech). FT=flow through, W=wash, E= eluate.

Annex IV. Observation of activity with drop tests

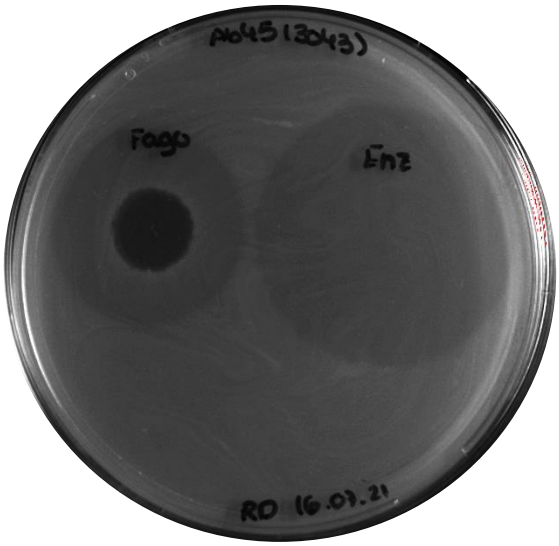

Figure A3. Activity of phage 3043 and its respective CPS depolymerase lytic. Activity was assessed against K38 strain bacterial lawn. On the left, the parental phage activity, with a plaque surrounded by a halo. On the right, K38-2 depolymerase activity with a halo zone.

Annex V. CD spectra and thermal unfolding curves

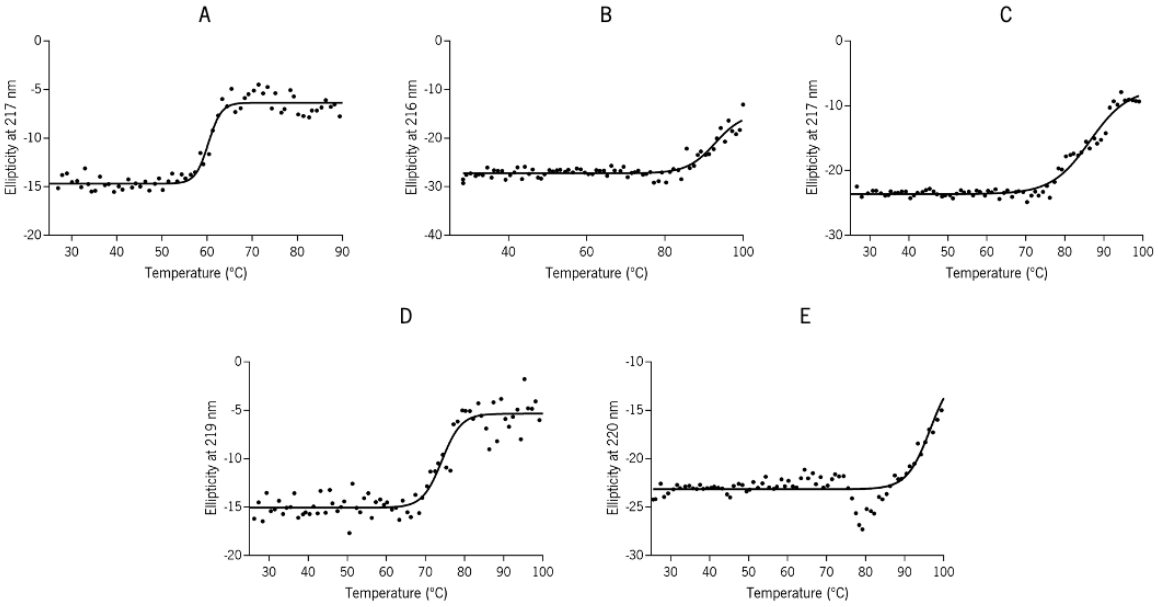

Figure A4. Melting temperature curves of CPS depolymerases. Thermal unfolding of K9 (**A**), K32 (**B**), K38-2 (**C**), K44 (**D**) and K67 (**E**) depolymerases. Measurements were performed at the enzymes negative dichroic minimum in potassium phosphate at pH 7 at heating rates 1°C/min, from 25 to 100°C.

Annex VI. K38-2 depolymerase activity on biofilms and planktonic cells

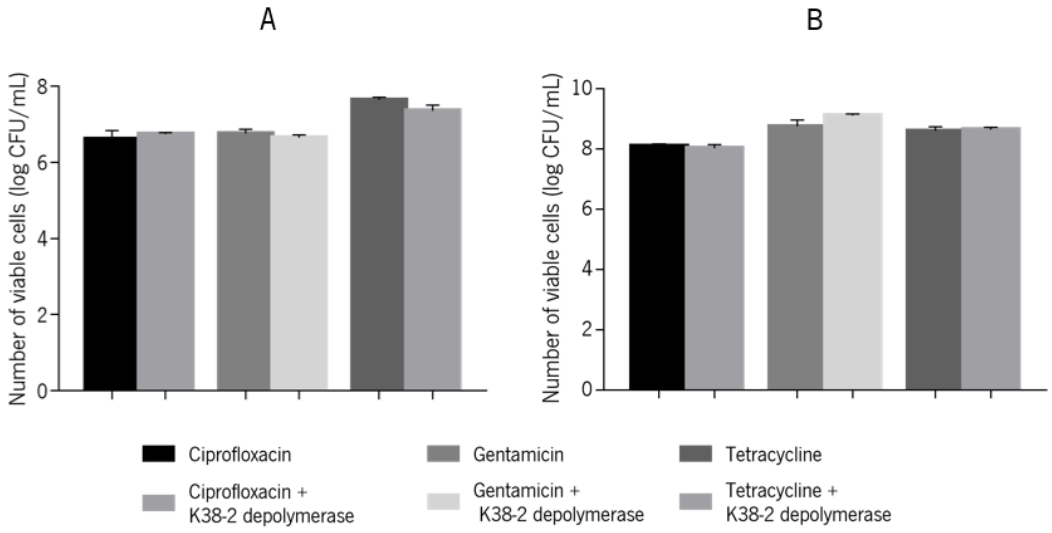

Figure A5. Synergetic effect of K38-2 depolymerase and ciprofloxacin, gentamicin and tetracycline antibiotics on 24h-old biofilm and planktonic cells. Potential 24h-old K38 biofilm disruption was assessed by quantification of viable cells after 6 of infection using 5 μM of K38-2 depolymerase and/or 5MIC of different antibiotics (**A**) Potential synergetic effect of K38-2 depolymerase (1 μM) and antibiotics (0.5MIC) after 4h of infection on K38 planktonic cells (**B**). Error bars represent standard deviation for two repeated experiments. Significance was determined by a Student *t* test between untreated and treated samples. * Statistically different (P <0.01).